# Accepted Manuscript

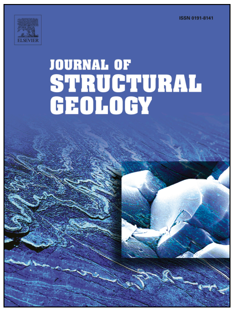


Defining the natural fracture network in a shale gas play and its cover succession: The case of the Utica Shale in eastern Canada

P. Ladevèze, S. Séjourné, C. Rivard, D. Lavoie, R. Lefebvre, A. Rouleau

PII: S0191-8141(17)30292-4

DOI: 10.1016/j.jsg.2017.12.007

Reference: SG 3574

To appear in: *Journal of Structural Geology*

Received Date: 17 March 2017

Revised Date: 6 November 2017

Accepted Date: 13 December 2017

Please cite this article as: Ladevèze, P., Séjourné, S., Rivard, C., Lavoie, D., Lefebvre, R., Rouleau, A., Defining the natural fracture network in a shale gas play and its cover succession: The case of the Utica Shale in eastern Canada, *Journal of Structural Geology* (2018), doi: 10.1016/j.jsg.2017.12.007.

# Defining the natural fracture network in a shale gas play and its cover succession: the case of the Utica Shale in eastern Canada

Ladevèze, P. [*,a,b], Séjourné, S.[c], Rivard, C. [b], Lavoie, D. [b], Lefebvre, R.[a], Rouleau, A.[d]

[a] *INRS – Centre Eau Terre Environnement, 490 rue de la Couronne, Québec City, QC G1K 9A9, Canada*

[b] *Geological Survey of Canada – Québec, 490 rue de la Couronne, Québec City, QC G1K 9A9, Canada*

[c] *Consulting geologist, Montréal, Canada*

[d] *UQAC, 555 Blvd. de l'Université, Chicoutimi, QC G7H 2B1, Canada*

[*] *Corresponding author: pierrelad@gmail.com*

**Keywords:** natural fracture characterization; analogs; conceptual models; shale gas; Utica Shale

**Abstract**

In the St. Lawrence sedimentary platform (eastern Canada), very little data are available between shallow fresh water aquifers and deep geological hydrocarbon reservoir units (here referred to as the intermediate zone). Characterization of this intermediate zone is crucial, as the latter controls aquifer vulnerability to operations carried out at depth. In this paper, the natural fracture networks in shallow aquifers and in the Utica shale gas reservoir are documented in an attempt to indirectly characterize the intermediate zone. This study used structural data from outcrops, shallow observation well logs and deep shale gas well logs to propose a conceptual model of the natural fracture network. Shallow and deep fractures were categorized into three sets of steeply-dipping fractures and into a set of bedding-parallel fractures. Some lithological and structural controls on fracture distribution were identified. The regional geologic history and similarities between the shallow and deep fracture datasets allowed the extrapolation of the fracture network characterization to the intermediate zone. This study thus highlights the benefits of using both datasets simultaneously, while they are generally interpreted separately. Recommendations are also proposed for future environmental assessment studies in which the existence of preferential flow pathways and potential upward fluid migration toward shallow aquifers need to be identified.

# 1 Introduction

For shale-dominated successions, there is a high interest in identifying natural fracture networks because they control the rock permeability (Barton et al., 1998; Berkowitz, 2002; Guerriero et al., 2013; Narr et al., 2006; Odling et al., 1999; Singhal and Gupta, 2010) and thus strongly influence fluid flow in the different stratigraphic units and potentially between deep prospective shale gas strata and shallow aquifers (CCA 2014; EPA 2016; Lefebvre, 2016).

However, the quantitative assessment of natural fractures can be challenging due to observational biases related to the methods that provide results at different scales (e.g. at the scale of outcrops, wells or seismic lines) and to the data that are sparsely or irregularly distributed. The inherent incompleteness of data is exacerbated in the so-called “intermediate” zone (or caprock). There is generally a lack of observation in this zone because it is located between shallow aquifers studied for hydrogeological purpose and the deep reservoir that has been characterized for hydrocarbon exploration/production. The characterization of this zone is crucial to properly understand the dynamic of potential contaminants migration to shallow aquifers.

Fracture observations on outcrops are often used as analogs for deep reservoirs (Antonellini and Mollema, 2000; Gale et al., 2014; Larsen et al., 2010; Lavenu et al., 2013; Vitale et al., 2012). Hence, the extrapolation of fracture data from outcrops and shallow hydrogeological wells, or from the deep reservoir where well log data and other geoscience information abound, may appear to be a promising approach to characterize the intermediate zone. However, the use of ‘shallow’ or ‘deep’ datasets as analogs is not always possible and certainly not straightforward; the controls on fracture distribution in a sedimentary succession have to be carefully identified to fully assess the fracture patterns. At shallow depths, surface weathering can enhance fracture apertures and be possibly responsible for fractures filling with minerals that are not representative of deep units. Furthermore, uplift or unroofing can initiate fracture propagation (Engelder, 1985; English, 2012; Gale et al., 2014). Therefore, the presence of unloading fractures oriented according to either a residual or a contemporary stress field will affect the shallow rock mass (Engelder, 1985). To the contrary, some fracture generation processes can occur only at significant depths due to an increase of the greatest compressive stress during regional shortening, a decrease in the least compressive stress caused by regional extension or an increase in pore pressure (Gillespie et al., 2001). Therefore, to be able to use some shallow and deep fracture sets as analogs, it must first be demonstrated that outcropping fractures are not solely the expression of near-surface events and were most likely formed at significant depths (at least comparable with the reservoir depth).

In this paper, we aim at integrating multisource data (outcrops, shallow and deep acoustic and electric well logs) that have different observation scales to obtain a sound interpretation of the fracture network affecting a shale gas play in southern Quebec (Saint-Édouard area, approximately 65 km southwest of Quebec City; location in Fig. 1). An emphasis is put on the characterization of the intermediate zone which potentially controls contaminants migration to subsurface. The proposed methodology could be of interest for other studies in shale dominated successions where there is a lack of data in the intermediate zone.

## 2 Regional tectonostratigraphic setting

### 2.1 *The St. Lawrence Platform*

In southern Quebec, the St. Lawrence Platform is bounded by the Canadian Shield to the NW and by the Appalachian mountain belt to the SE. The portion of interest of the St. Lawrence Platform (here referred as the SLP) comprises the area roughly between Montréal and Quebec City. This Cambrian-Ordovician depositional element is divided in two tectonostratigraphic domains: the autochthonous and the parautochthonous domains (Castonguay et al., 2010; St-Julien and Hubert, 1975) (Fig. 1). At the base of the autochthonous domain, Cambrian-Ordovician rift and passive margin units unconformably overlie the Grenville crystalline rocks (Lavoie et al., 2012) (Fig. 2). These passive margin units include the Potsdam Group sandstones and conglomerates and the Beekmantown Group dolomites and limestones. Those two groups are covered by Middle to Upper Ordovician units deposited in a foreland basin setting (Lavoie, 2008) (Fig. 2). The progressively deepening-upward carbonate units of the succeeding Chazy, Black River and Trenton groups, and the Utica Shale, were then covered by the overlying Upper Ordovician turbidite and molasse units of the Sainte-Rosalie, Lorraine and Queenston groups. The Utica Shale constitutes a prospective unit for shale gas in southern Quebec (Dietrich et al., 2011; Hamblin, 2006; Lavoie, 2008; Lavoie et al., 2014).

The SLP units have recorded a polyphased structural history (Pinet et al., 2014) and thus display a complex structural pattern. These events include Middle and Late Ordovician normal faulting that started at the inception of the foreland basin phase (Thériault, 2007), shortening during the Taconian orogeny (Tremblay and Pinet, 2016), and some post-Ordovician folding (Pinet et al., 2008) and faulting (Sasseville et al., 2008; Tremblay et al., 2013). Normal faults (including the Jacques-Cartier River fault, Fig. 5) are steeply-dipping to the south and displace the basement, the basal units of the platform and its upper units in the autochthonous domain (possibly including the Utica Shale and Lorraine Group). These faults were reactivated several times during and after the building of the Appalachians, documented evidence of movement is known for the late Silurian Salinic Orogeny and the opening of modern Atlantic (Castonguay et al., 2001; Faure et al., 2004; Konstantinovskaya et al., 2009; Sasseville et al., 2012; Séjourné et al., 2003; Tremblay and Pinet, 2016). A summary of the depositional environment and the major tectonic events that affected rock of the SLP is presented in Fig. 3.

In the autochthonous domain, the near surface Upper Ordovician units (post-Utica Shale) are folded by the regional Chambly-Fortierville syncline. This fold is asymmetric with more steeply-dipping beds in the southern flank (28°) than in the northern flank (10°) (Fig. 4a). Its axis is roughly parallel to the limit between the SLP and the Appalachians. To the southeast, the Aston fault and the Logan's Line belong to a regional thrust-fault system that limits the parautochthonous domain (Fig. 2 and Fig. 5). Reprocessing and reinterpretation of an industrial 2D seismic line (using two well calibration points) was proposed in (Lavoie et al., 2016) and showed that in the Saint-Édouard area, the parautochthonous domain forms a triangle zone delimited to the northwest by a NW-dipping backthrust and by the SW-dipping the Logan's Line to the SE (Fig. 5). The existence of a triangle zone bounding the southern limb of the Chambly-Fortierville is supported by previous interpretations done in the SLP (Castonguay et al., 2006; Castonguay et al., 2003; Konstantinovskaya et al., 2009). These thrusts/backthrusts are associated with the Middle to Late Ordovician Taconian Orogeny (St-Julien and Hubert, 1975). In the parautochthonous domain, a southeast-dipping system of thrust faults displays imbricated thrust geometries (Castonguay et al., 2006; Séjourné et al., 2003; St-Julien et al., 1983). Some northeast-striking folds also affect the parautochthonous units (Fig. 4b). The Logan's Line marks the fault-contact between the SLP and the allochthonous external Humber zone (St-Julien and Hubert, 1975) (Fig. 5).

The present-day in-situ maximum horizontal stress ($SH_{max}$) orientation is NE–SW in the SLP as previously proposed using borehole breakouts orientations (inferred from four-arm dipmeter caliper data) (Konstantinovskaya et al., 2012). This trend is relatively consistent with the large-scale trend documented in eastern North America (Heidbach et al., 2009; Zoback, 1992). The stresses/pressure gradients estimated in the platform indicate a strike-slip stress regime (Konstantinovskaya et al., 2012). As the regional faults of the SLP are oblique to the actual $SH_{max}$, a reactivation of these structures under the current stress field remains possible (Konstantinovskaya et al., 2012) but has not yet been documented.

Organic matter reflectance data indicates that at least 3 and 4.7 km of sediments have been eroded in the SLP (Sikander and Pittion, 1978) and in the frontal part of the Chaudière Nappe in the Quebec City area (Ogunyomi et al., 1980), respectively. Later studies showed that there was an increasing thickness of eroded sediments from about 5 to 7 km from northeast to southwest in the SLP (Héroux and Bertrand, 1991; Yang and Hesse, 1993).

### 2.2 *The intermediate zone (caprock) and reservoir units of the Saint-Édouard area*

The Utica Shale is overlain by autochthonous units (the Nicolet Formation - Lorraine Group and the Lotbinière Formation – Sainte-Rosalie Group) and parautochthonous units (Les Fonds Formation – Sainte-Rosalie Group). These units constitute the intermediate zone (caprock) in the Saint-Édouard study area.

The Utica Shale (Upper Ordovician) is made of limy mudstone that contains centi- to decimetric interbeds of shaley limestone (Globensky, 1987; Lavoie et al., 2008; Theriault, 2012). It is divided in two members (Upper and Lower). The Lower Utica Shale contains more limestone interbeds than the Upper Utica Shale. In the Saint-Édouard area, the thickness of the Utica Shale ranges from 200 to 400 m (Fig. 5). The autochthonous Lotbinière Formation (Sainte-Rosalie Group) and the parautochthonous Les Fonds Formation (Sainte-Rosalie Group) are time- and facies correlative units of the Utica Shale (Lavoie et al., 2016) (Fig. 2). The Utica Shale, Lotbinière and Les Fonds formations display a similar lithofacies of black calcareous mudstone with thin beds of impure fine-grained limestone but differs by their organofacies (Lavoie et al., 2016). The Lotbinière Formation is made of gray-black micaceous shale with rare interbeds of calcareous siltstones (thickness <10 cm) and is outcropping north of the Jacques-Cartier River normal fault (Belt et al., 1979; Clark and Globensky, 1973). In the parautochthonous domain, the Les Fonds Formation is mainly composed of shale with less abundant fine-grained limestones and conglomerates (Comeau et al., 2004). The Nicolet Formation (Lorraine Group, Upper Ordovician) is slightly younger compared to the previous three units (Comeau et al., 2004) and is mostly made of gray to dark-gray shale with centi- to decimetric (rarely metric) siltstone interbeds (Clark and Globensky, 1973; Globensky, 1987). Upward, there is a decrease of the shale content and an increase in the number and thickness of the sandstone beds (Clark and Globensky, 1976). In the Saint-Édouard area, the thickness of autochthonous and parautochthonous intermediate zone units (i.e., above the Utica Shale) progressively increases from 400 m to 1900 m from northwest to southeast (Fig. 5).

**Insert Fig. 1 to 5 here.**

## 3 Methodology

In this study, the term “fracture” refers to metric scale planar discontinuities that affect the rock mass without visible displacement.

### 3.1 *Data sources*

Fracture data were collected and compiled in the Saint-Édouard area using different methods. Fifteen outcrops were investigated (Fig. 1). Borehole logs includes acoustic, optical and electric logs that have different resolutions. Typically, electric logs have a higher resolution than acoustic and optical tools. Interpretation were then done in the light of these scale differences. Acoustic and optical televiewer logs from eleven shallow (15 to 147 m deep in the bedrock) groundwater monitoring wells drilled for the project (Crow and Ladevèze, 2015) were also studied. Moreover, Formation Micro Imager (FMI) data from three deep shale gas wells were interpreted. The wells referenced by the oil and gas geoscience information system of the Ministère des Ressources naturelles of Quebec under the numbers A266/A276 (Leclercville n°1), A279 (Fortierville n°1) and A283 (Sainte-Gertrude n°1) were used. To simplify the nomenclature in the current paper, they are hereafter referred to as A, B and C, respectively (Fig. 1). FMI data from the vertical sections of wells A, B and C cover the following ranges of depth: 1470-2080 m for well A, 560-2320 m for well B and 590-2050 m for well C; this includes the Utica Shale and variable portions of the overlying Lorraine Group. Each of these wells also includes a horizontal section (“horizontal leg”) in the Utica Shale (1000, 970 and 920 m long, for wells A, B and C respectively) for which FMI data was also available. For a history of the recent shale gas exploration in the study area, refer to Lavoie et al. (2014) and Rivard et al. (2014). The characteristics of the measurement stations are summarized in Table 1.

**Insert Table 1 here.**

## 3.2 *Fracture assessment*

Common geometrical attributes of fractures were measured: attitude, spacing, crosscutting relationships between fractures and other geological structures (such as syn-sedimentary concretions). These attributes were documented all along the boreholes using acoustic and electrical logs. As most of the outcrops were limited in size and were displaying only sparsely distributed fractures, their attributes were systematically measured in the exposed surfaces.

### *3.2.1 Fracture sets*

For each measurement station (outcrop or well), fracture poles were plotted on stereonets using the *SpheriStat*™ software (Stesky, 2010). Contoured density diagrams were used to identify the mean position of the fracture sets. The poles density contours of borehole data were corrected for sampling bias (underestimation of the frequencies for the fracture planes that are sub-parallel to the observation line) using the method of Terzaghi (1965). A weight function of the angle $\beta$ between the fracture plane and the observation line was attributed to all fracture densities. This weight $w$ is expressed as: $w=(\sin \beta)^{-1}$ (Terzaghi, 1965). Even if mathematically valid, fracture planes with low $\beta$ values are overestimated with this method (Park and West, 2002). For this reason, an arbitrary 10° blind zone was used in the analysis (fractures sub-parallel to the observation-line are excluded).

When clear crosscutting relationships were observed on outcrops, the relative timing of fracture sets formation could be defined. In borehole data, it was rarely possible to identify such relationships. In this case, the main attitude for fracture set attitudes were compared to adjacent outcrops data (if existing) to define a hypothetical relative timing for the formation of the fracture sets.

If fracture poles are scattered in stereonets, only the maximum pole concentration is taken into account. To better identify the major fracture sets in such cases (generally the case of outcrops or shallow wells that displays significant folding), a fold test was performed on fracture data in order to calculate the fracture attitudes prior to folding events. Results from this test were also used to further assess the relative chronology of fracture sets formation and folding. The rotation applied to fracture attitudes corresponds to the angle of rotation of the bedding plane after a folding event. Two generations of folds have previously been documented in the autochthonous domain in the Saint-Édouard area: F-I (first generation: Chambly-Fortierville syncline) and F-II (second generation) (Pinet, 2011). To consider the effect of the two generations of folds, the analysis was performed in two steps. First, the fracture plans were replaced back to their original attitude prior to F-II folding. As the F-II fold axes are sub-horizontal, the first step consists in correcting the strike direction of fracture planes according to the strike angle between fold-I and fold-II axes. The second step aims at correcting the fracture plans back to their attitude prior to F-I folding. This was done by tilting back the fracture planes around the F-I axis (N233/04, Fig. 4) with an angle corresponding to the structural dip (angle between the bedding plane attitudes in each measurement station and the horizontal). In the parautochthonous domain, a single folding event was easily observable in the field and fracture plans were back-tilted along the regional F-I axis (N235/03 Fig. 4). A better fracture set concentration after rotation is a strong indicator of its pre-folding origin. To quantify the degree of concentration of attitude data, the parameter k was calculated for both the original and rotated fracture sets. This parameter quantifies the degree of data dispersion on a sphere/stereonet (Fisher, 1953). The higher the values of k, the more the data are concentrated in the stereonet (Fiore Allwardt et al., 2007).

#### *3.2.2 Fractures distribution*

In the document, the term “spacing” refers here to the perpendicular distance between two adjacent fracture planes of similar attitude. Measuring or estimating spacing thus requires first a classification of the fractures into coherent fracture attitude set. The fractures densities correspond to the number of fractures (regardless of their attitudes) per unit distance along a line. They were calculated along the wells using a counting window of various lengths. Each fracture density value was then normalized by the window lengths. All fracture densities were corrected using the Terzaghi method. In the same way, fracture frequencies correspond to the number of fractures from a specific set per unit distance along a line.

To further explore the process of fracturing in siltstone units, the fracture spacing was plotted against bed thicknesses (fractures are bed-confined in siltstone to the contrary of shale in the studied area). Values of the ratio of fracture spacing to layer thickness (the slope of the curve) were extracted from these plots and used to determine if the fracture network has attained saturation, a concept describing the situation where whatever the applied strain, fracture spacing has attained a lower limit (or an upper limit for fracture densities) that is proportional to bed thickness (Bai et al., 2000; Wu and D. Pollard, 1995).

Geostatistical tools were used to assess the degree of spatial correlation of each fracture set (Chilès, 1988; Escuder Viruete et al., 2001; Miller, 1979; Tavchandjian et al., 1997; Valley, 2007; Villaescusa and Brown, 1990). In other words, the use of geostatistics can help define the spatial organization of fractures when they seem to have a totally random spatial distribution in the rock mass. The knowledge of the spatial distribution of fractures can be used to develop discrete fracture network (DFN) models to further assess the fracture control on fluid flow (Caine and Tomusiak, 2003; Dershowitz et al., 1998; Min et al., 2004; Surrette et al., 2008).

Variogram analyses were thus performed on spacing data for each fracture set in the horizontal section of the three deep wells. A formal definition of the experimental variogram γ(h) ($m^2$) for fracture spacing data is presented in Eq. (1).

$$\gamma(h) = \frac{1}{2n}\sum_{i=1}^{n}\left[z(x_i) - z(x_i + h_i)\right]^2 \qquad \text{Eq. (1)}$$

where, $n$ is the number of fractures separated by a distance $h$ (this calculation interval is also called "lag"), $z(x_i)$ is the fracture spacing value at the distance $x_i$. An experimental variogram presents the γ values successively calculated for increasing $h$ values. The shape of the experimental variogram is used to assess if the available data have a spatial correlation that could be represented by a theoretical model. If so, the nugget value in the experimental variogram must be lower than the variance of the entire dataset for the correlation in fracture spacing to be considered present (reflecting fracture clustering). The range value in the variogram provides the maximum distance for fracture spacing clustering. In geological terms, this range of influence means that two samples spaced farther apart than this distance are likely not correlated (and thus considered independent) (Miller, 1979).

#### *3.2.3 Fracture and rock mechanical properties*

The potential for fracture propagation in rocks is controlled by their brittleness (Ding et al., 2012; Lai et al., 2015; Meng et al., 2015). The Brittleness Index is an empirical parameter that is widely used to quantify the ability of a rock unit to fracture (Wang et al., 2015). In the Saint-Édouard area, this parameter was previously estimated from borehole logs acquired in the deep gas wells using the Grieser and Bray (2007) and the Glorioso and Rattia (2012) methods (Séjourné, 2017). These methods are respectively based on the acoustic (compressional and shear wave velocity logs) and mineralogical (derived from elemental spectroscopy logs) properties of the shale. In the current paper, the relationship between fracture densities and brittleness variations in the Lorraine Group and Utica Shale was explored.

# 4 Results

## 4.1 *Fractures in shales*

Two fracture types were observed in shale units: steeply-dipping fractures (F1, F2 and F3) and bedding-parallel fractures (BPF). Examples of observed fractures on outcrops are presented in Fig. 6. In the vast majority of outcrops, fractures are planar and exhibit clear crosscutting relationships. For this reason, it was possible to sort the high-angle fractures in three sets that are designated according to their relative order of formation (F1, F2 and F3 sets; F1 is the older set). Fractures were also only bed-confined in siltstones.

To facilitate the classification of fractures in sets, a fold test analysis was done using data from outcrops and shallow wells that were affected by folding events that could be clearly identified in the field (i.e. outcrops affected by folds F-II and F-I). Fracture attitudes from outcrops and values of the associated parameter $k$ (which quantifies the data concentration in the stereonets) are presented in Fig. 8. In the autochthonous domain, an improved concentration of fracture poles was obtained for F1 and F2 sets after rotation prior to the second generation of folds (F-II). Then, removing the effects of F-I fold improved even more the concentration of F1 fractures, but had no effect on the concentration of F2 fractures. This strongly suggests a pre-F-I folding origin for the F1 set, and a pre- to syn-F-II origin for F2 fractures. To the contrary, the concentration of the F3 fracture set was reduced after removing both F-II and F-I effects, thus supporting a syn- to post F-II folding origin for this F3 set. One fold generation was clearly observed in the parautochthonous domain (other fold generations may exist but were hardly observable on outcrops).

This regional folding corresponds to the first fold generation (F-I) documented in the autochthonous domain. The fold test showed that a better concentration was obtained for the F1 set when rotated prior to folding, confirming a potential pre-F-I origin for F1 fractures. Results for the F2 fracture set show a slight, probably poorly significant, reduction of concentration and the timing remains not well constrained on the basis of the fold test.

Fracture sets F1 and F2 are pervasive in both the autochthonous and parautochthonous domains. They strike NE (F1) and NW (F2) (Fig. 7), with F2 abutting against F1 (Fig. 6a and b). F1 and F2 are perpendicular to each other and orthogonally crosscut the bedding planes (S0). F1 fractures are locally concentrated in corridors (as in Fig. 6b). The third fracture set (F3) is only documented in the autochthonous domain. F3 strikes WNW and is sub-vertical (dip >80°) whatever the bedding planes attitudes (Fig. 7). F3 generally crosscuts F1 and F2 and was not observed at all sites. All three fracture sets were documented in shallow and deep data. Finally the BPF were only observed at shallow depth.

Detailed fracture length measurements were limited to the size of the outcrops. Thus, only semi-quantitative fracture length estimations are here proposed. Fracture lengths for the F1 and F2 sets were approximately between 2 and 5 m. The maximum observed fracture lengths were ranging between 10 and 30 m. F1 fractures display lengths higher than F2 fractures, as F2 abut F1 fractures. Due to the limited number of outcropping F3 fractures, no realistic estimate of fracture lengths for this set was possible. Finally, because some fractures locally extend beyond the limit of the outcropping areas, length estimation values must be considered with caution.

Some intervals in the black shales of the Lotbinière Formation (northern part of the study area) display oval-shaped carbonate concretions (maximum diameter of up to 1.5 m; length-to-width ratio around 1.5). The metabolic activity of sulfate-reducing and methanogen bacteria that occurred shortly after the inception of burial of organic matter-rich sediments under anoxic conditions are responsible for the formation of these concretions (Mozley and Davis, 2005). In the Lotbinière Formation, 15 fractures were identified passing around such concretions without crosscutting them (Fig. 6c). Such a relationship is interpreted as an indicator of natural fractures propagation in the presence of abnormal fluid pressure in response to the shale thermal maturation and to the gas generation in a context of deep burial (McConaughy and Engelder, 1999).

**Insert fig. 6 to 8 here.**

Statistics on fracture spacing data from outcrops and boreholes are presented in Fig. 9. Median values in shale outcrops are significantly for F1 than for F2 (0.20 to 0.28 m for F1; 2.4 to 2.93 m for F2). The same trend is observed in the shale gas wells (0.14 m for F1 and 2.93 m for F2). Lower and upper quartiles for fracture spacing also extend over a significantly larger interval for the F2 set than for the F1 set, suggesting a more scattered spatial distribution of F2 fractures, especially in the Utica Shale. In the deep wells, the mean value for F3 spacing (0.11 m) is slightly lower than that of the F1 value.

**Insert fig. 9 here.**

To the contrary of F2 fractures, both F1 and F3 fractures spacing data from outcrops and shale gas wells seems to follow a power law distribution (exponent values around 1), see Fig. 10. In this figure, spacing value less than 0.05m (resolution of the observation methods) and higher than 10 m (upper limit of statistical homogeneity) were excluded for the regression calculation. Following Bonnet et al. (2001), this may reflect the scale invariance of the fracture spacing for these two sets. The existence of the power law distribution must be interpreted with care as our dataset is affected by both censoring bias (high fracture spacing is not sampled due to the limited size of outcrops and well sections) and truncation bias (limitation due to tools resolution). Then, the scale range of observations did not extend two orders of magnitude as suggested by Bonnet et al. (2001). Despite this limitation, the specific trend for F2 fractures distribution may be explained by the relative timing of fracture formation. If F2 fractures lengths are constrained by F1 spacing, F2 spacing may not be scale invariant. This further support the possibility of a successive formation of F1 and F2 fractures.

**Insert fig. 10 here.**

All experimental variograms of the fracture sets obtained from horizontal legs of wells A, B and C show nugget values much lower than the variance of the entire sample (Fig. 11), implying that there is a correlation in fracture spacing. Therefore, fracture distributions display some clustering. F1 fractures display ranges values between 30 and 150 m. Variograms for the F2 and F3 set display ranges from 12 to 30 m, and 60 to 100 m respectively. Some concentration of F1 fractures (with significantly higher F1 fracture frequencies than other fracture sets) were identified in the horizontal well A (in the Utica Shale). This high frequency of F1 fractures is consistent with outcrop observations where F1 fractures spacing are lower than F2 and F3 spacing. This may be interpreted as the presence of F1 fractures corridors (see for instance Fig. 12: F1 fractures are closely spaced on distances of around 40 m and separated by approximately 100 to 200 m).

**Insert fig. 11 and 12 here.**

In the deep zone, fracture density vertical profiles generally display localized fractured intervals separated by vertical distances ranging from 10 m to 300 m. Fig. 13 only presents the fracture density and Brittleness Index (BI) variation with depth for well B, but they can be considered representative of those found in wells A and C. Higher fracture densities and BI values were generally measured in the Utica Shale. This suggests that these two parameters could be correlated. In specific depth intervals in well B, some high fracture densities values correlates with low BI values (see the contact between the Upper and Lower Utica in Fig. 13). Geomechanical contrasts in the vicinity of these lithological contacts may explain the occurrence of these higher fracture density intervals.

**Insert fig. 13 here.**

### 4.2 *Fractures in siltstone interbeds*

Data from outcrops showed that the siltstone interbeds are crosscut by the same fracture sets as those cutting across the shale (F1, F2 and F3) (Fig. 14a and b). However, contrary to shale units, fractures are stratabound in siltstone units, with only a few F1 fractures intersecting both siltstone and shale beds (Fig. 14c). F1 fractures are also generally longer than F2 fractures. F2 fractures abut F1 fractures and F2 fracture lengths generally equal to F1 fracture spacings (Fig. 14b). Fracture density in the siltstone beds is significantly higher than in shale intervals, with spacings lower than 1 m for both F1 and F2 fracture sets. Fractures were regularly spaced all along the outcrops. There is also a strong correlation between siltstone bed thickness and fracture spacing as shown in Fig. 15b. The calculated ratios of fracture spacing to layer thickness are respectively 1.29 and 1.43 for the F1 and F2 fracture sets.

**Insert fig. 14 and 15 here.**

# 5 Discussion

## 5.1 *Fracture pattern*

### *5.1.1 Main controls on fracture distributions*

The differences in fracture distribution between the Lorraine Group shales and the Lorraine Group siltstones, and also between the Lorraine Group shales and the Utica Shale, suggest that these distributions are lithologically controlled.

Differences in fracture distributions were observed between shales and siltstones of the Lorraine Group. In Lorraine Group shales, the F1 spacing is lower than the F2 spacing (see a visual example in Fig. 6b) and F1 and F2 fracture are probably organized in corridors. In siltstone units of the Lorraine Group, F1 and F2 fractures are more homogeneously distributed and display equivalent spacing values (see a visual example in Fig. 14). Fractures in siltstone units are also limited by the bed thickness (which rarely exceeds 1 to 2 m) and this parameter is correlated with fracture spacing (Fig. 15); this was also observed in many sedimentary basins (Bai et al., 2000; Gross, 1993; Ji and Saruwatari, 1998; Ladeira and Price, 1981; Narr and Suppe, 1991). It was thus possible to evaluate the fracture saturation in siltstones, based on estimated fracture spacing to layer thickness ratios. According to the threshold interval of ratio values (0.8 to 1.2) proposed in Bai and Pollard (2000) and Bai et al. (2000), F1 and F2 fracture spacing would be at saturation in siltstone units (ratios of 1.29 and 1.43 respectively above the threshold interval of ratio values). Contrasts in mechanical properties between shales and sandstones (the sandstone being more brittle with a higher Young's modulus) induce a preferential fracturing of sandstones (Engelder, 1985; Laubach et al., 2009). This could explain the higher observed fractures densities in the siltstones of the SLP. However, this must be considered cautiously as mechanical property differences between siltstone and shale units were not estimated throughout the SLP. This estimation is challenged by the presence of a significant amount of clay in both units (Séjourné et al., 2013); see also the low BI variations in the proximity of siltstone/shale contacts (Fig. 13).

In the vertical sections of deep shale gas wells (depths > 500 m), higher fracture densities were measured in the Utica Shale compared to the Lorraine Group shales (Fig. 13). This is in agreement with the highly fractured horizontal portions of the shale gas wells completed into the Utica Shale compared to the lower density of steeply-dipping fractures observed in the outcropping Lorraine Group units. In contrast, fracture spacing and strike direction values are similar in the outcropping Lorraine Group units and in the deep Utica Shale (Fig. 7 and Fig. 9). This could be interpreted as fracture corridors being more common in the Utica Shale compared to caprock units. Therefore, when drilling a well through the entire sedimentary succession, there is higher probability of intersecting fracture swarms in the Utica Shale than in overlying units. The Utica Shale is more calcareous than the clayey Lorraine Group shale (Globensky, 1987; Lavoie et al., 2008; Theriault, 2012) resulting in overall higher Brittleness Index (BI) values for the Utica

Shale than the overlying shale units (Séjourné, 2017). Brittle shale units are more likely to be affected by a dense natural fracture network than ductile shale (Ding et al., 2012; Lai et al., 2015).

### *5.1.2 Use of analogs to characterize the caprock*

The relationships between the three fracture sets (F1, F2 and F3) and the two regional fold generations was assessed by applying a fold test on shallow fractures. This analysis supports a syn- to post F-II folding origin for the F3 set. Conversely, the F1 and F2 fractures were probably developed before (or possibly during for F2) the main deformation/folding episodes that shaped-up the SLP (F-II and F-I folds). Therefore, the nowadays shallow structures should have been formed at depth before the removal of the overburden by erosion. The presence at reservoir depths of F3 fractures also discards their potential shallow formation after erosion.

Vitrinite reflectance data has shown that, at least regionally, around 5 km of overburden have been eroded in the SLP (Héroux and Bertrand, 1991; Yang and Hesse, 1993). At these depths, the fractures propagate according to the regional stress field orientation and thus display common orientations. Because shallow and deep fracture networks display common characteristics (especially in terms of fracture attitudes and spacing) and because of the burial history of the Saint-Édouard area, it is suggested that shallow fractures in shallow units were formed at depth and hence, had recorded the same tectonic events as fractures in deep units. Consequently, shallow and deep observations can be used to assess the fracture pattern in the intermediate zone.

No conclusion can be drawn regarding the initiating mechanism for fracture propagation. The latter could result from an increase of the greatest compressive stress during regional shortening, a decrease in the least compressive stress caused by regional extension, or an increase in pore pressure (which could also be associated with the first two mechanisms). It must be noted that an abnormal pore pressure related to the thermal maturation of organic matter is more likely to have occurred in the Lotbinière Formation, Les Fonds Formation and Utica Shale, as these units display higher organic content than the Lorraine Group units (Haeri-Ardakani et al., 2015; Lavoie et al., 2016). In the Lotbinière Formation, the crosscutting relationship between fractures and calcareous concretions indicated that some fractures could have been initiated in a context of abnormal pore pressure.

The use of analogs can be controversial if the regional geologic history is not well understood. The presence of shallow unloading fractures that display the same attitudes as some of the deep fractures is not discarded. Nonetheless, as a deep fracture dataset was available in the area, it was possible to infer that the density of possible shallow unloading fractures (developed under the control of either thermal-elastic contraction during uplift or erosion) is likely marginal, as fracture spacings are comparable in both shallow and deep intervals.

#### *5.1.3 Conceptual models*

In the Saint-Édouard area, the steeply-dipping fractures and BPF are assumed to be pervasive throughout the sedimentary succession, from the shallow aquifers to the gas reservoir (Utica Shale) and hence, throughout the intermediate zone. The F1 and F2 sets are orthogonal to each other and to the bedding planes. F1 fractures may be concentrated in corridors but this pattern remains to be confirmed. F1 and F2 fracture sets are also present in siltstone units and observations on outcrops showed that these sets are more homogeneously distributed in this unit (similar F1 and F2 spacing values). A third fracture set (F3) was observed in the Utica Shale and locally in the Lorraine Group, where these fractures are more sparsely distributed. A fourth set, corresponding to BPF, was only observed in shallow shale units within the upper 60 m of bedrock. The observation of BPF was easier at shallow depth because their aperture is enhanced in this interval, probably as a consequence of glaciations/de-glaciations events or de-compaction in a context of erosion and uplift. However, some BPF should exist at depth in the study area as in many other shale successions (Gale et al., 2015; Gale et al., 2016; Wang and Gale, 2016).

A conceptual model integrating all the elements acquired about the fracture pattern affecting the sedimentary succession of the Saint-Édouard area is proposed in Fig. 16. Schematics of the fracture network were developed using two scales to better represent their characteristics and features: the mesoscale (1 km blocks in Fig. 16a, b and c) and the metric (local) scale (Fig. 16d and e). The size of the metric scale blocks corresponds to the representative elementary volume (REV) of the fracture network that affects each lithological unit (shale or siltstone). A REV is defined as the minimum volume of sampling domains beyond which its characteristics remain constant (Bear, 1972). The REV properties could be used to further explore the hydraulic controls of this fracture network in numerical models with a Discrete Fracture Networks (DFN) approach. For stratabound fractures, such as those in the siltstone units, the size of the REV (a metric scale block) should be at least one or two times larger than the mean fracture spacing (Odling et al., 1999). Thus, for the highly fractured siltstone units, a REV of 0.5 m size can be defined (Fig. 16e). For non-stratabound systems, such as in the shale units, it is recommended to define a REV larger than the maximum mean trace length of fractures (Voeckler, 2012); in fact, a size at least three times larger than the mean trace is suggested (Oda, 1985, 1988). The approximate maximum mean fracture length observed in shale units is 5 m. For this reason, a 15 m long REV is proposed (Fig. 16d). However, due to the lack of large outcropping areas in the Saint-Édouard area, more fracture length measurements would be recommended in neighbouring areas for a finer estimation of the REV dimensions in shale units. It must be kept in mind that these REV are theoretical volumes that could not exist in the field due to the complexity and continuity of fluid flow circulation in the fracture network (Kulatilake and Panda, 2000; Neuman, 1988). However, in a context of low porosity and permeability rock in the SLP (BAPE 2010; Séjourné, 2015; Séjourné et al., 2013), fluid circulation can only be envisioned through open fractures and very little within the matrix. Therefore, the definition of a REV is simply a first step to better assess the control of fractures on fluid flow.

**Insert fig. 16 here.**

## 5.2 *Implications for the assessment of potential upward fluid migration*

### *5.2.1 Limits of the conceptual model*

In the Saint-Édouard area, the caprock and shale gas reservoir are affected by several fracture sets that are pervasive throughout the region and the entire stratigraphic succession. The experimental variograms showed that fractures are clustered and the parameters extracted from semi-variograms could be used for other studies to generate simulation of stochastic fracture networks fracture (in DFN models for example). Scale-dependant change in structure, such as the existence of fracture corridors, could not be identified using these variogram as this approach assumes that fracture spacing is a scale-independent continuous variable. As a consequence to further assess the heterogeneity of this fracture pattern, gains could be obtained by the use of parameters such as lacunarity which describes the scale-dependant changes in fracture patterns (Roy, 2013; Roy et al., 2014). For the specific case of the Saint-Édouard area, more field data would be necessary to rigorously document this entire range of heterogeneity. At regional scale, the progressive deepening of the platform to the southeast may also have had a control on small and large scale fracturing but it could not be confirmed with the existing datasets in the studied area.

In addition, the outcropping areas were limited in size and number and borehole data cannot provide any direct observation of fracture lengths. As a consequence, the vertical extension of fractures, and thus the vertical continuity of the fracture network between the deep gas reservoir and shallow aquifers cannot be undoubtedly determined solely based on the currently available structural datasets. This highlights the limits of using analogs when regarding to the potential existence of large-scale preferential fluid flow pathways in a sedimentary succession. However, the approach is particularly useful in fracture network characterisation studies, to make up for the frequent lack of data in some specific geological intervals.

#### *5.2.2 New insights for the assessment of potential upward fluid migration*

As direct observations of the vertical extent of structural discontinuities are challenged by the limits of the available datasets and methods, data from other fields should be acquired to assess the potential of upward fluid migration through the caprock. For instance, isotopic signatures of gas in both rock and groundwater would provide good indicators to identify a potential hydraulic connection between the deep reservoir and the surficial aquifers. In addition, the assessment of the geomechanical properties of the different units within the intermediate zone would provide evidence of the presence or absence of ductile strata that would control the fracture length. To further explore the hydraulic controls imposed by the presence of fractures and faults, one should also consider the four following points: 1) the role of individual fractures on fluid flow and especially their aperture throughout the stratigraphy; 2) the existence of open fractures associated with regional-scale structural discontinuities, such as fault damage zones; 3) the evaluation of hydraulic properties of these regional-scale features; 4) the driving mechanisms that would support upward fluid flow in these pathways (if any) throughout the entire stratigraphic succession (deep shale gas reservoir, intermediate zone and shallow aquifers).

## 6 Conclusion

The natural fracture pattern in both the shallow aquifers and the deep shale gas reservoir of the Saint-Édouard area was characterized using a combination of fracture data from outcrops and well logs (acoustic, optical and micro-resistivity). Three steeply-dipping fracture sets, as well as bedding-parallel fractures were documented. The three high-angle fracture sets are common to both shallow and deep units with similar characteristics such as fracture attitude and spacing. For this reason and based on the regional geologic history, these fracture sets could be used as analogs for those within the intermediate zone for which little to no data were available. These fracture sets are pervasive throughout the region, but they are heterogeneously distributed. Conceptual models of the fracture pattern were developed at metric to kilometric scales. Nonetheless, due to the limitations of the observation methods and the near absence of data for the intermediate zone, the vertical extension of natural fractures, which represents a critical parameter for aquifer vulnerability, still remains elusive. The comprehensive assessment of the caprock integrity should also be based on geomechanical properties of the different caprock units, on gas and groundwater geochemistry to provide evidence for potential upward migration and on the definition of potential hydraulic properties of fractures, fault planes and associated damage zones identified in the Saint-Édouard area, as well as their *in situ* hydrological conditions.

This paper highlighted the benefits of combining datasets from the shallow and deep intervals in fracture network characterization. It also pointed out the limitations of using analogs to assess the potential impacts of shale gas activities on shallow fresh groundwater. Even if these results are strictly valid for the Saint-Édouard area, the methodology used to characterize the fracture network in the caprock interval using geoscience data from the shallow and deep geological intervals could be used in other shale gas plays where lithologies are dominated by shale units. The approach could also be used in other fields, such as in geothermal energy or deep geological carbon sequestration projects, where the fracture pattern and the integrity of a rock mass relative to fluid flow must be assessed.

## Acknowledgments

This project was part of the Environmental Geoscience Program of Natural Resources Canada. It also benefited from funding from the Energy Sector through the Eco-EII and PERD programs. The authors wish to thank Talisman Energy (now Repsol Oil & Gas Canada) and especially Marianne Molgat, as well as Charles Lamontagne of the Ministère du Développement durable, de l'Environnement et de la Lutte contre les Changements climatiques (MDDELCC) du Québec for providing well logs data. The land owners are also thanked for the access to outcrops and drilling sites. Authors are very grateful to André Guy Tranquille Temgoua, Xavier Malet and Elena Konstantinovskaya for field support. Authors wish to thank Nicolas Pinet for his careful review of the manuscript and relevant comments. Erwan Gloaguen is also thanked for his helpful comments. This paper is GSC contribution 33012.

## References


Antonellini, M., Mollema, P.N., 2000. A natural analog for a fractured and faulted reservoir in dolomite: Triassic Sella Group, northern Italy. AAPG Bulletin 84, 314-344.

Bai, T., Pollard, D.D., 2000. Fracture spacing in layered rocks: a new explanation based on the stress transition. Journal of Structural Geology 22, 43-57.

Bai, T., Pollard, D.D., Gao, H., 2000. Explanation for fracture spacing in layered materials. Nature 403, 753-756.

BAPE, 2010. Comparaison des shales d’Utica et de Lorraine avec des shales en exploitation, Réponse de la l'APGQ aux questions de la Commission du BAPE sur les gaz de schiste. Available at: http://www.bape.gouv.qc.ca/sections/mandats/Gaz_de_schiste/documents/DB25%20tableau%20de%20shales.pdf (accessed february 2017). Bureau d’Audiences Publiques sur l’Environnement (BAPE) DB25.

Barton, A., Hickman, S., Morin, R., 1998. Reservoir-Scale fracture permeability in the Dixie Valley, Nevada, geolthermal field Twenty-Third Workshop on Geothermal Reservoir Engineering SGP-TR-158, 299-306.

Bear, J., 1972. Dynamics of fluids in porous media. Dover Publications, inc., New York.

Belt, E.S., Riva, J., Bussières, L., 1979. Revision and correlation of late Middle Ordovician stratigraphy northeast of Quebec City. Canadian Journal of Earth Sciences 16, 1467-1483.

Berkowitz, B., 2002. Characterizing flow and transport in fractured geological media: A review. Advances in Water Resources 25, 861-884.

Bonnet, E., Bour, O., Odling, N.E., Davy, P., Main, I., Cowie, P., Berkowitz, B., 2001. Scaling of fracture systems in geological media. Reviews of Geophysics - AGU 39, 3.

Caine, J.S., Tomusiak, S.R.A., 2003. Brittle structures and their role in controlling porosity and permeability in a complex Precambrian crystalline-rock aquifer system in the Colorado Rocky Mountain Front Range. Geological Society of America Bulletin 115, 1410-1424.

Castonguay, S., Dietrich, J., Lavoie, D., Laliberté, J.-Y., 2010. Structure and petroleum plays of the St. Lawrence Platform and Appalachians in southern Quebec: insights from interpretation of MRNQ seismic reflection data. Bulletin of Canadian Petroleum Geology 58, 219-234.

Castonguay, S., Dietrich, J., Shinduke, R., Laliberté, J.-Y., 2006. Nouveau regard sur l'architecture de la Plate-forme du Saint-Laurent et des Appalaches du sud du Québec par le retraitement des profils de sismique réflexion M-2001, M-2002 et M-2003. Commission géologique du Canada, Dossier Public 5328, 19.

Castonguay, S., Séjourné, S., Dietrich, J., 2003. The Appalachian structural front in southern Quebec: Seismic and field evidence for complex structures and a triangle zone at the edge of the foreland thrust belt:. First annual joint meeting of the Geological Society of America – Northeastern Section and the Atlantic Geoscience Society, Halifax 2003, On line: http://gsa.confex.com/gsa/2003NE/finalprogram/abstract_51232.htm.

Castonguay, S.b., Ruffet, G., Tremblay, A., F├⌐raud, G., 2001. Tectonometamorphic evolution of the Southern Quebec Appalachians: 40Ar/39 Ar evidence for Middle Ordovician crustal thickening and Silurian-Early Devonian exhumation of the internal Humber zone. 113, 144-160.

CCA, 2014. Environmental impacts of shale gas extraction in Canada. Available at http://www.scienceadvice.ca/uploads/eng/assessments%20and%20publications%20and%20news%20releases/shale%20gas/shalegas_fullreporten.pdf (accessed february 2017). Council of Canadian Academies (CCA), 292.

Chilès, J., 1988. Fractal and geostatistical methods for modeling of a fracture network. Mathematical Geology 20, 631-654.

Clark, T.H., Globensky, Y., 1973. Portneuf et parties de St-Raymond et de Lyster - Comtés de Portneuf et de Lotbinière. Ministère des Richesses Naturelles, Direction Générale des Mines, Rapport Géologique 148.

Clark, T.H., Globensky, Y., 1976. Région de Bécancour. 165.

Comeau, F.A., Kirkwood, D., Malo, M., Asselin, E., Bertrand, R., 2004. Taconian mélanges in the parautochthonous zone of the Quebec Appalachians revisited: implications for foreland basin and thrust belt evolution. Canadian Journal of Earth Sciences 41, 1473-1490.

Crow, H.L., Ladevèze, P., 2015. Downhole geophysical data collected in 11 boreholes near St.-Édouard-de-Lotbinière, Québec. Geological Survey of Canada, Open File 7768, 48.

Dershowitz, B., LaPointe, P., Eiben, T., Wei, L., 1998. Integration of Discrete Feature Network Methods with Conventional Simulator Approaches. Society of Petroleum Engineers SPE-49069-MS.

Dietrich, J., Lavoie, D., Hannigan, P., Pinet, N., Castonguay, S., Giles, P., Hamblin, A.P., 2011. Geological setting and resource potential of conventional petroleum plays in Paleozoic basins in eastern Canada. Bulletin of Canadian Petroleum Geology 59, 54-84.

Ding, W., Li, C., Li, C., Xu, C., Jiu, K., Zeng, W., Wu, L., 2012. Fracture development in shale and its relationship to gas accumulation. Geoscience Frontiers 3, 97-105.

Engelder, T., 1985. Loading paths to joint propagation during a tectonic cycle: an example from the Appalachian Plateau, U.S.A. Journal of Structural Geology 7, 459-476.

English, J.M., 2012. Thermomechanical origin of regional fracture systems. AAPG Bulletin 96, 1597-1625.

EPA, 2016. Hydraulic Fracturing for Oil and Gas: Impacts from the Hydraulic Fracturing Water Cycle on Drinking Water Resources in the United States (Final Report). Available at: www.epa.gov/hfstudy (accessed february 2017). U.S. Environmental Protection Agency (EPA), Washington, DC EPA/600/R-16/236F, 666.

Escuder Viruete, J., Carbonell, R., Jurado, M.J., Martí, D., Pérez-Estaún, A., 2001. Two-dimensional geostatistical modeling and prediction of the fracture system in the Albala Granitic Pluton, SW Iberian Massif, Spain. Journal of Structural Geology 23, 2011-2023.

Faure, S., Tremblay, A., Malo, M., 2004. Reconstruction of Taconian and Acadian paleostress regimes in the Quebec and northern New Brunswick Appalachians. Canadian Journal of Earth Sciences 41, 619-634.

Fiore Allwardt, P., Bellahsen, N., Pollard, D.D., 2007. Curvature and fracturing based on global positioning system data collected at Sheep Mountain anticline, Wyoming. Geosphere 3, 408-421.

Fisher, R., 1953. Dispersion on a Sphere. Proceedings of the Royal Society of London A: Mathematical, Physical and Engineering Sciences 217, 295-305.

Gale, J., Ukar, E., Elliott, S.J., Wang, Q., 2015. Bedding-Parallel Fractures in Shales: Characterization, Prediction and Importance, AAPG Annual Convention and Exhibition, Denver, CO., USA, May 31 - June 3, 2015.

Gale, J.F., Ukar, E., Wang, Q., Elliott, S.J., 2016. Bedding-Parallel Fractures in Shales, AAPG Annual Convention and Exhibition, Calgary, Alberta, Canada, June 22, 2016.

Gale, J.F.W., Laubach, S.E., Olson, J.E., Eichhubl, P., Fall, A., 2014. Natural fractures in shale: A review and new observations. AAPG Bulletin 98, 2165-2216.

Gillespie, P.A., Walsh, J.J., Watterson, J., Bonson, C.G., Manzocchi, T., 2001. Scaling relationships of joint and vein arrays from The Burren, Co. Clare, Ireland. Journal of Structural Geology 23, 183-201.

Globensky, Y., 1987. Géologie des Basses Terres du Saint-Laurent. Direction Générale de l'Exploration Géologique et minérale du Québec, Gouvernement du Québec MM 85-02.

Glorioso, J.C., Rattia, A., 2012. Unconventional reservoirs: Basic petrophysical concepts for shale gas, SPE/EAGE European Unconventional Resources Conference & Exhibition-From Potential to Production. SPE, Vienna, Austria.

Grieser, W.V., Bray, J.M., 2007. Identification of Production Potential in Unconventional Reservoirs, Production and Operations Symposium. Society of Petroleum Engineers, Oklahoma City, Oklahoma, U.S.A. .

Gross, M.R., 1993. The origin and spacing of cross joints: examples from the Monterey Formation, Santa Barbara Coastline, California. Journal of Structural Geology 15, 737-751.

Guerriero, V., Mazzoli, S., Iannace, A., Vitale, S., Carravetta, A., Strauss, C., 2013. A permeability model for naturally fractured carbonate reservoirs. Marine and Petroleum Geology 40, 115-134.

Haeri-Ardakani, O., Sanei, H., Lavoie, D., Chen, Z., Jiang, C., 2015. Geochemical and petrographic characterization of the Upper Ordovician Utica Shale, southern Quebec, Canada. International Journal of Coal Geology 138, 83-94.

Hamblin, A.P., 2006. The "Shale Gas" concept in Canada: a preliminary inventory of possibilities. Geological Survey of Canada, Open File 5389, 103.

Heidbach, O., Tingay, M., Barth, A., Reinecker, J., Kurfeß, D., Müller, B., 2009. The World Stress Map, in: 2008, S.E.b.o.t.W.d.r. (Ed.). Helmholtz Centre Potsdam - GFZ German Research Centre for Geosciences, Commission de la Carte Géologique du Monde / Commission for the Geological Map of the World.

Héroux, Y., Bertrand, R., 1991. Maturation thermique de la matière organique dans un bassin du Paléozoïque inférieur, Basses-Terres du Saint-Laurent, Québec, Canada. Canadian Journal of Earth Sciences 28, 1019-1030.

Ji, S., Saruwatari, K., 1998. A revised model for the relationship between joint spacing and layer thickness. Journal of Structural Geology 20, 1495-1508.

Konstantinovskaya, E., Malo, M., Castillo, D.A., 2012. Present-day stress analysis of the St. Lawrence Lowlands sedimentary basin (Canada) and implications for caprock integrity during CO2 injection operations. Tectonophysics 518-521, 119-137.

Konstantinovskaya, E., Rodriguez, D., Kirkwood, D., Harris, L., Thériault, R., 2009. Effects of basement structure, sedimentation and erosion on thrust wedge geometry: an example from the Quebec Appalachians and analogue models. Bulletin of Canadian Petroleum Geology 57, 34-62.

Kulatilake, P.H.S.W., Panda, B.B., 2000. Effect of Block Size and Joint Geometry on Jointed Rock Hydraulics and REV. Journal of Engineering Mechanics 126.

Ladeira, F.L., Price, N.J., 1981. Relationship between fracture spacing and bed thickness. Journal of Structural Geology 3, 179-183.

Lai, J., Wang, G., Huang, L., Li, W., Ran, Y., Wang, D., Zhou, Z., Chen, J., 2015. Brittleness index estimation in a tight shaly sandstone reservoir using well logs. Journal of Natural Gas Science and Engineering 27, Part 3, 1536-1545.

Larsen, B., Grunnaleite, I., Gudmundsson, A., 2010. How fracture systems affect permeability development in shallow-water carbonate rocks: An example from the Gargano Peninsula, Italy. Journal of Structural Geology 32, 1212-1230.

Laubach, S.E., Olson, J.E., Gross, M.R., 2009. Mechanical and fracture stratigraphy. AAPG Bulletin 93, 1413-1426.

Lavenu, A.P., Lamarche, J., Gallois, A., Gauthier, B.D., 2013. Tectonic versus diagenetic origin of fractures in a naturally fractured carbonate reservoir analog (Nerthe anticline, southeastern France). AAPG Bulletin 97, 2207-2232.

Lavoie, D., 2008. Chapter 3 Appalachian Foreland Basin of Canada, in: Andrew, D.M. (Ed.), Sedimentary Basins of the World. Elsevier, pp. 65-103.

Lavoie, D., Desrochers, A., Dix, G., Knight, I., Salad Hersi, O., 2012. The Great American Carbonate Bank in Eastern Canada: An Overview. In: Derby, J.R., Fritz, R.D., Longacre, S.A., Morgan, W.A., Sternbach, C.A. (Eds.), The Great American Carbonate Bank. The Geology and Economic Resources of the Cambrian–Ordovician Sauk Megasequence of Laurentia. AAPG Memoirs 98, 499-523.

Lavoie, D., Hamblin, A.P., Theriault, R., Beaulieu, J., Kirkwood, D., 2008. The Upper Ordovician Utica Shales and Lorraine Group flysch in southern Québec: Tectonostratigraphic setting and significance for unconventional gas. Commission géologique du Canada, Open File 5900, 56.

Lavoie, D., Pinet, N., Bordeleau, G., Ardakani, O.H., Ladevèze, P., Duchesne, M.J., Rivard, C., Mort, A., Brake, V., Sanei, H., Malet, X., 2016. The Upper Ordovician black shales of southern Quebec (Canada) and their significance for naturally occurring hydrocarbons in shallow groundwater. International Journal of Coal Geology 158, 44-64.

Lavoie, D., Rivard, C., Lefebvre, R., Séjourné, S., Thériault, R., Duchesne, M.J., Ahad, J.M.E., Wang, B., Benoit, N., Lamontagne, C., 2014. The Utica Shale and gas play in southern Quebec: Geological and hydrogeological syntheses and methodological approaches to groundwater risk evaluation. International Journal of Coal Geology 126, 77-91.

Lefebvre, R., 2016. Mechanisms leading to potential impacts of shale gas development on groundwater quality. Wiley Interdisciplinary Reviews: Water, n/a-n/a.

McConaughy, D.T., Engelder, T., 1999. Joint interaction with embedded concretions: joint loading configurations inferred from propagation paths. Journal of Structural Geology 21, 1637-1652.

Meng, F., Zhou, H., Zhang, C., Xu, R., Lu, J., 2015. Evaluation Methodology of Brittleness of Rock Based on Post-Peak Stress–Strain Curves. Rock Mech Rock Eng 48, 1787-1805.

Miller, S.M., 1979. Determination of spatial dependence in fracture set characteristics by geostatistical methods, Department of mining and geological engineering. The University of Arizona, p. 122.

Min, K.-B., Jing, L., Stephansson, O., 2004. Determining the equivalent permeability tensor for fractured rock masses using a stochastic REV approach: Method and application to the field data from Sellafield, UK. Hydrogeology Journal 12, 497-510.

Mozley, P.S., Davis, J.M., 2005. Internal structure and mode of growth of elongate calcite concretions: Evidence for small-scale, microbially induced, chemical heterogeneity in groundwater. Geological Society of America Bulletin 117, 1400-1412.

Narr, W., Schechter, D.W., Thompson, L.B., 2006. Naturally fractured reservoir characterization. Richardson, TX: Society of Petroleum Engineers.

Narr, W., Suppe, J., 1991. Joint spacing in sedimentary rocks. Journal of Structural Geology 13, 1037-1048.

Neuman, S.P., 1988. Stochastic Continuum Representation of Fractured Rock Permeability as an Alternative to the REV and Fracture Network Concepts, in: Custodio, E., Gurgui, A., Ferreira, J.P.L. (Eds.), Groundwater Flow and Quality Modelling. Springer Netherlands, Dordrecht, pp. 331-362.

Oda, M., 1985. Permeability tensor for discontinuous rock masses. Geotechnique 35, 483-495.

Oda, M., 1988. A method for evaluating the representative elementary volume based on joint survey of rock masses. Canadian Geotechnical Journal 25, 440-447.

Odling, N.E., Gillespie, P., Bourgine, B., Castaing, C., Chiles, J.P., Christensen, N.P., Fillion, E., Genter, A., Olsen, C., Thrane, L., Trice, R., Aarseth, E., Walsh, J.J., Watterson, J., 1999. Variations in fracture system geometry and their implications for fluid flow in fractures hydrocarbon reservoirs. Petroleum Geoscience 5, 373-384.

Ogunyomi, O., Hesse, R., Heroux, Y., 1980. Pre-Orogenic and Synorogenic Diagenesis and Anchimetamorphism in Lower Paleozoic Continental Margin Sequences of the Northern Appalachians in and Around Quebec City, Canada. Bulletin of Canadian Petroleum Geology 28, 559-577.

Park, H.J., West, T.R., 2002. Sampling bias of discontinuity orientation caused by linear sampling technique. Engineering Geology 66, 99-110.

Pinet, N., 2011. Deformation in the Utica Shale and Lorraine Group, Saint Lawrence Lowlands, Québec. Geological Survey of Canada, Open File 6952, 12.

Pinet, N., Duchesne, M., Lavoie, D., Bolduc, A.e., Long, B., 2008. Surface and subsurface signatures of gas seepage in the St. Lawrence Estuary (Canada): Significance to hydrocarbon exploration. Marine and Petroleum Geology 25, 271-288.

Pinet, N., Lavoie, D., Keating, P., Duchesne, M., 2014. The St Lawrence Platform and Appalachian deformation front in the St Lawrence Estuary and adjacent areas (Quebec, Canada): structural complexity revealed by magnetic and seismic imaging. Geological Magazine 151, 996-1012.

Rivard, C., Lavoie, D., Lefebvre, R., Séjourné, S., Lamontagne, C., Duchesne, M., 2014. An overview of Canadian shale gas production and environmental concerns. International Journal of Coal Geology 126, 64-76.

Roy, A., 2013. Scale-dependent heterogeneity in fracture data sets and grayscale images. The University of Tennesee.

Roy, A., Perfect, E., Dunne, W.M., McKay, L.D., 2014. A technique for revealing scale-dependent patterns in fracture spacing data. Journal of Geophysical Research: Solid Earth 119, 5979-5986.

Sasseville, C., Clauer, N., Tremblay, A., 2012. Timing of fault reactivation in the upper crust of the St. Lawrence rift system, Canada, by K–Ar dating of illite-rich fault rocks1. Canadian Journal of Earth Sciences 49, 637-652.

Sasseville, C., Tremblay, A., Clauer, N., Liewig, N., 2008. K–Ar age constraints on the evolution of polydeformed fold–thrust belts: The case of the Northern Appalachians (southern Quebec). Journal of Geodynamics 45, 99-119.

Séjourné, S., 2015. Caractérisation des réseaux de fractures naturelles, de la porosité et de la saturation en eau du Shale d'Utica et de sa couverture par l'analyse des diagraphies de forages pétroliers dans la région de Saint-Édouard, Québec. Commission Géologique du Canada, Dossier Public 7980, 60.

Séjourné, S., 2017. Étude géomécanique du Shale d'Utica et de sa couverture d'après les puits pétroliers et gaziers de la région de Saint-Édouard-de-Lotbinière, Québec. Commission Géologique du Canada, Dossier Public 8196, 54.

Séjourné, S., Dietrich, J., Malo, M., 2003. Seismic characterization of the structural front of southern Quebec Appalachians. Bulletin of Canadian Petroleum Geology 51, 29-44.

Séjourné, S., Lefebvre, R., Malet, X., Lavoie, D., 2013. Synthèse géologique et hydrogéologique du Shale d'Utica et des unités sus-jacentes (Lorraine, Queenston et dépots meubles), Basses-Terres du Saint-Laurent, Québec. Commission Géologique du Canada, Dossier Public 7338, 165.

Sikander, A., Pittion, J., 1978. Reflectance studies on organic matter in lower Paleozoic sediments of Quebec. Bulletin of Canadian Petroleum Geology 26, 132-151.

Singhal, B.B.S., Gupta, R.P., 2010. Applied Hydrogeology of Fractured Rocks. Springer Netherlands.

St-Julien, P., Hubert, C., 1975. Evolution of the Taconian orogen in the Quebec Appalachians. American Journal of Science 275-A, 337-362.

St-Julien, P., Slivitsky, A., Feininger, T., 1983. A deep structural profile across the Appalachians of southern Quebec. Geological Society of America Memoirs 158, 103-112.

Stesky, M., 2010. Pangea Scientific - Spheristat Version 3.1 - User's Manual.

Surrette, M., Allen, D.M., Journeay, M., 2008. Regional evaluation of hydraulic properties in variably fractured rock using a hydrostructural domain approach. Hydrogeology Journal 16, 11-30.

Tavchandjian, O., Rouleau, A., Archambault, G., Daigneault, R., Marcotte, D., 1997. Geostatistical analysis of fractures in shear zones in the Chibougamau area: applications to structural geology. Tectonophysics 269, 51-63.

Terzaghi, R.D., 1965. Sources of error in joint surveys. Geotechnique 15 (3), 287-304.

Theriault, R., 2012. Caractérisation du Shale d'Utica et du Groupe de Lorraine, Basses-Terres du Saint-Laurent - Partie 2 : Interprétation Géologique, in: Québec, M.d.R.N.e.F. (Ed.), p. 80.

Thériault, R., 2007. Trenton/Black River Hydrothermal Dolomite Reservoirs in Québec: The Emergence of a New and Highly Promising Play along the St. Lawrence Platform. American Association of Petroleum Geologists. Eastern Section Annual Meeting, Abstract with Programs 57.

Tremblay, A., Pinet, N., 2016. Late Neoproterozoic to Permian tectonic evolution of the Quebec Appalachians, Canada. Earth-Science Reviews 160, 131-170.

Tremblay, A., Roden-Tice, M.K., Brandt, J.A., Megan, T.W., 2013. Mesozoic fault reactivation along the St. Lawrence rift system, eastern Canada: Thermochronologic evidence from apatite fission-track dating. Geological Society of America Bulletin 125, 794-810.

Valley, B.C., 2007. The relation between natural fracturing and stress heterogeneities in deep-seated crystalline rocks at Soultz-sous-Forêts (France). Swiss Federal Institute of Technology (ETH), Zurich, p. 277.

Villaescusa, E., Brown, E.T., 1990. Characterizing joint spatial correlations using geostatistical methods, in: C. A. Barton and O. Stephansson, B. (Ed.), Rock Joints.

Vitale, S., Dati, F., Mazzoli, S., Ciarcia, S., Guerriero, V., Iannace, A., 2012. Modes and timing of fracture network development in poly-deformed carbonate reservoir analogues, Mt. Chianello, southern Italy. Journal of Structural Geology 37, 223-235.

Voeckler, H., 2012. Modeling deep groundwater flow throught fractured bedrock in a mountainous headwater catchment using a coupled surface water-groundwater model, Okanagan basin, British Columbia. The University of British Columbia, Vancouver, p. 433.

Wang, D., Ge, H., Wang, X., Wang, J., Meng, F., Suo, Y., Han, P., 2015. A novel experimental approach for fracability evaluation in tight-gas reservoirs. Journal of Natural Gas Science and Engineering 23, 239-249.

Wang, Q., Gale, J.F., 2016. Characterizing Bedding-Parallel Fractures in Shale: Aperture-Size Distributions and Spatial Organization, AAPG Annual Convention and Exhibition, Calgary, Alberta, Canada, June 22, 2016.

Wu, H., D. Pollard, D., 1995. An experimental study of the relationship between joint spacing and layer thickness. Journal of Structural Geology 17, 887-905.

Yang, C., Hesse, R., 1993. Diagenesis and anchimetamorphism in an overthrust belt, external domain of the Taconian Orogen, southern Canadian Applachians-II. Paleogeothermal gradients derived from maturation of different types of organic matter. Organic Geochemistry 20, 381-403.

Zoback, M.L., 1992. First- and second-order patterns of stress in the lithosphere: The World Stress Map Project. Journal of Geophysical Research: Solid Earth 97, 11703-11728.

Table 1. List of measurement stations

Fig. 1. The Saint-Édouard area location and its geological context: a. location of the St. Lawrence Platform; b. geological framework of the St. Lawrence Platform (modified from Globensky (1987)); c. geological map of the Saint-Édouard area (Clark and Globensky, 1973; Globensky, 1987; Lavoie et al., 2016; Thériault and Beauséjour, 2012). Faults represented as dashed lines indicate interpreted shallow faults projected from seismic data. J.-C. River fault: Jacques-Cartier River fault; C.-F. syncline: Chambly-Fortierville syncline ; Gp. : Group ; Fm. : Formation.

Fig. 2. Stratigraphy of the Saint-Édouard area units (modified from Konstantinovskaya et al. (2014). Gp. : Group ; Fm. : Formation.

Fig. 3. Tectonic calendar recorded in the studied area, modified from Lavoie (2008).

Fig. 4. Stereographic projection (lower hemisphere Schmidt stereodiagram) of the bedding plane attitudes measured  in the autochthonous (a.) and parautochthonous (b.) domains. Each pole corresponds to the mean bedding plane attitude measured on each outcrop and shallow well in the Saint-Édouard area. C.F. syncline: Chambly-Fortierville syncline; n: number of measurement sites (outcrops or wells).

Fig. 5. Cross-section in the Saint-Édouard area (see Fig. 1 for location). Interpretation proposed by Lavoie et al. (2016) and based on industrial seismic data. Gp: Group.

Fig. 6. Examples of fracture observations on outcropping shales: a. and b. Fracture sets 1 and 2 abutting relationships in the outcropping Lorraine Group (a; site 10) and Les Fonds Formations (b; site 17). The gray dots highlight the abutting relationships between fracture sets; d. example of a fracture that abuts a calcareous concretion at site 6.

Fig. 7. Attitudes of the fracture sets identified in wells and outcrops intersecting shales in the Saint-Édouard area. The mean fracture sets and bedding planes attitudes estimated for each station are compiled in the "synthesis" stereonets. Fracture and bedding planes poles are plotted in a lower hemisphere Schmidt representation. For outcrop data, contoured densities are not significant as they vary with the number of features measured in each outcrop (a function of the outcrop and well dimensions); densities were corrected for the sampling bias in borehole data. J.-C.: Jacques-Cartier; C.-F.: Chambly-Fortierville; n: number of fractures for each outcrop/well; L: length of the well section logged;

Fig. 8. Fracture attitudes variations during the fold test. The fracture data used in the analysis comes from outcrops 5 & 7 to 16 (autochthonous) and from outcrop 17 and wells #10, 11 and 13 (parautochthonous). Fault and fold axis locations presented in the maps were initially described in Clark and Globensky (1973) and Pinet (2011). F-I and F-II: first and second generations folds. Two folds generations were identified in the autochthonous domain and one folding event was

identified in the parautochthonous domain. The parameter k quantifies the degree of data concentration (higher values correspond to highly concentrated data).

Fig. 9. Fracture spacing measured on outcrops of the Lorraine Group shale (15 sites) and in three deep well horizontal legs located in the Utica Shale. The box plot diagrams show, from right to left, maximum, upper quartile (75th percentile), median value, lower quartile (25th percentile) and minimum fracture spacing for the F1, F2 and F3 fracture sets.

Fig. 10. Fracture spacing distributions from outcrops and deep wells. The number of F3 fracture spacings measured in outcrops was insufficient to present meaningful results.

Fig. 11. Experimental variograms for spacing of fractures with respect to the distance lag h along the horizontal legs of the deep wells (Utica Shale). A moving average curve was added for a better identification of the trends in the calculated variograms. The horizontal line corresponds to the variance of the entire fracture spacing sample. This representation highlights the limit beyond which fracture spacing is not correlated (range) for F1, F2 and F3.

Fig. 12. Fracture densities in the horizontal leg of the deep shale gas well A (Utica Shale). Fracture frequencies were calculated using a 20 m window length every 5 m.

Fig. 13. Fracture density and rock brittleness at depth: a. example of fracture density variation with depth in the deep vertical well B. Fracture densities were calculated using a 5 m window

length every 1 m and the values were corrected for sampling bias; b: mineralogical and acoustic Brittleness Index variations with depth (data from Séjourné (2017)).

Fig. 14. Examples of fractures affecting siltstone beds (a and c: site 9; b: top view of the outcrop at site 11). The gray dots highlight the abutting relationships between fracture sets.

Fig. 15. Geometrical characteristics of fractures in siltstone units: a. Examples of fracture attitudes measured in siltstone outcrops at sites 9 and 11; b. Linear relationship between fracture spacing and siltstone bed thickness (data from outcrops 1, 6, 13 & 19); the term ratio in the plots corresponds to the fracture spacing to layer thickness ratio; the location of sites is shown in Fig. 1.

Fig. 16. Conceptual models of the fracture patterns: a. caprock units of the autochthonous domain; b. caprock units of the parautochthonous domain; c. deep shale gas reservoir. In a. and b., the shallow aquifers are not specifically represented because they are affected by the same fracture network than the caprock units. The fracture network is also represented at a smaller scale in REVs: d. shale units; e. siltstone interbeds.

| Measurement station | ID | UTM coordinates (NAD83 19N) | | | Lithology | Group | Number of fractures | Outcrop size (approxima-tivelly) / borehole lenght in the bedrock (m) | Outcrop or well direction (°N) |
|---|---|---|---|---|---|---|---|---|---|
| | | X (m) | Y (m) | UTM Zone | | | | | |
| Outcrop (river bed) | 1 | 263815 | 5151764 | 19T | Shale | Queenston | 33 | 60 | 90 |
| Outcrop (river bed) | 2 | 263877 | 5152879 | 19T | Shale | Lorraine | 49 | 50 | 120 |
| Outcrop (river bed) | 3 | 270891 | 5161970 | 19T | Shale | Lorraine | 5 | 10 | 10 |
| Outcrop (river bed) | 4 | 272323 | 5160028 | 19T | Shale | Lorraine | 45 | 15 | 340 |
| Outcrop (river bed) | 5 | 279520 | 5159255 | 19T | Shale | Lorraine | 22 | 20 | 90 |
| Outcrop (river bed) | 6 | 278734 | 5169518 | 19T | Shale | Sainte-Rosalie | 126 | 4 x 20 | 44; 120; 150; 160 |
| Outcrop (river bed) | 7 | 285270 | 5166177 | 19T | Shale | Lorraine | 29 | 60 | 160 |
| Outcrop (river bed) | 8 | 289280 | 5167441 | 19T | Shale | Lorraine | 29 | 15 | 10 |
| Outcrop (vertical wall) | 9 | 290718 | 5167411 | 19T | Siltstones | Lorraine | 18 | 20 | 40 |
| Outcrop (river bed) | 10 | 290937 | 5167320 | 19T | Shale | Lorraine | 35 | 50 | 160 |
| Outcrop (vertical wall) | 11 | 291434 | 5167412 | 19T | Siltstones | Lorraine | 28 | 150 | 90 |
| Outcrop (vertical wall) | 12 | 294107 | 5167496 | 19T | Shale | Lorraine | 13 | 20 | 70 |
| Outcrop (vertical wall) | 13 | 294715 | 5167631 | 19T | Shale | Lorraine | 46 | 20 | 70 |
| Outcrop (vertical wall) | 14 | 294989 | 5167677 | 19T | Shale | Lorraine | 7 | 20 | 70 |
| Outcrop (river bed) | 15 | 296619 | 5167487 | 19T | Shale | Lorraine | 12 | 10 | 0 |
| Outcrop (river bed) | 16 | 296866 | 5168006 | 19T | Shale | Lorraine | 17 | 50 | 140 |
| Outcrop (river bed) | 17 | 299783 | 5169320 | 19T | Shale | Sainte-Rosalie | 120 | 2 x 20 | 130; 30 |
| Shallow well | 1 | 281370 | 5168963 | 19T | Shale | Sainte-Rosalie | 10 | 47 | vertical |
| Shallow well | 2 | 287925 | 5155391 | 19T | Shale | Sainte-Rosalie | 42 | 46 | vertical |
| Shallow well | 3 | 282584 | 5158820 | 19T | Shale & Siltstone | Lorraine | 50 | 30 | vertical |
| Shallow well | 4 | 288214 | 5157504 | 19T | Shale | Sainte-Rosalie | 39 | 20 | vertical |
| Shallow well | 7 | 276263 | 5164099 | 19T | Shale | Lorraine | 19 | 40 | vertical |
| Shallow well | 8 | 277620 | 5162758 | 19T | Shale & Siltstone | Lorraine | 49 | 50 | vertical |
| Shallow well | 10 | 286450 | 5157073 | 19T | Shale | Sainte-Rosalie | 25 | 15 | vertical |
| Shallow well | 11 | 286396 | 5156776 | 19T | Shale | Sainte-Rosalie | 19 | 50 | vertical |
| Shallow well | 13 | 286807 | 5156653 | 19T | Shale | Sainte-Rosalie | 2 | 59 | vertical |
| Shallow well | 21 | 287026 | 5156377 | 19T | Shale | Sainte-Rosalie | 52 | 148 | vertical |
| Deep well | A | 280035 | 5154051 | 19T | Shale | Sainte-Rosalie | 96 | 424 | vertical |
| Deep well | B | 269837 | 5152004 | 19T | Shale | Sainte-Rosalie | 1354 | 1758 | vertical |
| Deep well | C | 707892 | 5133892 | 18T | Shale | Sainte-Rosalie | 812 | 1165 | vertical |
| Deep well | A | 280035 | 5154051 | 19T | Shale | Lorraine | 56 | 195 | vertical |
| Deep well | B | 269837 | 5152004 | 19T | Shale | Lorraine | 1325 | 255 | vertical |
| Deep well | C | 707892 | 5133892 | 18T | Shale | Lorraine | 588 | 275 | vertical |
| Horizontal well | A | 280035 | 5154051 | 19T | Shale | Lorraine | 2085 | 1020 | 316 |
| Horizontal well | B | 269837 | 5152004 | 19T | Shale | Lorraine | 3254 | 600 | 316 |
| Horizontal well | C | 707892 | 5133892 | 18T | Shale | Lorraine | 1986 | 950 | 307 |

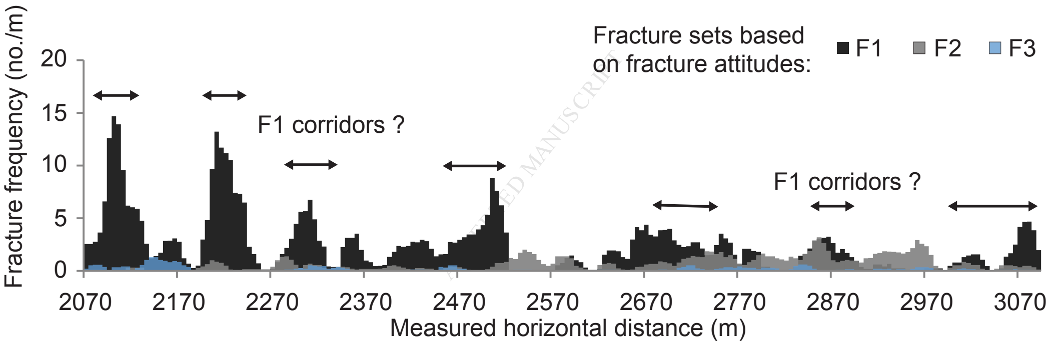

Fracture frequency (no./m)
20
15
10
5
0
Fracture sets based on fracture attitudes:
F1
F2
F3
F1 corridors ?
F1 corridors ?
2070
2170
2270
2370
2470
2570
2670
2770
2870
2970
3070
Measured horizontal distance (m)

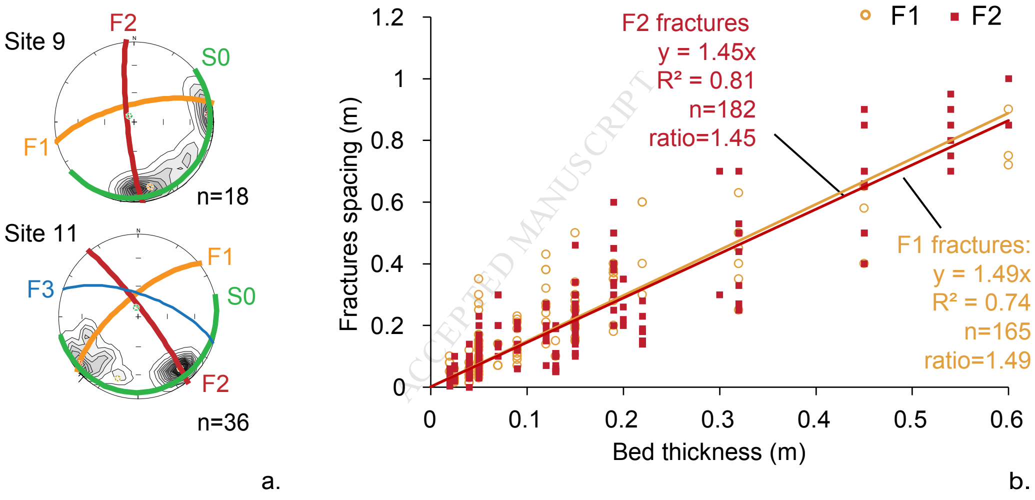

Site 9
F2
S0
F1
n=18
Site 11
F1
F3
S0
F2
n=36
a.
F1
F2
F2 fractures
y = 1.45x
R² = 0.81
n=182
ratio=1.45
F1 fractures:
y = 1.49x
R² = 0.74
n=165
ratio=1.49
Fractures spacing (m)
Bed thickness (m)
0
0.2
0.4
0.6
0.8
1
1.2
0
0.1
0.2
0.3
0.4
0.5
0.6
b.

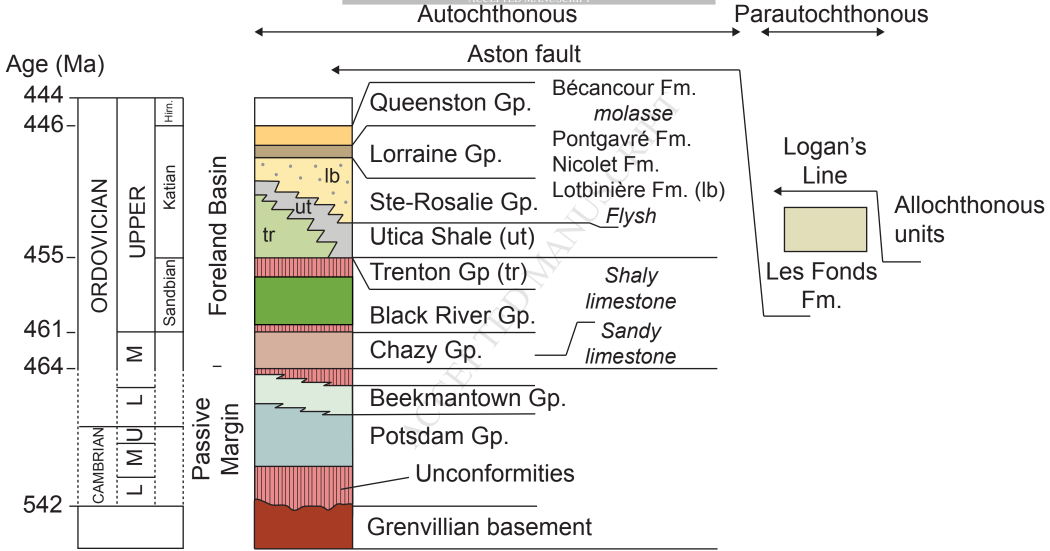

Autochthonous
Parautochthonous
Aston fault
Age (Ma)
444
446
455
461
464
542
ORDOVICIAN
CAMBRIAN
UPPER
M
L
U
M
L
Hirn.
Katian
Sandbian
Foreland Basin
Passive Margin
lb
ut
tr
Queenston Gp.
Lorraine Gp.
Ste-Rosalie Gp.
Utica Shale (ut)
Trenton Gp (tr)
Black River Gp.
Chazy Gp.
Beekmantown Gp.
Potsdam Gp.
Unconformities
Grenvillian basement
Bécancour Fm.
molasse
Pontgavré Fm.
Nicolet Fm.
Lotbinière Fm. (lb)
Flysh
Shaly limestone
Sandy limestone
Logan's Line
Allochthonous units
Les Fonds Fm.

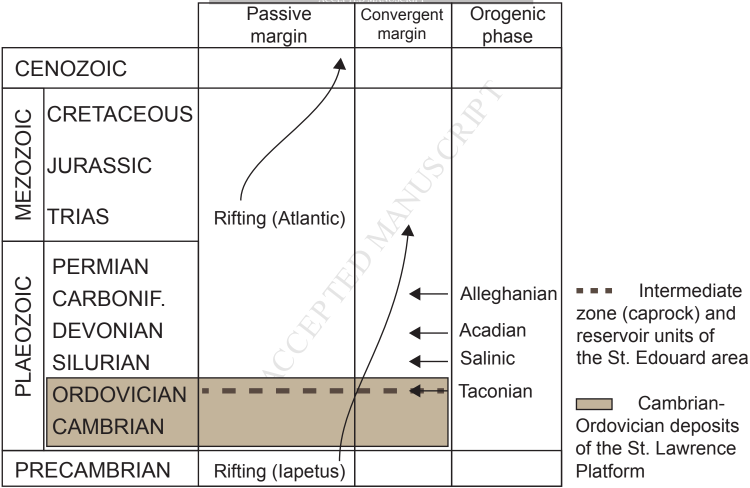

Passive margin
Convergent margin
Orogenic phase
CENOZOIC
MEZOZOIC
CRETACEOUS
JURASSIC
TRIAS
Rifting (Atlantic)
PLAEOZOIC
PERMIAN
CARBONIF.
DEVONIAN
SILURIAN
ORDOVICIAN
CAMBRIAN
Alleghanian
Acadian
Salinic
Taconian
PRECAMBRIAN
Rifting (Iapetus)
Intermediate zone (caprock) and reservoir units of the St. Edouard area
Cambrian-Ordovician deposits of the St. Lawrence Platform

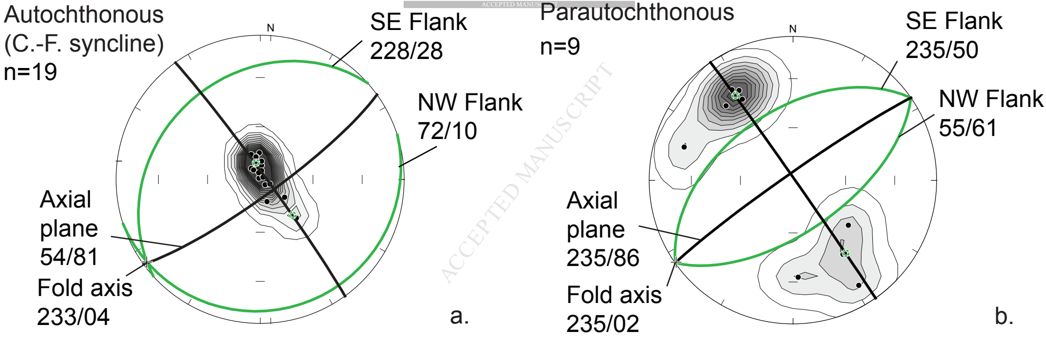
Autochthonous
(C.-F. syncline)
n=19
N
SE Flank
228/28
NW Flank
72/10
Axial
plane
54/81
Fold axis
233/04
a.
Parautochthonous
n=9
N
SE Flank
235/50
NW Flank
55/61
Axial
plane
235/86
Fold axis
235/02
b.

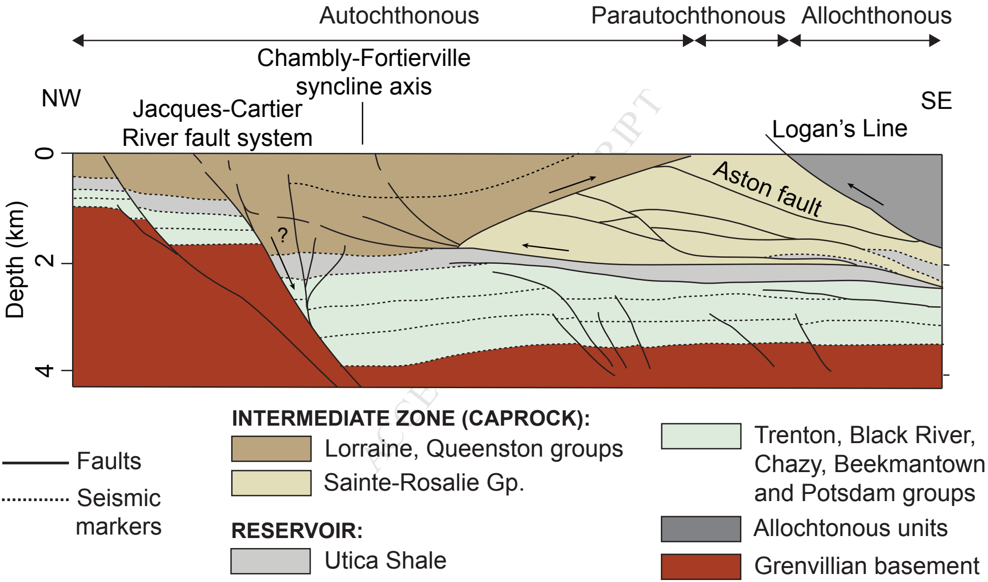
Autochthonous
Parautochthonous
Allochthonous
Chambly-Fortierville
syncline axis
NW
SE
Jacques-Cartier
River fault system
Logan's Line
Aston fault
?
Depth (km)
0
2
4
INTERMEDIATE ZONE (CAPROCK):
Lorraine, Queenston groups
Sainte-Rosalie Gp.
RESERVOIR:
Utica Shale
Faults
Seismic
markers
Trenton, Black River,
Chazy, Beekmantown
and Potsdam groups
Allochtonous units
Grenvillian basement

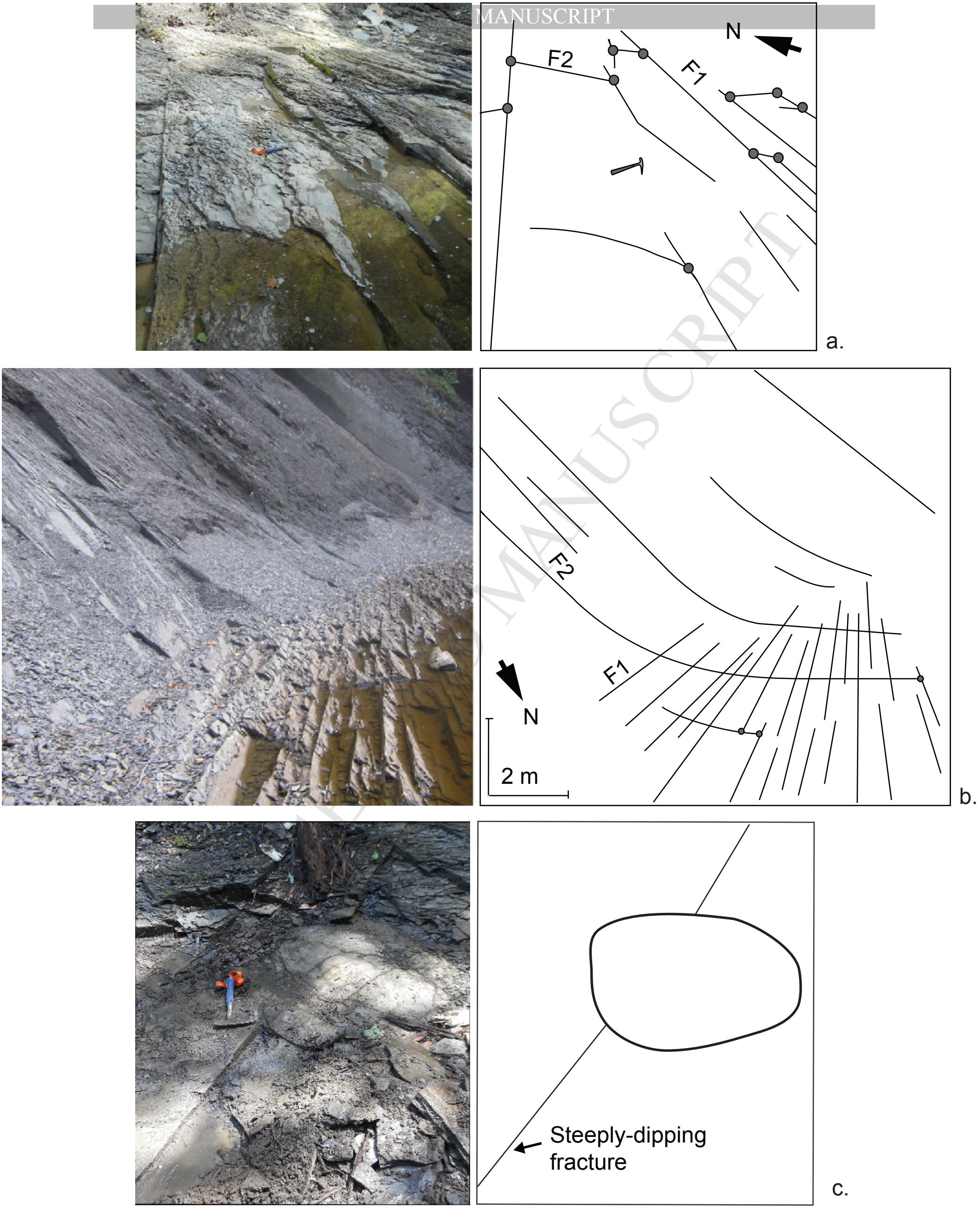
N
F2
F1
a.
F2
F1
N
2 m
b.
Steeply-dipping
fracture
c.

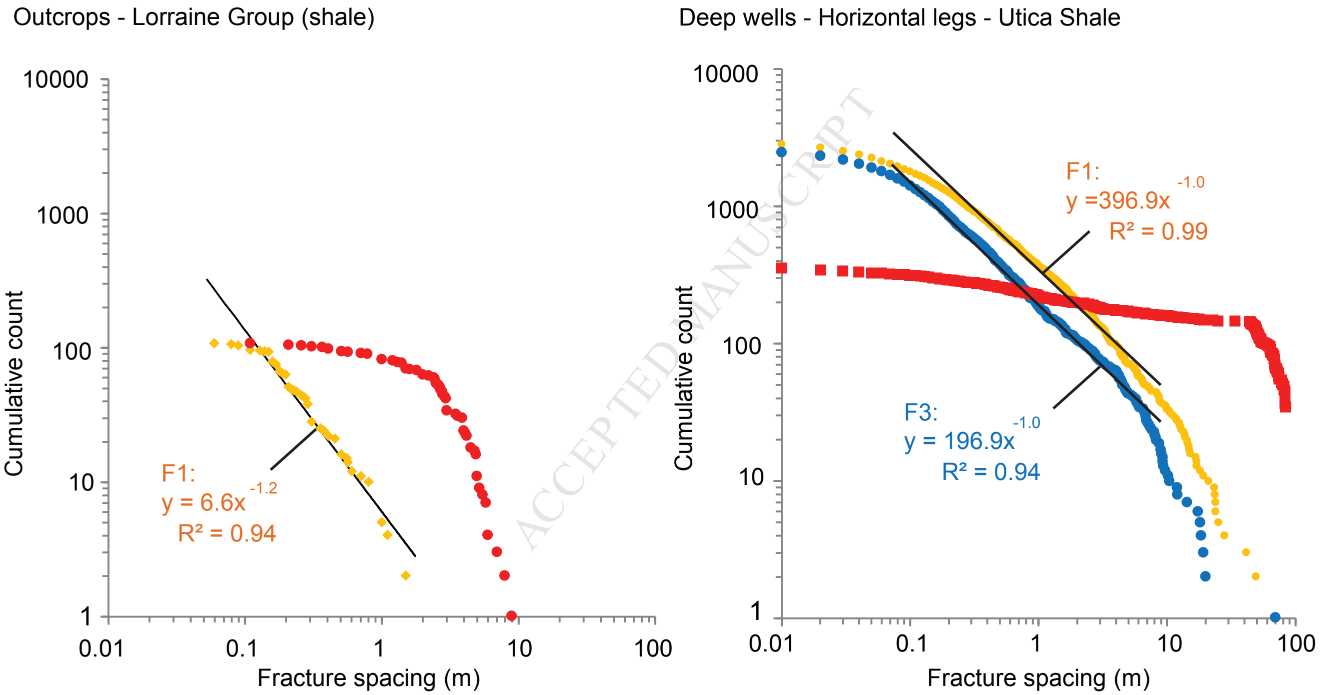
Outcrops - Lorraine Group (shale)
Cumulative count
10000
1000
100
10
1
0.01
0.1
1
10
100
Fracture spacing (m)
F1:
y = 6.6x-1.2
R² = 0.94
Deep wells - Horizontal legs - Utica Shale
Cumulative count
10000
1000
100
10
1
0.01
0.1
1
10
100
Fracture spacing (m)
F1:
y =396.9x-1.0
R² = 0.99
F3:
y = 196.9x-1.0
R² = 0.94

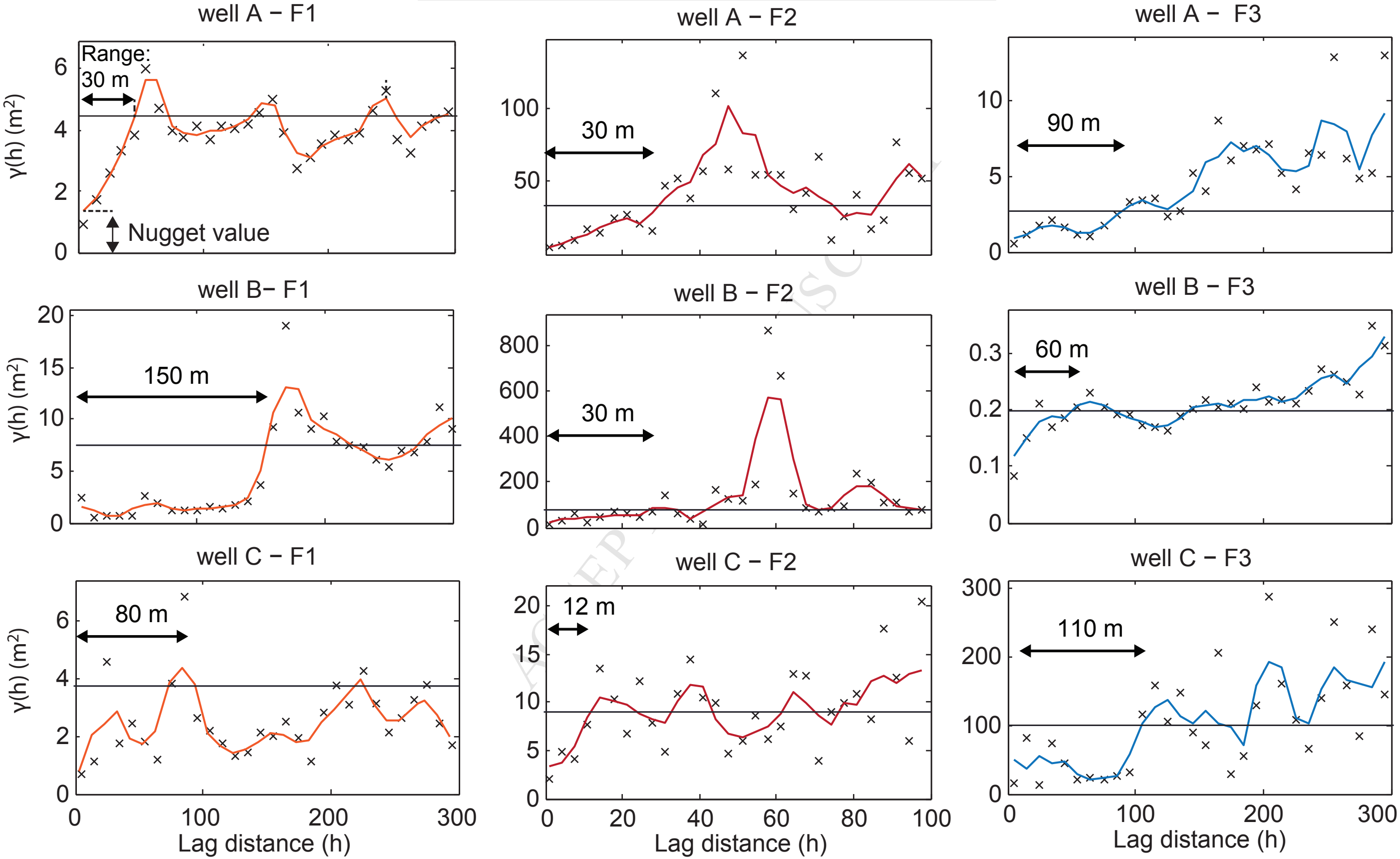

well A − F1
Range:
30 m
Nugget value
well A − F2
30 m
well A − F3
90 m
well B− F1
150 m
well B − F2
30 m
well B − F3
60 m
well C − F1
80 m
well C − F2
12 m
well C − F3
110 m
γ(h) (m²)
Lag distance (h)

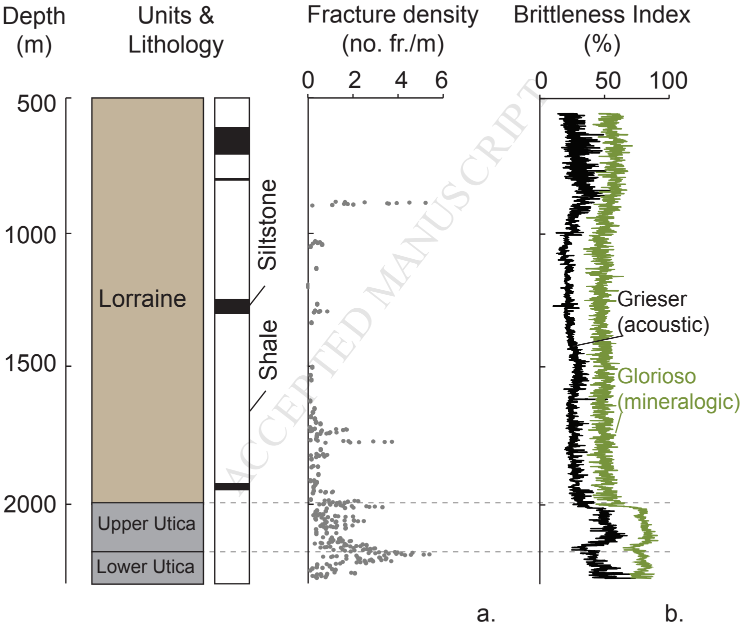
Depth (m)
Units & Lithology
Fracture density (no. fr./m)
Brittleness Index (%)
0
2
4
6
0
50
100
500
1000
1500
2000
Lorraine
Upper Utica
Lower Utica
Siltstone
Shale
Grieser (acoustic)
Glorioso (mineralogic)
a.
b.

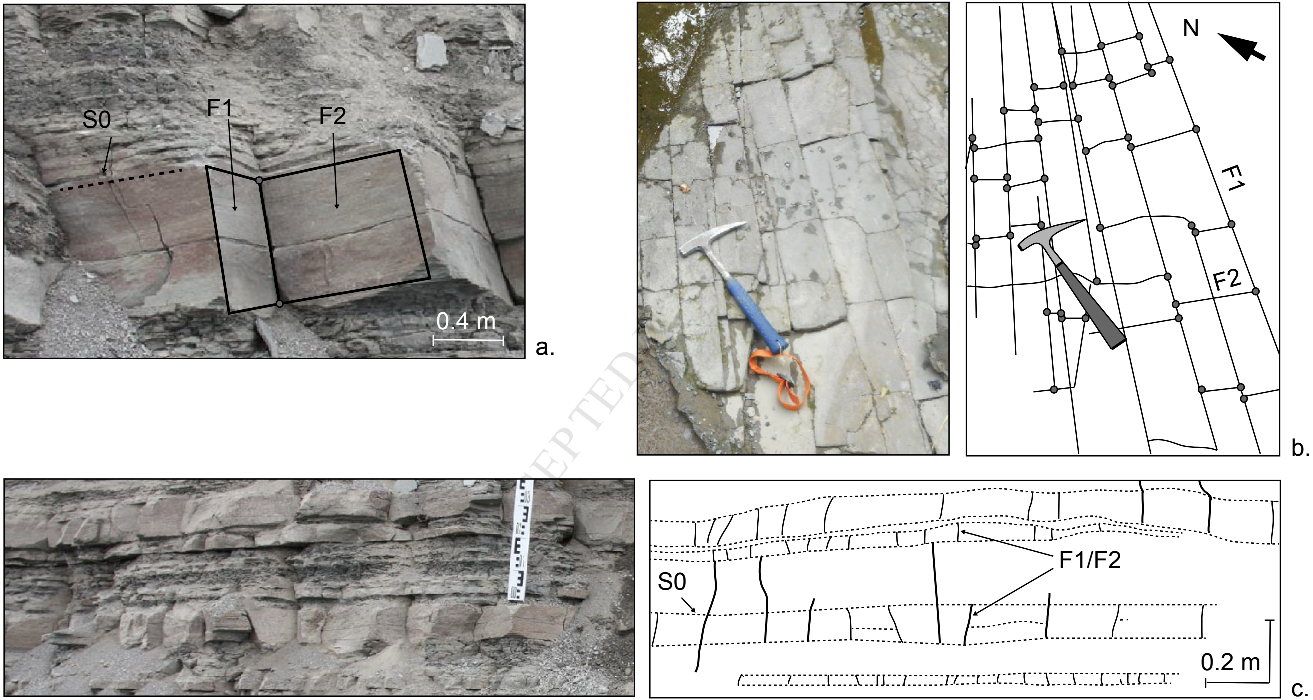
S0
F1
F2
0.4 m
a.
N
F1
F2
b.
F1/F2
S0
0.2 m
c.

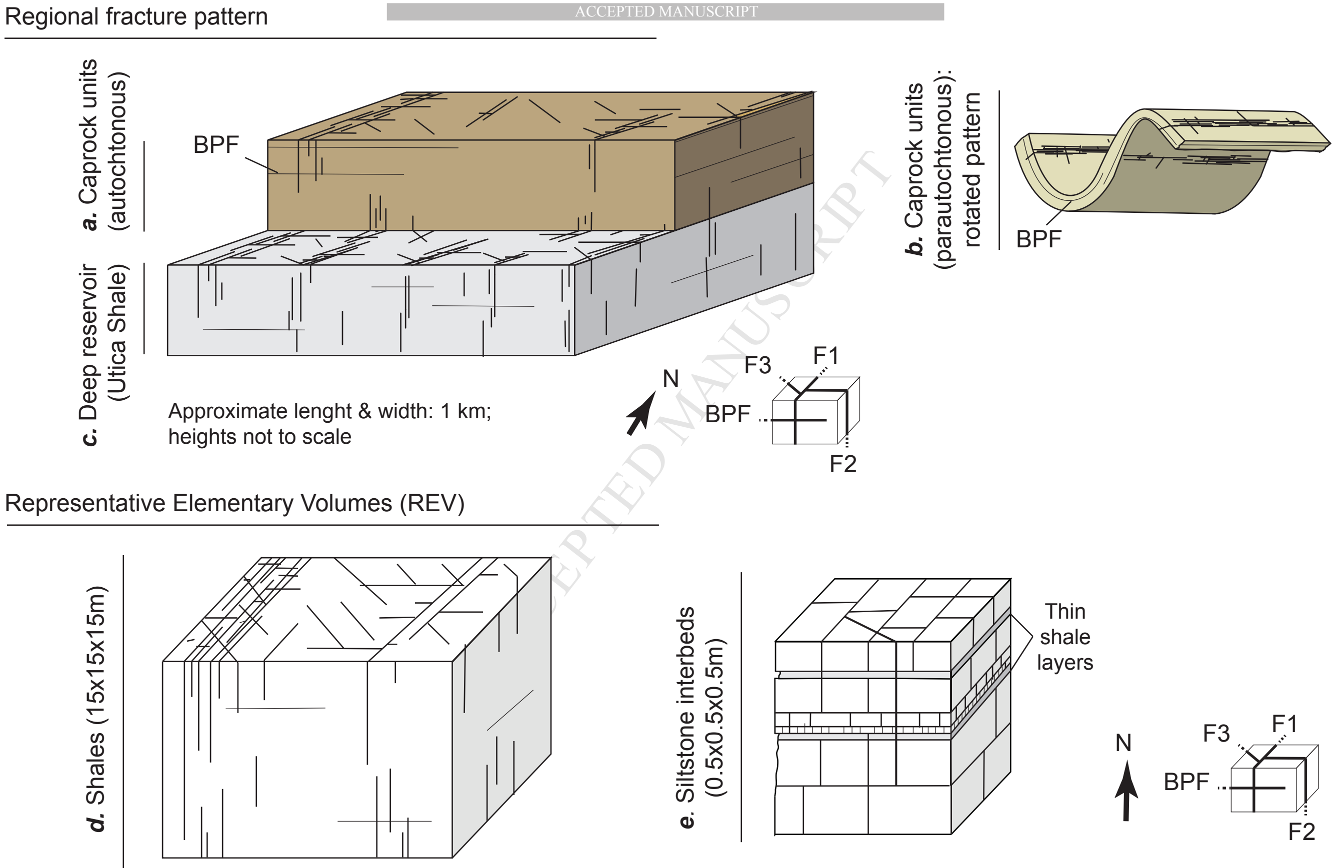
Regional fracture pattern
a. Caprock units (autochtonous)
BPF
b. Caprock units (parautochtonous): rotated pattern
BPF
c. Deep reservoir (Utica Shale)
Approximate lenght & width: 1 km;
heights not to scale
N
F3
F1
BPF
F2
Representative Elementary Volumes (REV)
d. Shales (15x15x15m)
e. Siltstone interbeds (0.5x0.5x0.5m)
Thin
shale
layers
N
F3
F1
BPF
F2

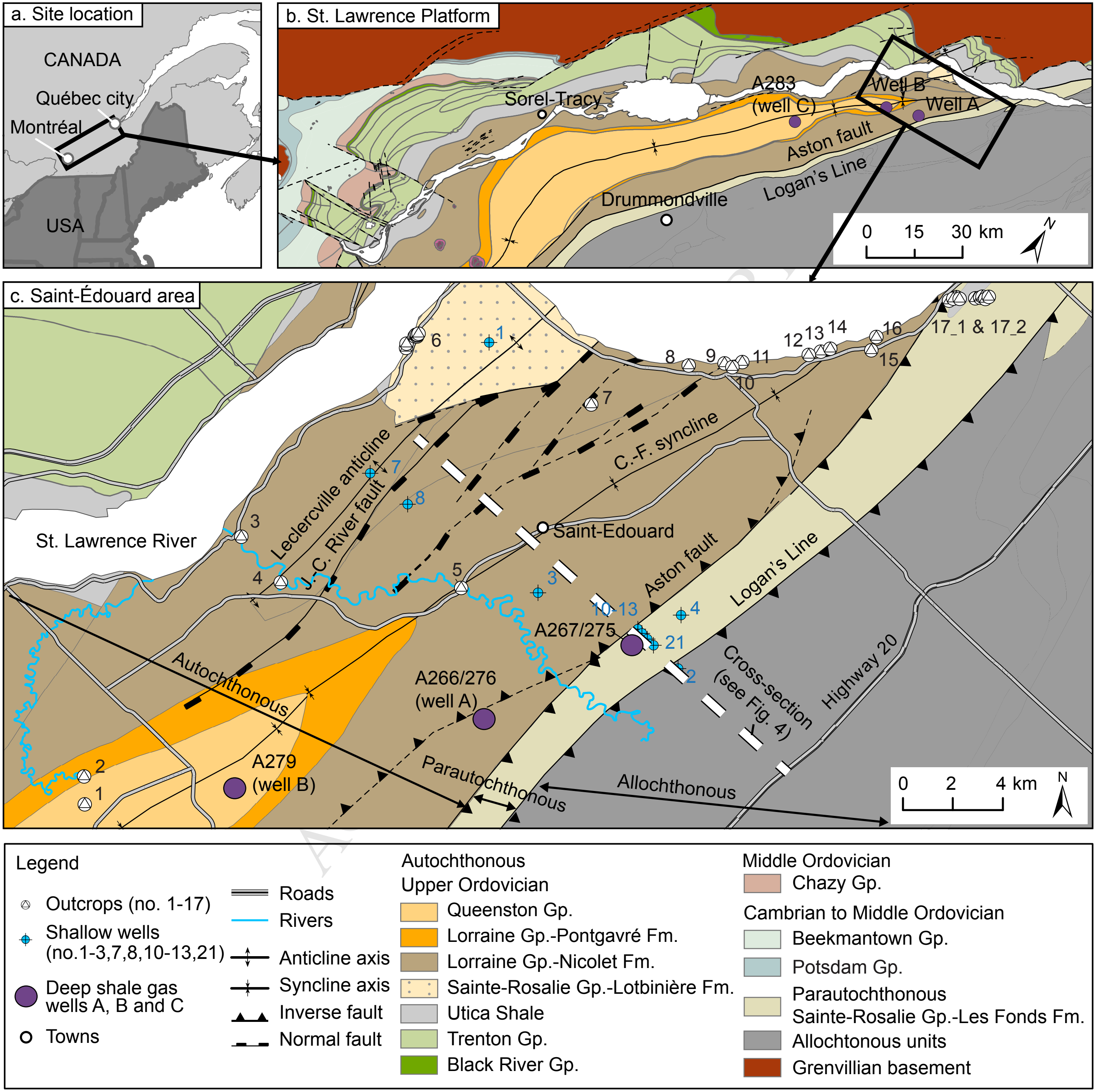
a. Site location
CANADA
Québec city
Montréal
USA
b. St. Lawrence Platform
Sorel-Tracy
A283
(well C)
Well B
Well A
Aston fault
Logan's Line
Drummondville
0 15 30 km
N
c. Saint-Édouard area
St. Lawrence River
Leclercville anticline
J. C. River fault
C.-F. syncline
Saint-Edouard
Aston fault
Logan's Line
A267/275
A266/276
(well A)
A279
(well B)
Autochthonous
Parautochthonous
Allochthonous
Cross-section
(see Fig. 4)
Highway 20
17_1 & 17_2
10-13
21
0 2 4 km
N
Legend
Outcrops (no. 1-17)
Shallow wells
(no.1-3,7,8,10-13,21)
Deep shale gas
wells A, B and C
Towns
Roads
Rivers
Anticline axis
Syncline axis
Inverse fault
Normal fault
Autochthonous
Upper Ordovician
Queenston Gp.
Lorraine Gp.-Pontgavré Fm.
Lorraine Gp.-Nicolet Fm.
Sainte-Rosalie Gp.-Lotbinière Fm.
Utica Shale
Trenton Gp.
Black River Gp.
Middle Ordovician
Chazy Gp.
Cambrian to Middle Ordovician
Beekmantown Gp.
Potsdam Gp.
Parautochthonous
Sainte-Rosalie Gp.-Les Fonds Fm.
Allochtonous units
Grenvillian basement

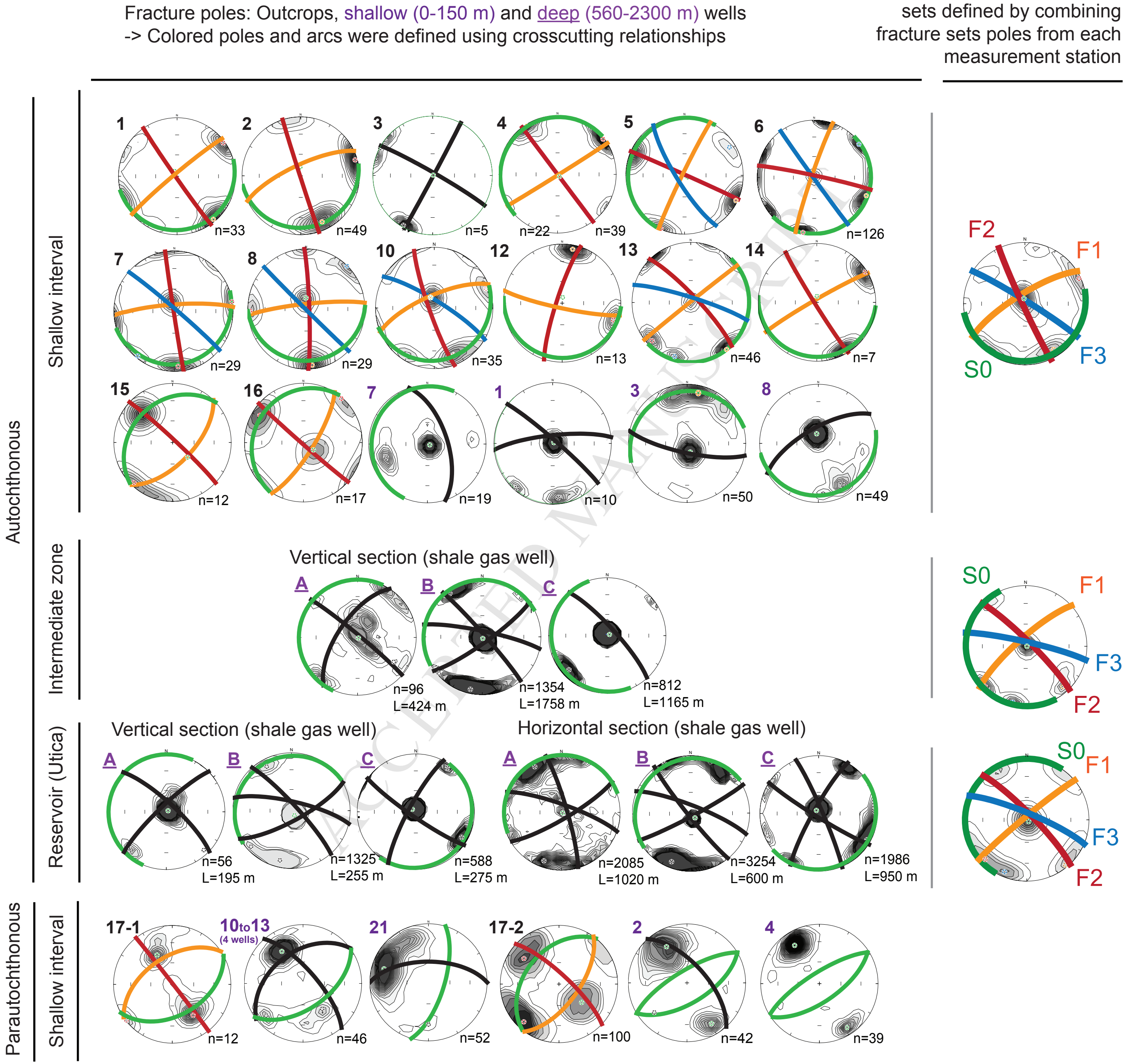
Fracture poles: Outcrops, shallow (0-150 m) and deep (560-2300 m) wells
-> Colored poles and arcs were defined using crosscutting relationships
Synthesis: -> major fracture sets defined by combining fracture sets poles from each measurement station
Autochthonous
Shallow interval
1
2
3
4
5
6
n=33
n=49
n=5
n=22
n=39
n=126
7
8
10
12
13
14
n=29
n=29
n=35
n=13
n=46
n=7
15
16
7
1
3
8
n=12
n=17
n=19
n=10
n=50
n=49
F2
F1
S0
F3
Intermediate zone
Vertical section (shale gas well)
A
B
C
n=96
L=424 m
n=1354
L=1758 m
n=812
L=1165 m
Reservoir (Utica)
Vertical section (shale gas well)
Horizontal section (shale gas well)
n=56
L=195 m
n=1325
L=255 m
n=588
L=275 m
n=2085
L=1020 m
n=3254
L=600 m
n=1986
L=950 m
Parautochthonous
17-1
10to13
(4 wells)
21
17-2
2
4
n=12
n=46
n=52
n=100
n=42
n=39

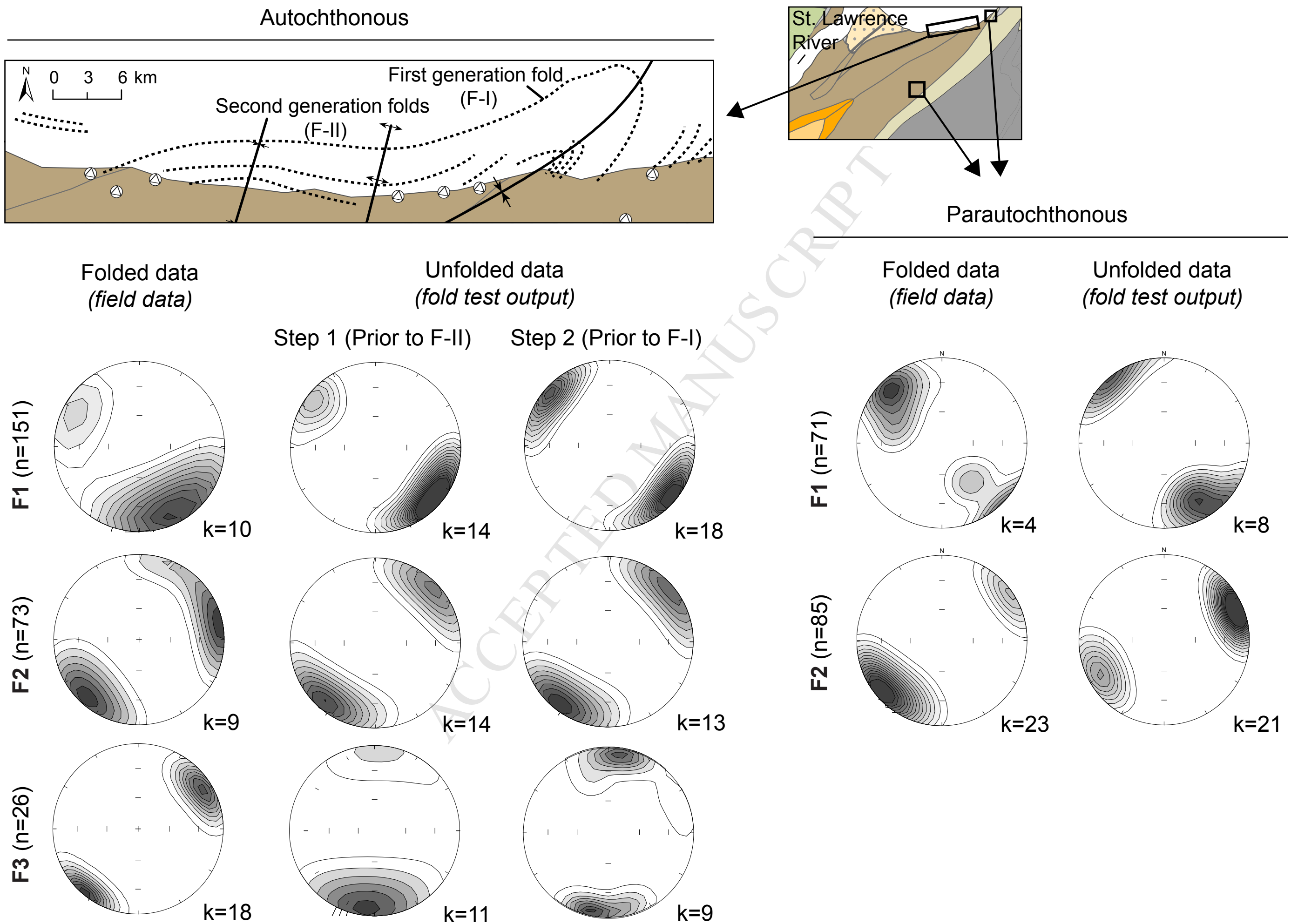

Autochthonous
N
0 3 6 km
First generation fold
(F-I)
Second generation folds
(F-II)
St. Lawrence
River
Parautochthonous
Folded data
(field data)
Unfolded data
(fold test output)
Step 1 (Prior to F-II)
Step 2 (Prior to F-I)
F1 (n=151)
k=10
k=14
k=18
F2 (n=73)
k=9
k=14
k=13
F3 (n=26)
k=18
k=11
k=9
Folded data
(field data)
Unfolded data
(fold test output)
F1 (n=71)
k=4
k=8
F2 (n=85)
k=23
k=21

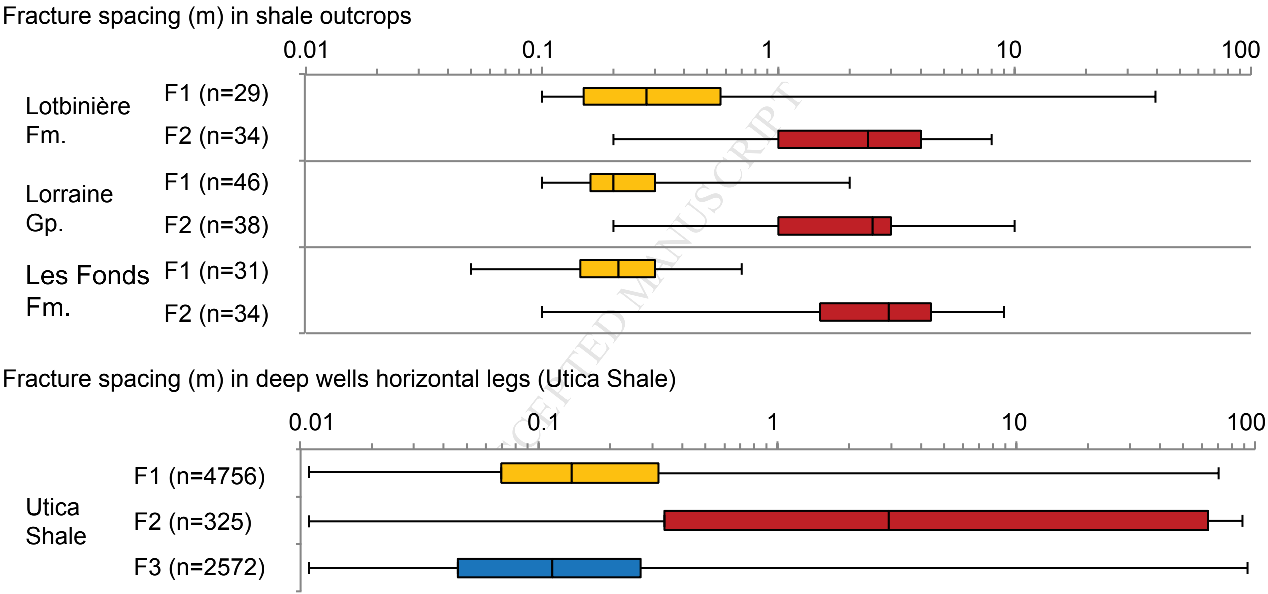

Fracture spacing (m) in shale outcrops
0.01
0.1
1
10
100
Lotbinière Fm.
F1 (n=29)
F2 (n=34)
Lorraine Gp.
F1 (n=46)
F2 (n=38)
Les Fonds Fm.
F1 (n=31)
F2 (n=34)
Fracture spacing (m) in deep wells horizontal legs (Utica Shale)
0.01
0.1
1
10
100
Utica Shale
F1 (n=4756)
F2 (n=325)
F3 (n=2572)

Elsevier Editorial System(tm) for Journal of Structural Geology
Manuscript Draft

Manuscript Number: SG-D-17-00079R2

Title: Defining the natural fracture network in a shale gas play and its cover succession: the case of the Utica Shale in eastern Canada

Article Type: SI:Spatial arrangement

Keywords: natural fracture characterization; analogs; conceptual models; shale gas; Utica Shale

Corresponding Author: Mr. Pierre Ladevèze,

Corresponding Author's Institution: INRS & Geological Survey of Canada

First Author: Pierre Ladevèze

Order of Authors: Pierre Ladevèze; Stephan Séjourné; Christine Rivard; Denis Lavoie; René Lefebvre; Alain Rouleau

Manuscript Region of Origin: CANADA

Abstract: In the St. Lawrence sedimentary platform (eastern Canada), very little data are available between shallow fresh water aquifers and deep geological hydrocarbon reservoir units (here referred to as the intermediate zone). Characterization of this intermediate zone is crucial, as the latter controls aquifer vulnerability to operations carried out at depth. In this paper, the natural fracture networks in shallow aquifers and in the Utica shale gas reservoir are documented in an attempt to indirectly characterize the intermediate zone. This study used structural data from outcrops, shallow observation well logs and deep shale gas well logs to propose a conceptual model of the natural fracture network. Shallow and deep fractures were categorized into three sets of steeply-dipping fractures and into a set of bedding-parallel fractures. Some lithological and structural controls on fracture distribution were identified. The regional geologic history and similarities between the shallow and deep fracture datasets allowed the extrapolation of the fracture network characterization to the intermediate zone. This study thus highlights the benefits of using both datasets simultaneously, while they are generally interpreted separately. Recommendations are also proposed for future environmental assessment studies in which the existence of preferential flow pathways and potential upward fluid migration toward shallow aquifers need to be identified.

## Response to Reviewers

Dear Reviewer, I would like to thanks you for your comments and time reviewing our paper.

Please fin hereafter a modified version of the paper.

Sincerely,

Pierre Ladevèze.

**Corrections applied:**

**Reviewer**: Some minor corrections to be done:

Line 229: "Fracture distribution" .... ? what do you mean?

**Pierre L.:** Thanks for highlighting this error in the text, I have modified the text.

Line 288: Error! Reference source not found

The text has also been modified.

Line 310-312; You first say "fracture lengths reach from 10 to 30m" and then between 2 and 5 m for F1 and F2. Please clarify. And what about F3 ?

I have clarified these points in the text.

Line 331: "significantly for F1" significantly what ?

I have suppressed this sentence because it does not bring any value to the text.

Line 349: What about F3 ?

Unfortunately fracture spacing distributions could not be further used to assess the relative timing of fracture sets formation. However, crosscutting relationship observations and the fold test analysis brought strong evidences that support the formation of F3 fractures after the F1 and F2 sets.

Line 361: Why no F2 and F3 fracture corridors ? this question should also may be addressed in the discussion chapter.

This comment points out to the limits of our conceptual model (organization of the fracture sets in corridors). Concerning this aspect of the study, it would have been really interesting to improve our conceptual model with more field-based evidences. In our field dataset, only the potential existence of F1 fractures corridors could be identified. Even if a lot of fracture data is available in the Saint-Edouard area, existing data could not help to further assess this aspect. We have discussed the limits of the conceptual model in more details in the section discussion (section 5.2.1. Limits of the conceptual model). Finally, we would like to emphasis on the fact that the purpose of our paper is to propose an approach to characterize the intermediate zone using shallow and deep fracture data and also to highlight its interest in a context of unconventional gas development. In this context, we think that the previously discussed limitations did not affect the validity of our approach.

Line 424: "when drilling a deep vertical well". This is misleading. It is not because you drill deep but because you drill in the Utica Shale. Note also that drilling a vertical well might not be the best solution to intersect corridors.

Thanks for the comment, I have modified the sentence to avoid misinterpretations.

Figure 10: I am not convinced by your regression line for the deep wells. Despite apparently good R2, the lines do not fit the data. Do you apply the regression to all the data or only through the linear part of them? Indeed, you should apply two cutoffs, one for the small spacing values (the resolution limit around 0.1m) and one for the large value (limit of statistical homogeneity, around 20m). In a log-log plot a good correlation coefficient should be at least 0.97. 0.91 is definitively not a good one. Moreover, why do you have horizontally aligned data points? In a cumulative count plot, this should not happen.

I have modified the figure and the text in the section result. I had made an error when plotting the data (horizontally aligned points are now excluded). These points were affecting the quality of the regression. Following your comments, I have also applied two cut-offs for the regressions lines. The modifications were applied and I think that the figure looks better.

Figure 12: The F1 FC's seem to have some characteristic thicknesses (around 40m) and spacings (100 to 200 m). How does this relate to the variograms in Figure 11?

As the geometrical characteristics of the corridors remains to be confirmed, we only briefly discuss this point. I have added a sentence to highlight the geometrical characteristics of the F1 corridors observed on fig. 12. Moreover, concerning the use of variogram to better assess the existence of corridor, some new insights are presented in section 5.2.1. Significant gains can be obtained using variogram to assess the clustering of fractures. However, as spacing is a scale-independent continuous variable, variograms could not be used to further explore the geometrical characteristics of fracture corridors (a scale dependent characteristic of the fracture network).

Figure 15: regression line coefficient: to me 0.0059 and 0.046 do not mean anything. The regressions could be forced to 0 which is geologically sound.

I agree, thanks. DONE.

**Highlights**

- This study integrates shallow and deep multisource fracture datasets

- An analog approach was used to characterized the caprock of the Utica Shale reservoir

- Four fracture sets affects the entire shale succession

- A conceptual model of this fracture network is proposed

# Defining the natural fracture network in a shale gas play and its cover succession: the case of the Utica Shale in eastern Canada

Ladevèze, P. [*,a,b], Séjourné, S.[c], Rivard, C. [b], Lavoie, D. [b], Lefebvre, R.[a], Rouleau, A.[d]

[a] *INRS – Centre Eau Terre Environnement, 490 rue de la Couronne, Québec City, QC G1K 9A9, Canada*

[b] *Geological Survey of Canada – Québec, 490 rue de la Couronne, Québec City, QC G1K 9A9, Canada*

[c] *Consulting geologist, Montréal, Canada*

[d] *UQAC, 555 Blvd. de l'Université, Chicoutimi, QC G7H 2B1, Canada*

[*] *Corresponding author: pierrelad@gmail.com*

**Keywords:** natural fracture characterization; analogs; conceptual models; shale gas; Utica Shale

## Abstract

In the St. Lawrence sedimentary platform (eastern Canada), very little data are available between shallow fresh water aquifers and deep geological hydrocarbon reservoir units (here referred to as the intermediate zone). Characterization of this intermediate zone is crucial, as the latter controls aquifer vulnerability to operations carried out at depth. In this paper, the natural fracture networks in shallow aquifers and in the Utica shale gas reservoir are documented in an attempt to indirectly characterize the intermediate zone. This study used structural data from outcrops, shallow observation well logs and deep shale gas well logs to propose a conceptual model of the natural fracture network. Shallow and deep fractures were categorized into three sets of steeply-dipping fractures and into a set of bedding-parallel fractures. Some lithological and structural controls on fracture distribution were identified. The regional geologic history and similarities between the shallow and deep fracture datasets allowed the extrapolation of the fracture network characterization to the intermediate zone. This study thus highlights the benefits of using both datasets simultaneously, while they are generally interpreted separately. Recommendations are also proposed for future environmental assessment studies in which the existence of preferential flow pathways and potential upward fluid migration toward shallow aquifers need to be identified.

# 1 Introduction

For shale-dominated successions, there is a high interest in identifying natural fracture networks because they control the rock permeability (Barton et al., 1998; Berkowitz, 2002; Guerriero et al., 2013; Narr et al., 2006; Odling et al., 1999; Singhal and Gupta, 2010) and thus strongly influence fluid flow in the different stratigraphic units and potentially between deep prospective shale gas strata and shallow aquifers (CCA 2014; EPA 2016; Lefebvre, 2016).

However, the quantitative assessment of natural fractures can be challenging due to observational biases related to the methods that provide results at different scales (e.g. at the scale of outcrops, wells or seismic lines) and to the data that are sparsely or irregularly distributed. The inherent incompleteness of data is exacerbated in the so-called “intermediate” zone (or caprock). There is generally a lack of observation in this zone because it is located between shallow aquifers studied for hydrogeological purpose and the deep reservoir that has been characterized for hydrocarbon exploration/production. The characterization of this zone is crucial to properly understand the dynamic of potential contaminants migration to shallow aquifers.

Fracture observations on outcrops are often used as analogs for deep reservoirs (Antonellini and Mollema, 2000; Gale et al., 2014; Larsen et al., 2010; Lavenu et al., 2013; Vitale et al., 2012). Hence, the extrapolation of fracture data from outcrops and shallow hydrogeological wells, or from the deep reservoir where well log data and other geoscience information abound, may appear to be a promising approach to characterize the intermediate zone. However, the use of ‘shallow’ or ‘deep’ datasets as analogs is not always possible and certainly not straightforward; the controls on fracture distribution in a sedimentary succession have to be carefully identified to fully assess the fracture patterns. At shallow depths, surface weathering can enhance fracture apertures and be possibly responsible for fractures filling with minerals that are not representative of deep units. Furthermore, uplift or unroofing can initiate fracture propagation (Engelder, 1985; English, 2012; Gale et al., 2014). Therefore, the presence of unloading fractures oriented according to either a residual or a contemporary stress field will affect the shallow rock mass (Engelder, 1985). To the contrary, some fracture generation processes can occur only at significant depths due to an increase of the greatest compressive stress during regional shortening, a decrease in the least compressive stress caused by regional extension or an increase in pore pressure (Gillespie et al., 2001). Therefore, to be able to use some shallow and deep fracture sets as analogs, it must first be demonstrated that outcropping fractures are not solely the expression of near-surface events and were most likely formed at significant depths (at least comparable with the reservoir depth).

In this paper, we aim at integrating multisource data (outcrops, shallow and deep acoustic and electric well logs) that have different observation scales to obtain a sound interpretation of the fracture network affecting a shale gas play in southern Quebec (Saint-Édouard area, approximately 65 km southwest of Quebec City; location in Fig. 1). An emphasis is put on the characterization of the intermediate zone which potentially controls contaminants migration to subsurface. The proposed methodology could be of interest for other studies in shale dominated successions where there is a lack of data in the intermediate zone.

## 2 Regional tectonostratigraphic setting

### 2.1 *The St. Lawrence Platform*

In southern Quebec, the St. Lawrence Platform is bounded by the Canadian Shield to the NW and by the Appalachian mountain belt to the SE. The portion of interest of the St. Lawrence Platform (here referred as the SLP) comprises the area roughly between Montréal and Quebec City. This Cambrian-Ordovician depositional element is divided in two tectonostratigraphic domains: the autochthonous and the parautochthonous domains (Castonguay et al., 2010; St-Julien and Hubert, 1975) (Fig. 1). At the base of the autochthonous domain, Cambrian-Ordovician rift and passive margin units unconformably overlie the Grenville crystalline rocks (Lavoie et al., 2012) (Fig. 2). These passive margin units include the Potsdam Group sandstones and conglomerates and the Beekmantown Group dolomites and limestones. Those two groups are covered by Middle to Upper Ordovician units deposited in a foreland basin setting (Lavoie, 2008) (Fig. 2). The progressively deepening-upward carbonate units of the succeeding Chazy, Black River and Trenton groups, and the Utica Shale, were then covered by the overlying Upper Ordovician turbidite and molasse units of the Sainte-Rosalie, Lorraine and Queenston groups. The Utica Shale constitutes a prospective unit for shale gas in southern Quebec (Dietrich et al., 2011; Hamblin, 2006; Lavoie, 2008; Lavoie et al., 2014).

The SLP units have recorded a polyphased structural history (Pinet et al., 2014) and thus display a complex structural pattern. These events include Middle and Late Ordovician normal faulting that started at the inception of the foreland basin phase (Thériault, 2007), shortening during the Taconian orogeny (Tremblay and Pinet, 2016), and some post-Ordovician folding (Pinet et al., 2008) and faulting (Sasseville et al., 2008; Tremblay et al., 2013). Normal faults (including the Jacques-Cartier River fault, Fig. 5) are steeply-dipping to the south and displace the basement, the basal units of the platform and its upper units in the autochthonous domain (possibly including the Utica Shale and Lorraine Group). These faults were reactivated several times during and after the building of the Appalachians, documented evidence of movement is known for the late Silurian Salinic Orogeny and the opening of modern Atlantic (Castonguay et al., 2001; Faure et al., 2004; Konstantinovskaya et al., 2009; Sasseville et al., 2012; Séjourné et al., 2003; Tremblay and Pinet, 2016). A summary of the depositional environment and the major tectonic events that affected rock of the SLP is presented in Fig. 3.

In the autochthonous domain, the near surface Upper Ordovician units (post-Utica Shale) are folded by the regional Chambly-Fortierville syncline. This fold is asymmetric with more steeply-dipping beds in the southern flank (28°) than in the northern flank (10°) (Fig. 4a). Its axis is roughly parallel to the limit between the SLP and the Appalachians. To the southeast, the Aston fault and the Logan's Line belong to a regional thrust-fault system that limits the parautochthonous domain (Fig. 2 and Fig. 5). Reprocessing and reinterpretation of an industrial 2D seismic line (using two well calibration points) was proposed in (Lavoie et al., 2016) and showed that in the Saint-Édouard area, the parautochthonous domain forms a triangle zone delimited to the northwest by a NW-dipping backthrust and by the SW-dipping the Logan's Line to the SE (Fig. 5). The existence of a triangle zone bounding the southern limb of the Chambly-Fortierville is supported by previous interpretations done in the SLP (Castonguay et al., 2006; Castonguay et al., 2003; Konstantinovskaya et al., 2009). These thrusts/backthrusts are associated with the Middle to Late Ordovician Taconian Orogeny (St-Julien and Hubert, 1975). In the parautochthonous domain, a southeast-dipping system of thrust faults displays imbricated thrust geometries (Castonguay et al., 2006; Séjourné et al., 2003; St-Julien et al., 1983). Some northeast-striking folds also affect the parautochthonous units (Fig. 4b). The Logan's Line marks the fault-contact between the SLP and the allochthonous external Humber zone (St-Julien and Hubert, 1975) (Fig. 5).

The present-day in-situ maximum horizontal stress ($SH_{max}$) orientation is NE–SW in the SLP as previously proposed using borehole breakouts orientations (inferred from four-arm dipmeter caliper data) (Konstantinovskaya et al., 2012). This trend is relatively consistent with the large-scale trend documented in eastern North America (Heidbach et al., 2009; Zoback, 1992). The stresses/pressure gradients estimated in the platform indicate a strike-slip stress regime (Konstantinovskaya et al., 2012). As the regional faults of the SLP are oblique to the actual $SH_{max}$, a reactivation of these structures under the current stress field remains possible (Konstantinovskaya et al., 2012) but has not yet been documented.

Organic matter reflectance data indicates that at least 3 and 4.7 km of sediments have been eroded in the SLP (Sikander and Pittion, 1978) and in the frontal part of the Chaudière Nappe in the Quebec City area (Ogunyomi et al., 1980), respectively. Later studies showed that there was an increasing thickness of eroded sediments from about 5 to 7 km from northeast to southwest in the SLP (Héroux and Bertrand, 1991; Yang and Hesse, 1993).

### 2.2 *The intermediate zone (caprock) and reservoir units of the Saint-Édouard area*

The Utica Shale is overlain by autochthonous units (the Nicolet Formation - Lorraine Group and the Lotbinière Formation – Sainte-Rosalie Group) and parautochthonous units (Les Fonds Formation – Sainte-Rosalie Group). These units constitute the intermediate zone (caprock) in the Saint-Édouard study area.

The Utica Shale (Upper Ordovician) is made of limy mudstone that contains centi- to decimetric interbeds of shaley limestone (Globensky, 1987; Lavoie et al., 2008; Theriault, 2012). It is divided in two members (Upper and Lower). The Lower Utica Shale contains more limestone interbeds than the Upper Utica Shale. In the Saint-Édouard area, the thickness of the Utica Shale ranges from 200 to 400 m (Fig. 5). The autochthonous Lotbinière Formation (Sainte-Rosalie Group) and the parautochthonous Les Fonds Formation (Sainte-Rosalie Group) are time- and facies correlative units of the Utica Shale (Lavoie et al., 2016) (Fig. 2). The Utica Shale, Lotbinière and Les Fonds formations display a similar lithofacies of black calcareous mudstone with thin beds of impure fine-grained limestone but differs by their organofacies (Lavoie et al., 2016). The Lotbinière Formation is made of gray-black micaceous shale with rare interbeds of calcareous siltstones (thickness <10 cm) and is outcropping north of the Jacques-Cartier River normal fault (Belt et al., 1979; Clark and Globensky, 1973). In the parautochthonous domain, the Les Fonds Formation is mainly composed of shale with less abundant fine-grained limestones and conglomerates (Comeau et al., 2004). The Nicolet Formation (Lorraine Group, Upper Ordovician) is slightly younger compared to the previous three units (Comeau et al., 2004) and is mostly made of gray to dark-gray shale with centi- to decimetric (rarely metric) siltstone interbeds (Clark and Globensky, 1973; Globensky, 1987). Upward, there is a decrease of the shale content and an increase in the number and thickness of the sandstone beds (Clark and Globensky, 1976). In the Saint-Édouard area, the thickness of autochthonous and parautochthonous intermediate zone units (i.e., above the Utica Shale) progressively increases from 400 m to 1900 m from northwest to southeast (Fig. 5).

**Insert Fig. 1 to 5 here.**

## 3 Methodology

In this study, the term “fracture” refers to metric scale planar discontinuities that affect the rock mass without visible displacement.

### 3.1 *Data sources*

Fracture data were collected and compiled in the Saint-Édouard area using different methods. Fifteen outcrops were investigated (Fig. 1). Borehole logs includes acoustic, optical and electric logs that have different resolutions. Typically, electric logs have a higher resolution than acoustic and optical tools. Interpretation were then done in the light of these scale differences. Acoustic and optical televiewer logs from eleven shallow (15 to 147 m deep in the bedrock) groundwater monitoring wells drilled for the project (Crow and Ladevèze, 2015) were also studied. Moreover, Formation Micro Imager (FMI) data from three deep shale gas wells were interpreted. The wells referenced by the oil and gas geoscience information system of the Ministère des Ressources naturelles of Quebec under the numbers A266/A276 (Leclercville n°1), A279 (Fortierville n°1) and A283 (Sainte-Gertrude n°1) were used. To simplify the nomenclature in the current paper, they are hereafter referred to as A, B and C, respectively (Fig. 1). FMI data from the vertical sections of wells A, B and C cover the following ranges of depth: 1470-2080 m for well A, 560-2320 m for well B and 590-2050 m for well C; this includes the Utica Shale and variable portions of the overlying Lorraine Group. Each of these wells also includes a horizontal section (“horizontal leg”) in the Utica Shale (1000, 970 and 920 m long, for wells A, B and C respectively) for which FMI data was also available. For a history of the recent shale gas exploration in the study area, refer to Lavoie et al. (2014) and Rivard et al. (2014). The characteristics of the measurement stations are summarized in Table 1.

**Insert Table 1 here.**

## 3.2 *Fracture assessment*

Common geometrical attributes of fractures were measured: attitude, spacing, crosscutting relationships between fractures and other geological structures (such as syn-sedimentary concretions). These attributes were documented all along the boreholes using acoustic and electrical logs. As most of the outcrops were limited in size and were displaying only sparsely distributed fractures, their attributes were systematically measured in the exposed surfaces.

### *3.2.1 Fracture sets*

For each measurement station (outcrop or well), fracture poles were plotted on stereonets using the *SpheriStat™* software (Stesky, 2010). Contoured density diagrams were used to identify the mean position of the fracture sets. The poles density contours of borehole data were corrected for sampling bias (underestimation of the frequencies for the fracture planes that are sub-parallel to the observation line) using the method of Terzaghi (1965). A weight function of the angle $\beta$ between the fracture plane and the observation line was attributed to all fracture densities. This weight $w$ is expressed as: $w=(\sin\beta)^{-1}$ (Terzaghi, 1965). Even if mathematically valid, fracture planes with low $\beta$ values are overestimated with this method (Park and West, 2002). For this reason, an arbitrary 10° blind zone was used in the analysis (fractures sub-parallel to the observation-line are excluded).

When clear crosscutting relationships were observed on outcrops, the relative timing of fracture sets formation could be defined. In borehole data, it was rarely possible to identify such relationships. In this case, the main attitude for fracture set attitudes were compared to adjacent outcrops data (if existing) to define a hypothetical relative timing for the formation of the fracture sets.

If fracture poles are scattered in stereonets, only the maximum pole concentration is taken into account. To better identify the major fracture sets in such cases (generally the case of outcrops or shallow wells that displays significant folding), a fold test was performed on fracture data in order to calculate the fracture attitudes prior to folding events. Results from this test were also used to further assess the relative chronology of fracture sets formation and folding. The rotation applied to fracture attitudes corresponds to the angle of rotation of the bedding plane after a folding event. Two generations of folds have previously been documented in the autochthonous domain in the Saint-Édouard area: F-I (first generation: Chambly-Fortierville syncline) and F-II (second generation) (Pinet, 2011). To consider the effect of the two generations of folds, the analysis was performed in two steps. First, the fracture plans were replaced back to their original attitude prior to F-II folding. As the F-II fold axes are sub-horizontal, the first step consists in correcting the strike direction of fracture planes according to the strike angle between fold-I and fold-II axes. The second step aims at correcting the fracture plans back to their attitude prior to F-I folding. This was done by tilting back the fracture planes around the F-I axis (N233/04, Fig. 4) with an angle corresponding to the structural dip (angle between the bedding plane attitudes in each measurement station and the horizontal). In the parautochthonous domain, a single folding event was easily observable in the field and fracture plans were back-tilted along the regional F-I axis (N235/03 Fig. 4). A better fracture set concentration after rotation is a strong indicator of its pre-folding origin. To quantify the degree of concentration of attitude data, the parameter k was calculated for both the original and rotated fracture sets. This parameter quantifies the degree of data dispersion on a sphere/stereonet (Fisher, 1953). The higher the values of k, the more the data are concentrated in the stereonet (Fiore Allwardt et al., 2007).

*3.2.2 Fractures distribution*

In the document, the term “spacing” refers here to the perpendicular distance between two adjacent fracture planes of similar attitude. Measuring or estimating spacing thus requires first a classification of the fractures into coherent fracture attitude set. The fractures densities correspond to the number of fractures (regardless of their attitudes) per unit distance along a line. They were calculated along the wells using a counting window of various lengths. Each fracture density value was then normalized by the window lengths. All fracture densities were corrected using the Terzaghi method. In the same way, fracture frequencies correspond to the number of fractures from a specific set per unit distance along a line.

To further explore the process of fracturing in siltstone units, the fracture spacing was plotted against bed thicknesses (fractures are bed-confined in siltstone to the contrary of shale in the studied area). Values of the ratio of fracture spacing to layer thickness (the slope of the curve) were extracted from these plots and used to determine if the fracture network has attained saturation, a concept describing the situation where whatever the applied strain, fracture spacing has attained a lower limit (or an upper limit for fracture densities) that is proportional to bed thickness (Bai et al., 2000; Wu and D. Pollard, 1995).

Geostatistical tools were used to assess the degree of spatial correlation of each fracture set (Chilès, 1988; Escuder Viruete et al., 2001; Miller, 1979; Tavchandjian et al., 1997; Valley, 2007; Villaescusa and Brown, 1990). In other words, the use of geostatistics can help define the spatial organization of fractures when they seem to have a totally random spatial distribution in the rock mass. The knowledge of the spatial distribution of fractures can be used to develop discrete fracture network (DFN) models to further assess the fracture control on fluid flow (Caine and Tomusiak, 2003; Dershowitz et al., 1998; Min et al., 2004; Surrette et al., 2008).

Variogram analyses were thus performed on spacing data for each fracture set in the horizontal section of the three deep wells. A formal definition of the experimental variogram γ(h) ($m^2$) for fracture spacing data is presented in Eq. (1).

$$\gamma(h) = \frac{1}{2n}\sum_{i=1}^{n}\left[z(x_i) - z(x_i + h_i)\right]^2 \qquad \text{Eq. (1)}$$

where, *n* is the number of fractures separated by a distance *h* (this calculation interval is also called “lag”), $z(x_i)$ is the fracture spacing value at the distance $x_i$. An experimental variogram presents the γ values successively calculated for increasing *h* values. The shape of the experimental variogram is used to assess if the available data have a spatial correlation that could be represented by a theoretical model. If so, the nugget value in the experimental variogram must be lower than the variance of the entire dataset for the correlation in fracture spacing to be considered present (reflecting fracture clustering). The range value in the variogram provides the maximum distance for fracture spacing clustering. In geological terms, this range of influence means that two samples spaced farther apart than this distance are likely not correlated (and thus considered independent) (Miller, 1979).

### *3.2.3 Fracture and rock mechanical properties*

The potential for fracture propagation in rocks is controlled by their brittleness (Ding et al., 2012; Lai et al., 2015; Meng et al., 2015). The Brittleness Index is an empirical parameter that is widely used to quantify the ability of a rock unit to fracture (Wang et al., 2015). In the Saint-Édouard area, this parameter was previously estimated from borehole logs acquired in the deep gas wells using the Grieser and Bray (2007) and the Glorioso and Rattia (2012) methods (Séjourné, 2017). These methods are respectively based on the acoustic (compressional and shear wave velocity logs) and mineralogical (derived from elemental spectroscopy logs) properties of the shale. In the current paper, the relationship between fracture densities and brittleness variations in the Lorraine Group and Utica Shale was explored.

# 4 Results

## 4.1 *Fractures in shales*

Two fracture types were observed in shale units: steeply-dipping fractures (F1, F2 and F3) and bedding-parallel fractures (BPF). Examples of observed fractures on outcrops are presented in Fig. 6. In the vast majority of outcrops, fractures are planar and exhibit clear crosscutting relationships. For this reason, it was possible to sort the high-angle fractures in three sets that are designated according to their relative order of formation (F1, F2 and F3 sets; F1 is the older set). Fractures were also only bed-confined in siltstones.

To facilitate the classification of fractures in sets, a fold test analysis was done using data from outcrops and shallow wells that were affected by folding events that could be clearly identified in the field (i.e. outcrops affected by folds F-II and F-I). Fracture attitudes from outcrops and values of the associated parameter *k* (which quantifies the data concentration in the stereonets) are presented in Fig. 8. In the autochthonous domain, an improved concentration of fracture poles was obtained for F1 and F2 sets after rotation prior to the second generation of folds (F-II). Then, removing the effects of F-I fold improved even more the concentration of F1 fractures, but had no effect on the concentration of F2 fractures. This strongly suggests a pre-F-I folding origin for the F1 set, and a pre- to syn-F-II origin for F2 fractures. To the contrary, the concentration of the F3 fracture set was reduced after removing both F-II and F-I effects, thus supporting a syn- to post F-II folding origin for this F3 set. One fold generation was clearly observed in the parautochthonous domain (other fold generations may exist but were hardly observable on outcrops). This regional folding corresponds to the first fold generation (F-I) documented in the autochthonous domain. The fold test showed that a better concentration was obtained for the F1 set when rotated prior to folding, confirming a potential pre-F-I origin for F1 fractures. Results for the F2 fracture set show a slight, probably poorly significant, reduction of concentration and the timing remains not well constrained on the basis of the fold test.

Fracture sets F1 and F2 are pervasive in both the autochthonous and parautochthonous domains. They strike NE (F1) and NW (F2) (Fig. 7), with F2 abutting against F1 (Fig. 6a and b). F1 and F2 are perpendicular to each other and orthogonally crosscut the bedding planes (S0). F1 fractures are locally concentrated in corridors (as in Fig. 6b). The third fracture set (F3) is only documented in the autochthonous domain. F3 strikes WNW and is sub-vertical (dip >80°) whatever the bedding planes attitudes (Fig. 7). F3 generally crosscuts F1 and F2 and was not observed at all sites. All three fracture sets were documented in shallow and deep data. Finally the BPF were only observed at shallow depth.

Detailed fracture length measurements were limited to the size of the outcrops. Thus, only semi-quantitative fracture length estimations are here proposed. Fracture lengths for the F1 and F2 sets were approximately between 2 and 5 m. The maximum observed fracture lengths were ranging between 10 and 30 m. F1 fractures display lengths higher than F2 fractures, as F2 abut F1 fractures. Due to the limited number of outcropping F3 fractures, no realistic estimate of fracture lengths for this set was possible. Finally, because some fractures locally extend beyond the limit of the outcropping areas, length estimation values must be considered with caution.

Some intervals in the black shales of the Lotbinière Formation (northern part of the study area) display oval-shaped carbonate concretions (maximum diameter of up to 1.5 m; length-to-width ratio around 1.5). The metabolic activity of sulfate-reducing and methanogen bacteria that occurred shortly after the inception of burial of organic matter-rich sediments under anoxic conditions are responsible for the formation of these concretions (Mozley and Davis, 2005). In the Lotbinière Formation, 15 fractures were identified passing around such concretions without crosscutting them (Fig. 6c). Such a relationship is interpreted as an indicator of natural fractures propagation in the presence of abnormal fluid pressure in response to the shale thermal maturation and to the gas generation in a context of deep burial (McConaughy and Engelder, 1999).

**Insert fig. 6 to 8 here.**

Statistics on fracture spacing data from outcrops and boreholes are presented in Fig. 9. Median values in shale outcrops are significantly for F1 than for F2 (0.20 to 0.28 m for F1; 2.4 to 2.93 m for F2). The same trend is observed in the shale gas wells (0.14 m for F1 and 2.93 m for F2). Lower and upper quartiles for fracture spacing also extend over a significantly larger interval for the F2 set than for the F1 set, suggesting a more scattered spatial distribution of F2 fractures, especially in the Utica Shale. In the deep wells, the mean value for F3 spacing (0.11 m) is slightly lower than that of the F1 value.

**Insert fig. 9 here.**

To the contrary of F2 fractures, both F1 and F3 fractures spacing data from outcrops and shale gas wells seems to follow a power law distribution (exponent values around 1), see Fig. 10. In this figure, spacing value less than 0.05m (resolution of the observation methods) and higher than 10 m (upper limit of statistical homogeneity) were excluded for the regression calculation. Following Bonnet et al. (2001), this may reflect the scale invariance of the fracture spacing for these two sets. The existence of the power law distribution must be interpreted with care as our dataset is affected by both censoring bias (high fracture spacing is not sampled due to the limited size of outcrops and well sections) and truncation bias (limitation due to tools resolution). Then, the scale range of observations did not extend two orders of magnitude as suggested by Bonnet et al. (2001). Despite this limitation, the specific trend for F2 fractures distribution may be explained by the relative timing of fracture formation. If F2 fractures lengths are constrained by F1 spacing, F2 spacing may not be scale invariant. This further support the possibility of a successive formation of F1 and F2 fractures.

**Insert fig. 10 here.**

All experimental variograms of the fracture sets obtained from horizontal legs of wells A, B and C show nugget values much lower than the variance of the entire sample (Fig. 11), implying that there is a correlation in fracture spacing. Therefore, fracture distributions display some clustering. F1 fractures display ranges values between 30 and 150 m. Variograms for the F2 and F3 set display ranges from 12 to 30 m, and 60 to 100 m respectively. Some concentration of F1 fractures (with significantly higher F1 fracture frequencies than other fracture sets) were identified in the horizontal well A (in the Utica Shale). This high frequency of F1 fractures is consistent with outcrop observations where F1 fractures spacing are lower than F2 and F3 spacing. This may be interpreted as the presence of F1 fractures corridors (see for instance Fig. 12: F1 fractures are closely spaced on distances of around 40 m and separated by approximately 100 to 200 m).

**Insert fig. 11 and 12 here.**

In the deep zone, fracture density vertical profiles generally display localized fractured intervals separated by vertical distances ranging from 10 m to 300 m. Fig. 13 only presents the fracture density and Brittleness Index (BI) variation with depth for well B, but they can be considered representative of those found in wells A and C. Higher fracture densities and BI values were generally measured in the Utica Shale. This suggests that these two parameters could be correlated. In specific depth intervals in well B, some high fracture densities values correlates with low BI values (see the contact between the Upper and Lower Utica in Fig. 13). Geomechanical contrasts in the vicinity of these lithological contacts may explain the occurrence of these higher fracture density intervals.

**Insert fig. 13 here.**

### 4.2 *Fractures in siltstone interbeds*

Data from outcrops showed that the siltstone interbeds are crosscut by the same fracture sets as those cutting across the shale (F1, F2 and F3) (Fig. 14a and b). However, contrary to shale units, fractures are stratabound in siltstone units, with only a few F1 fractures intersecting both siltstone and shale beds (Fig. 14c). F1 fractures are also generally longer than F2 fractures. F2 fractures abut F1 fractures and F2 fracture lengths generally equal to F1 fracture spacings (Fig. 14b). Fracture density in the siltstone beds is significantly higher than in shale intervals, with spacings lower than 1 m for both F1 and F2 fracture sets. Fractures were regularly spaced all along the outcrops. There is also a strong correlation between siltstone bed thickness and fracture spacing as shown in Fig. 15b. The calculated ratios of fracture spacing to layer thickness are respectively 1.29 and 1.43 for the F1 and F2 fracture sets.

**Insert fig. 14 and 15 here.**

# 5 Discussion

## 5.1 *Fracture pattern*

### *5.1.1 Main controls on fracture distributions*

The differences in fracture distribution between the Lorraine Group shales and the Lorraine Group siltstones, and also between the Lorraine Group shales and the Utica Shale, suggest that these distributions are lithologically controlled.

Differences in fracture distributions were observed between shales and siltstones of the Lorraine Group. In Lorraine Group shales, the F1 spacing is lower than the F2 spacing (see a visual example in Fig. 6b) and F1 and F2 fracture are probably organized in corridors. In siltstone units of the Lorraine Group, F1 and F2 fractures are more homogeneously distributed and display equivalent spacing values (see a visual example in Fig. 14). Fractures in siltstone units are also limited by the bed thickness (which rarely exceeds 1 to 2 m) and this parameter is correlated with fracture spacing (Fig. 15); this was also observed in many sedimentary basins (Bai et al., 2000; Gross, 1993; Ji and Saruwatari, 1998; Ladeira and Price, 1981; Narr and Suppe, 1991). It was thus possible to evaluate the fracture saturation in siltstones, based on estimated fracture spacing to layer thickness ratios. According to the threshold interval of ratio values (0.8 to 1.2) proposed in Bai and Pollard (2000) and Bai et al. (2000), F1 and F2 fracture spacing would be at saturation in siltstone units (ratios of 1.29 and 1.43 respectively above the threshold interval of ratio values). Contrasts in mechanical properties between shales and sandstones (the sandstone being more brittle with a higher Young's modulus) induce a preferential fracturing of sandstones (Engelder, 1985; Laubach et al., 2009). This could explain the higher observed fractures densities in the siltstones of the SLP. However, this must be considered cautiously as mechanical property differences between siltstone and shale units were not estimated throughout the SLP. This estimation is challenged by the presence of a significant amount of clay in both units (Séjourné et al., 2013); see also the low BI variations in the proximity of siltstone/shale contacts (Fig. 13).

In the vertical sections of deep shale gas wells (depths > 500 m), higher fracture densities were measured in the Utica Shale compared to the Lorraine Group shales (Fig. 13). This is in agreement with the highly fractured horizontal portions of the shale gas wells completed into the Utica Shale compared to the lower density of steeply-dipping fractures observed in the outcropping Lorraine Group units. In contrast, fracture spacing and strike direction values are similar in the outcropping Lorraine Group units and in the deep Utica Shale (Fig. 7 and Fig. 9). This could be interpreted as fracture corridors being more common in the Utica Shale compared to caprock units. Therefore, when drilling a well through the entire sedimentary succession, there is higher probability of intersecting fracture swarms in the Utica Shale than in overlying units. The Utica Shale is more calcareous than the clayey Lorraine Group shale (Globensky, 1987; Lavoie et al., 2008; Theriault, 2012) resulting in overall higher Brittleness Index (BI) values for the Utica

Shale than the overlying shale units (Séjourné, 2017). Brittle shale units are more likely to be affected by a dense natural fracture network than ductile shale (Ding et al., 2012; Lai et al., 2015).

#### *5.1.2 Use of analogs to characterize the caprock*

The relationships between the three fracture sets (F1, F2 and F3) and the two regional fold generations was assessed by applying a fold test on shallow fractures. This analysis supports a syn- to post F-II folding origin for the F3 set. Conversely, the F1 and F2 fractures were probably developed before (or possibly during for F2) the main deformation/folding episodes that shaped-up the SLP (F-II and F-I folds). Therefore, the nowadays shallow structures should have been formed at depth before the removal of the overburden by erosion. The presence at reservoir depths of F3 fractures also discards their potential shallow formation after erosion.

Vitrinite reflectance data has shown that, at least regionally, around 5 km of overburden have been eroded in the SLP (Héroux and Bertrand, 1991; Yang and Hesse, 1993). At these depths, the fractures propagate according to the regional stress field orientation and thus display common orientations. Because shallow and deep fracture networks display common characteristics (especially in terms of fracture attitudes and spacing) and because of the burial history of the Saint-Édouard area, it is suggested that shallow fractures in shallow units were formed at depth and hence, had recorded the same tectonic events as fractures in deep units. Consequently, shallow and deep observations can be used to assess the fracture pattern in the intermediate zone.

No conclusion can be drawn regarding the initiating mechanism for fracture propagation. The latter could result from an increase of the greatest compressive stress during regional shortening, a decrease in the least compressive stress caused by regional extension, or an increase in pore pressure (which could also be associated with the first two mechanisms). It must be noted that an abnormal pore pressure related to the thermal maturation of organic matter is more likely to have occurred in the Lotbinière Formation, Les Fonds Formation and Utica Shale, as these units display higher organic content than the Lorraine Group units (Haeri-Ardakani et al., 2015; Lavoie et al., 2016). In the Lotbinière Formation, the crosscutting relationship between fractures and calcareous concretions indicated that some fractures could have been initiated in a context of abnormal pore pressure.

The use of analogs can be controversial if the regional geologic history is not well understood. The presence of shallow unloading fractures that display the same attitudes as some of the deep fractures is not discarded. Nonetheless, as a deep fracture dataset was available in the area, it was possible to infer that the density of possible shallow unloading fractures (developed under the control of either thermal-elastic contraction during uplift or erosion) is likely marginal, as fracture spacings are comparable in both shallow and deep intervals.

#### *5.1.3 Conceptual models*

In the Saint-Édouard area, the steeply-dipping fractures and BPF are assumed to be pervasive throughout the sedimentary succession, from the shallow aquifers to the gas reservoir (Utica Shale) and hence, throughout the intermediate zone. The F1 and F2 sets are orthogonal to each other and to the bedding planes. F1 fractures may be concentrated in corridors but this pattern remains to be confirmed. F1 and F2 fracture sets are also present in siltstone units and observations on outcrops showed that these sets are more homogeneously distributed in this unit (similar F1 and F2 spacing values). A third fracture set (F3) was observed in the Utica Shale and locally in the Lorraine Group, where these fractures are more sparsely distributed. A fourth set, corresponding to BPF, was only observed in shallow shale units within the upper 60 m of bedrock. The observation of BPF was easier at shallow depth because their aperture is enhanced in this interval, probably as a consequence of glaciations/de-glaciations events or de-compaction in a context of erosion and uplift. However, some BPF should exist at depth in the study area as in many other shale successions (Gale et al., 2015; Gale et al., 2016; Wang and Gale, 2016).

A conceptual model integrating all the elements acquired about the fracture pattern affecting the sedimentary succession of the Saint-Édouard area is proposed in Fig. 16. Schematics of the fracture network were developed using two scales to better represent their characteristics and features: the mesoscale (1 km blocks in Fig. 16a, b and c) and the metric (local) scale (Fig. 16d and e). The size of the metric scale blocks corresponds to the representative elementary volume (REV) of the fracture network that affects each lithological unit (shale or siltstone). A REV is defined as the minimum volume of sampling domains beyond which its characteristics remain constant (Bear, 1972). The REV properties could be used to further explore the hydraulic controls of this fracture network in numerical models with a Discrete Fracture Networks (DFN) approach. For stratabound fractures, such as those in the siltstone units, the size of the REV (a metric scale block) should be at least one or two times larger than the mean fracture spacing (Odling et al., 1999). Thus, for the highly fractured siltstone units, a REV of 0.5 m size can be defined (Fig. 16e). For non-stratabound systems, such as in the shale units, it is recommended to define a REV larger than the maximum mean trace length of fractures (Voeckler, 2012); in fact, a size at least three times larger than the mean trace is suggested (Oda, 1985, 1988). The approximate maximum mean fracture length observed in shale units is 5 m. For this reason, a 15 m long REV is proposed (Fig. 16d). However, due to the lack of large outcropping areas in the Saint-Édouard area, more fracture length measurements would be recommended in neighbouring areas for a finer estimation of the REV dimensions in shale units. It must be kept in mind that these REV are theoretical volumes that could not exist in the field due to the complexity and continuity of fluid flow circulation in the fracture network (Kulatilake and Panda, 2000; Neuman, 1988). However, in a context of low porosity and permeability rock in the SLP (BAPE 2010; Séjourné, 2015; Séjourné et al., 2013), fluid circulation can only be envisioned through open fractures and very little within the matrix. Therefore, the definition of a REV is simply a first step to better assess the control of fractures on fluid flow.

**Insert fig. 16 here.**

## 5.2 *Implications for the assessment of potential upward fluid migration*

### *5.2.1 Limits of the conceptual model*

In the Saint-Édouard area, the caprock and shale gas reservoir are affected by several fracture sets that are pervasive throughout the region and the entire stratigraphic succession. The experimental variograms showed that fractures are clustered and the parameters extracted from semi-variograms could be used for other studies to generate simulation of stochastic fracture networks fracture (in DFN models for example). Scale-dependant change in structure, such as the existence of fracture corridors, could not be identified using these variogram as this approach assumes that fracture spacing is a scale-independent continuous variable. As a consequence to further assess the heterogeneity of this fracture pattern, gains could be obtained by the use of parameters such as lacunarity which describes the scale-dependant changes in fracture patterns (Roy, 2013; Roy et al., 2014). For the specific case of the Saint-Édouard area, more field data would be necessary to rigorously document this entire range of heterogeneity. At regional scale, the progressive deepening of the platform to the southeast may also have had a control on small and large scale fracturing but it could not be confirmed with the existing datasets in the studied area.

In addition, the outcropping areas were limited in size and number and borehole data cannot provide any direct observation of fracture lengths. As a consequence, the vertical extension of fractures, and thus the vertical continuity of the fracture network between the deep gas reservoir and shallow aquifers cannot be undoubtedly determined solely based on the currently available structural datasets. This highlights the limits of using analogs when regarding to the potential existence of large-scale preferential fluid flow pathways in a sedimentary succession. However, the approach is particularly useful in fracture network characterisation studies, to make up for the frequent lack of data in some specific geological intervals.

#### *5.2.2 New insights for the assessment of potential upward fluid migration*

As direct observations of the vertical extent of structural discontinuities are challenged by the limits of the available datasets and methods, data from other fields should be acquired to assess the potential of upward fluid migration through the caprock. For instance, isotopic signatures of gas in both rock and groundwater would provide good indicators to identify a potential hydraulic connection between the deep reservoir and the surficial aquifers. In addition, the assessment of the geomechanical properties of the different units within the intermediate zone would provide evidence of the presence or absence of ductile strata that would control the fracture length. To further explore the hydraulic controls imposed by the presence of fractures and faults, one should also consider the four following points: 1) the role of individual fractures on fluid flow and especially their aperture throughout the stratigraphy; 2) the existence of open fractures associated with regional-scale structural discontinuities, such as fault damage zones; 3) the evaluation of hydraulic properties of these regional-scale features; 4) the driving mechanisms that would support upward fluid flow in these pathways (if any) throughout the entire stratigraphic succession (deep shale gas reservoir, intermediate zone and shallow aquifers).

## 6 Conclusion

The natural fracture pattern in both the shallow aquifers and the deep shale gas reservoir of the Saint-Édouard area was characterized using a combination of fracture data from outcrops and well logs (acoustic, optical and micro-resistivity). Three steeply-dipping fracture sets, as well as bedding-parallel fractures were documented. The three high-angle fracture sets are common to both shallow and deep units with similar characteristics such as fracture attitude and spacing. For this reason and based on the regional geologic history, these fracture sets could be used as analogs for those within the intermediate zone for which little to no data were available. These fracture sets are pervasive throughout the region, but they are heterogeneously distributed. Conceptual models of the fracture pattern were developed at metric to kilometric scales. Nonetheless, due to the limitations of the observation methods and the near absence of data for the intermediate zone, the vertical extension of natural fractures, which represents a critical parameter for aquifer vulnerability, still remains elusive. The comprehensive assessment of the caprock integrity should also be based on geomechanical properties of the different caprock units, on gas and groundwater geochemistry to provide evidence for potential upward migration and on the definition of potential hydraulic properties of fractures, fault planes and associated damage zones identified in the Saint-Édouard area, as well as their *in situ* hydrological conditions.

This paper highlighted the benefits of combining datasets from the shallow and deep intervals in fracture network characterization. It also pointed out the limitations of using analogs to assess the potential impacts of shale gas activities on shallow fresh groundwater. Even if these results are strictly valid for the Saint-Édouard area, the methodology used to characterize the fracture network in the caprock interval using geoscience data from the shallow and deep geological intervals could be used in other shale gas plays where lithologies are dominated by shale units. The approach could also be used in other fields, such as in geothermal energy or deep geological carbon sequestration projects, where the fracture pattern and the integrity of a rock mass relative to fluid flow must be assessed.

## Acknowledgments

This project was part of the Environmental Geoscience Program of Natural Resources Canada. It also benefited from funding from the Energy Sector through the Eco-EII and PERD programs. The authors wish to thank Talisman Energy (now Repsol Oil & Gas Canada) and especially Marianne Molgat, as well as Charles Lamontagne of the Ministère du Développement durable, de l'Environnement et de la Lutte contre les Changements climatiques (MDDELCC) du Québec for providing well logs data. The land owners are also thanked for the access to outcrops and drilling sites. Authors are very grateful to André Guy Tranquille Temgoua, Xavier Malet and Elena Konstantinovskaya for field support. Authors wish to thank Nicolas Pinet for his careful review of the manuscript and relevant comments. Erwan Gloaguen is also thanked for his helpful comments. This paper is GSC contribution 33012.

## References


Antonellini, M., Mollema, P.N., 2000. A natural analog for a fractured and faulted reservoir in dolomite: Triassic Sella Group, northern Italy. AAPG Bulletin 84, 314-344.

Bai, T., Pollard, D.D., 2000. Fracture spacing in layered rocks: a new explanation based on the stress transition. Journal of Structural Geology 22, 43-57.

Bai, T., Pollard, D.D., Gao, H., 2000. Explanation for fracture spacing in layered materials. Nature 403, 753-756.

BAPE, 2010. Comparaison des shales d'Utica et de Lorraine avec des shales en exploitation, Réponse de la l'APGQ aux questions de la Commission du BAPE sur les gaz de schiste. Available at: http://www.bape.gouv.qc.ca/sections/mandats/Gaz_de_schiste/documents/DB25%20tableau%20de%20shales.pdf (accessed february 2017). Bureau d'Audiences Publiques sur l'Environnement (BAPE) DB25.

Barton, A., Hickman, S., Morin, R., 1998. Reservoir-Scale fracture permeability in the Dixie Valley, Nevada, geolthermal field Twenty-Third Workshop on Geothermal Reservoir Engineering SGP-TR-158, 299-306.

Bear, J., 1972. Dynamics of fluids in porous media. Dover Publications, inc., New York.

Belt, E.S., Riva, J., Bussières, L., 1979. Revision and correlation of late Middle Ordovician stratigraphy northeast of Quebec City. Canadian Journal of Earth Sciences 16, 1467-1483.

Berkowitz, B., 2002. Characterizing flow and transport in fractured geological media: A review. Advances in Water Resources 25, 861-884.

Bonnet, E., Bour, O., Odling, N.E., Davy, P., Main, I., Cowie, P., Berkowitz, B., 2001. Scaling of fracture systems in geological media. Reviews of Geophysics - AGU 39, 3.

Caine, J.S., Tomusiak, S.R.A., 2003. Brittle structures and their role in controlling porosity and permeability in a complex Precambrian crystalline-rock aquifer system in the Colorado Rocky Mountain Front Range. Geological Society of America Bulletin 115, 1410-1424.

Castonguay, S., Dietrich, J., Lavoie, D., Laliberté, J.-Y., 2010. Structure and petroleum plays of the St. Lawrence Platform and Appalachians in southern Quebec: insights from interpretation of MRNQ seismic reflection data. Bulletin of Canadian Petroleum Geology 58, 219-234.

Castonguay, S., Dietrich, J., Shinduke, R., Laliberté, J.-Y., 2006. Nouveau regard sur l'architecture de la Plate-forme du Saint-Laurent et des Appalaches du sud du Québec par le retraitement des profils de sismique réflexion M-2001, M-2002 et M-2003. Commission géologique du Canada, Dossier Public 5328, 19.

Castonguay, S., Séjourné, S., Dietrich, J., 2003. The Appalachian structural front in southern Quebec: Seismic and field evidence for complex structures and a triangle zone at the edge of the foreland thrust belt:. First annual joint meeting of the Geological Society of America – Northeastern Section and the Atlantic Geoscience Society, Halifax 2003, On line: http://gsa.confex.com/gsa/2003NE/finalprogram/abstract_51232.htm.

Castonguay, S.b., Ruffet, G., Tremblay, A., F├⌐raud, G., 2001. Tectonometamorphic evolution of the Southern Quebec Appalachians: 40Ar/39 Ar evidence for Middle Ordovician crustal thickening and Silurian-Early Devonian exhumation of the internal Humber zone. 113, 144-160.

CCA, 2014. Environmental impacts of shale gas extraction in Canada. Available at http://www.scienceadvice.ca/uploads/eng/assessments%20and%20publications%20and%20news%20releases/shale%20gas/shalegas_fullreporten.pdf (accessed february 2017). Council of Canadian Academies (CCA), 292.

Chilès, J., 1988. Fractal and geostatistical methods for modeling of a fracture network. Mathematical Geology 20, 631-654.

Clark, T.H., Globensky, Y., 1973. Portneuf et parties de St-Raymond et de Lyster - Comtés de Portneuf et de Lotbinière. Ministère des Richesses Naturelles, Direction Générale des Mines, Rapport Géologique 148.

Clark, T.H., Globensky, Y., 1976. Région de Bécancour. 165.

Comeau, F.A., Kirkwood, D., Malo, M., Asselin, E., Bertrand, R., 2004. Taconian mélanges in the parautochthonous zone of the Quebec Appalachians revisited: implications for foreland basin and thrust belt evolution. Canadian Journal of Earth Sciences 41, 1473-1490.

Crow, H.L., Ladevèze, P., 2015. Downhole geophysical data collected in 11 boreholes near St.-Édouard-de-Lotbinière, Québec. Geological Survey of Canada, Open File 7768, 48.

Dershowitz, B., LaPointe, P., Eiben, T., Wei, L., 1998. Integration of Discrete Feature Network Methods with Conventional Simulator Approaches. Society of Petroleum Engineers SPE-49069-MS.

Dietrich, J., Lavoie, D., Hannigan, P., Pinet, N., Castonguay, S., Giles, P., Hamblin, A.P., 2011. Geological setting and resource potential of conventional petroleum plays in Paleozoic basins in eastern Canada. Bulletin of Canadian Petroleum Geology 59, 54-84.

Ding, W., Li, C., Li, C., Xu, C., Jiu, K., Zeng, W., Wu, L., 2012. Fracture development in shale and its relationship to gas accumulation. Geoscience Frontiers 3, 97-105.

Engelder, T., 1985. Loading paths to joint propagation during a tectonic cycle: an example from the Appalachian Plateau, U.S.A. Journal of Structural Geology 7, 459-476.

English, J.M., 2012. Thermomechanical origin of regional fracture systems. AAPG Bulletin 96, 1597-1625.

EPA, 2016. Hydraulic Fracturing for Oil and Gas: Impacts from the Hydraulic Fracturing Water Cycle on Drinking Water Resources in the United States (Final Report). Available at: www.epa.gov/hfstudy (accessed february 2017). U.S. Environmental Protection Agency (EPA), Washington, DC EPA/600/R-16/236F, 666.

Escuder Viruete, J., Carbonell, R., Jurado, M.J., Martí, D., Pérez-Estaún, A., 2001. Two-dimensional geostatistical modeling and prediction of the fracture system in the Albala Granitic Pluton, SW Iberian Massif, Spain. Journal of Structural Geology 23, 2011-2023.

Faure, S., Tremblay, A., Malo, M., 2004. Reconstruction of Taconian and Acadian paleostress regimes in the Quebec and northern New Brunswick Appalachians. Canadian Journal of Earth Sciences 41, 619-634.

Fiore Allwardt, P., Bellahsen, N., Pollard, D.D., 2007. Curvature and fracturing based on global positioning system data collected at Sheep Mountain anticline, Wyoming. Geosphere 3, 408-421.

Fisher, R., 1953. Dispersion on a Sphere. Proceedings of the Royal Society of London A: Mathematical, Physical and Engineering Sciences 217, 295-305.

Gale, J., Ukar, E., Elliott, S.J., Wang, Q., 2015. Bedding-Parallel Fractures in Shales: Characterization, Prediction and Importance, AAPG Annual Convention and Exhibition, Denver, CO., USA, May 31 - June 3, 2015.

Gale, J.F., Ukar, E., Wang, Q., Elliott, S.J., 2016. Bedding-Parallel Fractures in Shales, AAPG Annual Convention and Exhibition, Calgary, Alberta, Canada, June 22, 2016.

Gale, J.F.W., Laubach, S.E., Olson, J.E., Eichhubl, P., Fall, A., 2014. Natural fractures in shale: A review and new observations. AAPG Bulletin 98, 2165-2216.

Gillespie, P.A., Walsh, J.J., Watterson, J., Bonson, C.G., Manzocchi, T., 2001. Scaling relationships of joint and vein arrays from The Burren, Co. Clare, Ireland. Journal of Structural Geology 23, 183-201.

Globensky, Y., 1987. Géologie des Basses Terres du Saint-Laurent. Direction Générale de l'Exploration Géologique et minérale du Québec, Gouvernement du Québec MM 85-02.

Glorioso, J.C., Rattia, A., 2012. Unconventional reservoirs: Basic petrophysical concepts for shale gas, SPE/EAGE European Unconventional Resources Conference & Exhibition-From Potential to Production. SPE, Vienna, Austria.

Grieser, W.V., Bray, J.M., 2007. Identification of Production Potential in Unconventional Reservoirs, Production and Operations Symposium. Society of Petroleum Engineers, Oklahoma City, Oklahoma, U.S.A. .

Gross, M.R., 1993. The origin and spacing of cross joints: examples from the Monterey Formation, Santa Barbara Coastline, California. Journal of Structural Geology 15, 737-751.

Guerriero, V., Mazzoli, S., Iannace, A., Vitale, S., Carravetta, A., Strauss, C., 2013. A permeability model for naturally fractured carbonate reservoirs. Marine and Petroleum Geology 40, 115-134.

Haeri-Ardakani, O., Sanei, H., Lavoie, D., Chen, Z., Jiang, C., 2015. Geochemical and petrographic characterization of the Upper Ordovician Utica Shale, southern Quebec, Canada. International Journal of Coal Geology 138, 83-94.

Hamblin, A.P., 2006. The “Shale Gas” concept in Canada: a preliminary inventory of possibilities. Geological Survey of Canada, Open File 5389, 103.

Heidbach, O., Tingay, M., Barth, A., Reinecker, J., Kurfeß, D., Müller, B., 2009. The World Stress Map, in: 2008, S.E.b.o.t.W.d.r. (Ed.). Helmholtz Centre Potsdam - GFZ German Research Centre for Geosciences, Commission de la Carte Géologique du Monde / Commission for the Geological Map of the World.

Héroux, Y., Bertrand, R., 1991. Maturation thermique de la matière organique dans un bassin du Paléozoïque inférieur, Basses-Terres du Saint-Laurent, Québec, Canada. Canadian Journal of Earth Sciences 28, 1019-1030.

Ji, S., Saruwatari, K., 1998. A revised model for the relationship between joint spacing and layer thickness. Journal of Structural Geology 20, 1495-1508.

Konstantinovskaya, E., Malo, M., Castillo, D.A., 2012. Present-day stress analysis of the St. Lawrence Lowlands sedimentary basin (Canada) and implications for caprock integrity during CO2 injection operations. Tectonophysics 518-521, 119-137.

Konstantinovskaya, E., Rodriguez, D., Kirkwood, D., Harris, L., Thériault, R., 2009. Effects of basement structure, sedimentation and erosion on thrust wedge geometry: an example from the Quebec Appalachians and analogue models. Bulletin of Canadian Petroleum Geology 57, 34-62.

Kulatilake, P.H.S.W., Panda, B.B., 2000. Effect of Block Size and Joint Geometry on Jointed Rock Hydraulics and REV. Journal of Engineering Mechanics 126.

Ladeira, F.L., Price, N.J., 1981. Relationship between fracture spacing and bed thickness. Journal of Structural Geology 3, 179-183.

Lai, J., Wang, G., Huang, L., Li, W., Ran, Y., Wang, D., Zhou, Z., Chen, J., 2015. Brittleness index estimation in a tight shaly sandstone reservoir using well logs. Journal of Natural Gas Science and Engineering 27, Part 3, 1536-1545.

Larsen, B., Grunnaleite, I., Gudmundsson, A., 2010. How fracture systems affect permeability development in shallow-water carbonate rocks: An example from the Gargano Peninsula, Italy. Journal of Structural Geology 32, 1212-1230.

Laubach, S.E., Olson, J.E., Gross, M.R., 2009. Mechanical and fracture stratigraphy. AAPG Bulletin 93, 1413-1426.

Lavenu, A.P., Lamarche, J., Gallois, A., Gauthier, B.D., 2013. Tectonic versus diagenetic origin of fractures in a naturally fractured carbonate reservoir analog (Nerthe anticline, southeastern France). AAPG Bulletin 97, 2207-2232.

Lavoie, D., 2008. Chapter 3 Appalachian Foreland Basin of Canada, in: Andrew, D.M. (Ed.), Sedimentary Basins of the World. Elsevier, pp. 65-103.

Lavoie, D., Desrochers, A., Dix, G., Knight, I., Salad Hersi, O., 2012. The Great American Carbonate Bank in Eastern Canada: An Overview. In: Derby, J.R., Fritz, R.D., Longacre, S.A., Morgan, W.A., Sternbach, C.A. (Eds.), The Great American Carbonate Bank. The Geology and Economic Resources of the Cambrian–Ordovician Sauk Megasequence of Laurentia. AAPG Memoirs 98, 499-523.

Lavoie, D., Hamblin, A.P., Theriault, R., Beaulieu, J., Kirkwood, D., 2008. The Upper Ordovician Utica Shales and Lorraine Group flysch in southern Québec: Tectonostratigraphic setting and significance for unconventional gas. Commission géologique du Canada, Open File 5900, 56.

Lavoie, D., Pinet, N., Bordeleau, G., Ardakani, O.H., Ladevèze, P., Duchesne, M.J., Rivard, C., Mort, A., Brake, V., Sanei, H., Malet, X., 2016. The Upper Ordovician black shales of southern Quebec (Canada) and their significance for naturally occurring hydrocarbons in shallow groundwater. International Journal of Coal Geology 158, 44-64.

Lavoie, D., Rivard, C., Lefebvre, R., Séjourné, S., Thériault, R., Duchesne, M.J., Ahad, J.M.E., Wang, B., Benoit, N., Lamontagne, C., 2014. The Utica Shale and gas play in southern Quebec: Geological and hydrogeological syntheses and methodological approaches to groundwater risk evaluation. International Journal of Coal Geology 126, 77-91.

Lefebvre, R., 2016. Mechanisms leading to potential impacts of shale gas development on groundwater quality. Wiley Interdisciplinary Reviews: Water, n/a-n/a.

McConaughy, D.T., Engelder, T., 1999. Joint interaction with embedded concretions: joint loading configurations inferred from propagation paths. Journal of Structural Geology 21, 1637-1652.

Meng, F., Zhou, H., Zhang, C., Xu, R., Lu, J., 2015. Evaluation Methodology of Brittleness of Rock Based on Post-Peak Stress–Strain Curves. Rock Mech Rock Eng 48, 1787-1805.

Miller, S.M., 1979. Determination of spatial dependence in fracture set characteristics by geostatistical methods, Department of mining and geological engineering. The University of Arizona, p. 122.

Min, K.-B., Jing, L., Stephansson, O., 2004. Determining the equivalent permeability tensor for fractured rock masses using a stochastic REV approach: Method and application to the field data from Sellafield, UK. Hydrogeology Journal 12, 497-510.

Mozley, P.S., Davis, J.M., 2005. Internal structure and mode of growth of elongate calcite concretions: Evidence for small-scale, microbially induced, chemical heterogeneity in groundwater. Geological Society of America Bulletin 117, 1400-1412.

Narr, W., Schechter, D.W., Thompson, L.B., 2006. Naturally fractured reservoir characterization. Richardson, TX: Society of Petroleum Engineers.

Narr, W., Suppe, J., 1991. Joint spacing in sedimentary rocks. Journal of Structural Geology 13, 1037-1048.

Neuman, S.P., 1988. Stochastic Continuum Representation of Fractured Rock Permeability as an Alternative to the REV and Fracture Network Concepts, in: Custodio, E., Gurgui, A., Ferreira, J.P.L. (Eds.), Groundwater Flow and Quality Modelling. Springer Netherlands, Dordrecht, pp. 331-362.

Oda, M., 1985. Permeability tensor for discontinuous rock masses. Geotechnique 35, 483-495.

Oda, M., 1988. A method for evaluating the representative elementary volume based on joint survey of rock masses. Canadian Geotechnical Journal 25, 440-447.

Odling, N.E., Gillespie, P., Bourgine, B., Castaing, C., Chiles, J.P., Christensen, N.P., Fillion, E., Genter, A., Olsen, C., Thrane, L., Trice, R., Aarseth, E., Walsh, J.J., Watterson, J., 1999. Variations in fracture system geometry and their implications for fluid flow in fractures hydrocarbon reservoirs. Petroleum Geoscience 5, 373-384.

Ogunyomi, O., Hesse, R., Heroux, Y., 1980. Pre-Orogenic and Synorogenic Diagenesis and Anchimetamorphism in Lower Paleozoic Continental Margin Sequences of the Northern Appalachians in and Around Quebec City, Canada. Bulletin of Canadian Petroleum Geology 28, 559-577.

Park, H.J., West, T.R., 2002. Sampling bias of discontinuity orientation caused by linear sampling technique. Engineering Geology 66, 99-110.

Pinet, N., 2011. Deformation in the Utica Shale and Lorraine Group, Saint Lawrence Lowlands, Québec. Geological Survey of Canada, Open File 6952, 12.

Pinet, N., Duchesne, M., Lavoie, D., Bolduc, A.e., Long, B., 2008. Surface and subsurface signatures of gas seepage in the St. Lawrence Estuary (Canada): Significance to hydrocarbon exploration. Marine and Petroleum Geology 25, 271-288.

Pinet, N., Lavoie, D., Keating, P., Duchesne, M., 2014. The St Lawrence Platform and Appalachian deformation front in the St Lawrence Estuary and adjacent areas (Quebec, Canada): structural complexity revealed by magnetic and seismic imaging. Geological Magazine 151, 996-1012.

Rivard, C., Lavoie, D., Lefebvre, R., Séjourné, S., Lamontagne, C., Duchesne, M., 2014. An overview of Canadian shale gas production and environmental concerns. International Journal of Coal Geology 126, 64-76.

Roy, A., 2013. Scale-dependent heterogeneity in fracture data sets and grayscale images. The University of Tennessee.

Roy, A., Perfect, E., Dunne, W.M., McKay, L.D., 2014. A technique for revealing scale-dependent patterns in fracture spacing data. Journal of Geophysical Research: Solid Earth 119, 5979-5986.

Sasseville, C., Clauer, N., Tremblay, A., 2012. Timing of fault reactivation in the upper crust of the St. Lawrence rift system, Canada, by K–Ar dating of illite-rich fault rocks1. Canadian Journal of Earth Sciences 49, 637-652.

Sasseville, C., Tremblay, A., Clauer, N., Liewig, N., 2008. K–Ar age constraints on the evolution of polydeformed fold–thrust belts: The case of the Northern Appalachians (southern Quebec). Journal of Geodynamics 45, 99-119.

Séjourné, S., 2015. Caractérisation des réseaux de fractures naturelles, de la porosité et de la saturation en eau du Shale d'Utica et de sa couverture par l'analyse des diagraphies de forages pétroliers dans la région de Saint-Édouard, Québec. Commission Géologique du Canada, Dossier Public 7980, 60.

Séjourné, S., 2017. Étude géomécanique du Shale d’Utica et de sa couverture d’après les puits pétroliers et gaziers de la région de Saint-Édouard-de-Lotbinière, Québec. Commission Géologique du Canada, Dossier Public 8196, 54.

Séjourné, S., Dietrich, J., Malo, M., 2003. Seismic characterization of the structural front of southern Quebec Appalachians. Bulletin of Canadian Petroleum Geology 51, 29-44.

Séjourné, S., Lefebvre, R., Malet, X., Lavoie, D., 2013. Synthèse géologique et hydrogéologique du Shale d'Utica et des unités sus-jacentes (Lorraine, Queenston et dépots meubles), Basses-Terres du Saint-Laurent, Québec. Commission Géologique du Canada, Dossier Public 7338, 165.

Sikander, A., Pittion, J., 1978. Reflectance studies on organic matter in lower Paleozoic sediments of Quebec. Bulletin of Canadian Petroleum Geology 26, 132-151.

Singhal, B.B.S., Gupta, R.P., 2010. Applied Hydrogeology of Fractured Rocks. Springer Netherlands.

St-Julien, P., Hubert, C., 1975. Evolution of the Taconian orogen in the Quebec Appalachians. American Journal of Science 275-A, 337-362.

St-Julien, P., Slivitsky, A., Feininger, T., 1983. A deep structural profile across the Appalachians of southern Quebec. Geological Society of America Memoirs 158, 103-112.

Stesky, M., 2010. Pangea Scientific - Spheristat Version 3.1 - User's Manual.

Surrette, M., Allen, D.M., Journeay, M., 2008. Regional evaluation of hydraulic properties in variably fractured rock using a hydrostructural domain approach. Hydrogeology Journal 16, 11-30.

Tavchandjian, O., Rouleau, A., Archambault, G., Daigneault, R., Marcotte, D., 1997. Geostatistical analysis of fractures in shear zones in the Chibougamau area: applications to structural geology. Tectonophysics 269, 51-63.

Terzaghi, R.D., 1965. Sources of error in joint surveys. Geotechnique 15 (3), 287-304.

Theriault, R., 2012. Caractérisation du Shale d'Utica et du Groupe de Lorraine, Basses-Terres du Saint-Laurent - Partie 2 : Interprétation Géologique, in: Québec, M.d.R.N.e.F. (Ed.), p. 80.

Thériault, R., 2007. Trenton/Black River Hydrothermal Dolomite Reservoirs in Québec: The Emergence of a New and Highly Promising Play along the St. Lawrence Platform. American Association of Petroleum Geologists. Eastern Section Annual Meeting, Abstract with Programs 57.

Tremblay, A., Pinet, N., 2016. Late Neoproterozoic to Permian tectonic evolution of the Quebec Appalachians, Canada. Earth-Science Reviews 160, 131-170.

Tremblay, A., Roden-Tice, M.K., Brandt, J.A., Megan, T.W., 2013. Mesozoic fault reactivation along the St. Lawrence rift system, eastern Canada: Thermochronologic evidence from apatite fission-track dating. Geological Society of America Bulletin 125, 794-810.

Valley, B.C., 2007. The relation between natural fracturing and stress heterogeneities in deep-seated crystalline rocks at Soultz-sous-Forêts (France). Swiss Federal Institute of Technology (ETH), Zurich, p. 277.

Villaescusa, E., Brown, E.T., 1990. Characterizing joint spatial correlations using geostatistical methods, in: C. A. Barton and O. Stephansson, B. (Ed.), Rock Joints.

Vitale, S., Dati, F., Mazzoli, S., Ciarcia, S., Guerriero, V., Iannace, A., 2012. Modes and timing of fracture network development in poly-deformed carbonate reservoir analogues, Mt. Chianello, southern Italy. Journal of Structural Geology 37, 223-235.

Voeckler, H., 2012. Modeling deep groundwater flow throught fractured bedrock in a mountainous headwater catchment using a coupled surface water-groundwater model, Okanagan basin, British Columbia. The University of British Columbia, Vancouver, p. 433.

Wang, D., Ge, H., Wang, X., Wang, J., Meng, F., Suo, Y., Han, P., 2015. A novel experimental approach for fracability evaluation in tight-gas reservoirs. Journal of Natural Gas Science and Engineering 23, 239-249.

Wang, Q., Gale, J.F., 2016. Characterizing Bedding-Parallel Fractures in Shale: Aperture-Size Distributions and Spatial Organization, AAPG Annual Convention and Exhibition, Calgary, Alberta, Canada, June 22, 2016.

Wu, H., D. Pollard, D., 1995. An experimental study of the relationship between joint spacing and layer thickness. Journal of Structural Geology 17, 887-905.

Yang, C., Hesse, R., 1993. Diagenesis and anchimetamorphism in an overthrust belt, external domain of the Taconian Orogen, southern Canadian Applachians-II. Paleogeothermal gradients derived from maturation of different types of organic matter. Organic Geochemistry 20, 381-403.

Zoback, M.L., 1992. First- and second-order patterns of stress in the lithosphere: The World Stress Map Project. Journal of Geophysical Research: Solid Earth 97, 11703-11728.

Table 1. List of measurement stations

Fig. 1. The Saint-Édouard area location and its geological context: a. location of the St. Lawrence Platform; b. geological framework of the St. Lawrence Platform (modified from Globensky (1987)); c. geological map of the Saint-Édouard area (Clark and Globensky, 1973; Globensky, 1987; Lavoie et al., 2016; Thériault and Beauséjour, 2012). Faults represented as dashed lines indicate interpreted shallow faults projected from seismic data. J.-C. River fault: Jacques-Cartier River fault; C.-F. syncline: Chambly-Fortierville syncline ; Gp. : Group ; Fm. : Formation.

Fig. 2. Stratigraphy of the Saint-Édouard area units (modified from Konstantinovskaya et al. (2014). Gp. : Group ; Fm. : Formation.

Fig. 3. Tectonic calendar recorded in the studied area, modified from Lavoie (2008).

Fig. 4. Stereographic projection (lower hemisphere Schmidt stereodiagram) of the bedding plane attitudes measured in the autochthonous (a.) and parautochthonous (b.) domains. Each pole corresponds to the mean bedding plane attitude measured on each outcrop and shallow well in the Saint-Édouard area. C.F. syncline: Chambly-Fortierville syncline; n: number of measurement sites (outcrops or wells).

Fig. 5. Cross-section in the Saint-Édouard area (see Fig. 1 for location). Interpretation proposed by Lavoie et al. (2016) and based on industrial seismic data. Gp: Group.

Fig. 6. Examples of fracture observations on outcropping shales: a. and b. Fracture sets 1 and 2 abutting relationships in the outcropping Lorraine Group (a; site 10) and Les Fonds Formations (b; site 17). The gray dots highlight the abutting relationships between fracture sets; d. example of a fracture that abuts a calcareous concretion at site 6.

Fig. 7. Attitudes of the fracture sets identified in wells and outcrops intersecting shales in the Saint-Édouard area. The mean fracture sets and bedding planes attitudes estimated for each station are compiled in the “synthesis” stereonets. Fracture and bedding planes poles are plotted in a lower hemisphere Schmidt representation. For outcrop data, contoured densities are not significant as they vary with the number of features measured in each outcrop (a function of the outcrop and well dimensions); densities were corrected for the sampling bias in borehole data. J.-C.: Jacques-Cartier; C.-F.: Chambly-Fortierville; n: number of fractures for each outcrop/well; L: length of the well section logged;

Fig. 8. Fracture attitudes variations during the fold test. The fracture data used in the analysis comes from outcrops 5 & 7 to 16 (autochthonous) and from outcrop 17 and wells #10, 11 and 13 (parautochthonous). Fault and fold axis locations presented in the maps were initially described in Clark and Globensky (1973) and Pinet (2011). F-I and F-II: first and second generations folds. Two folds generations were identified in the autochthonous domain and one folding event was

identified in the parautochthonous domain. The parameter k quantifies the degree of data concentration (higher values correspond to highly concentrated data).

Fig. 9. Fracture spacing measured on outcrops of the Lorraine Group shale (15 sites) and in three deep well horizontal legs located in the Utica Shale. The box plot diagrams show, from right to left, maximum, upper quartile (75th percentile), median value, lower quartile (25th percentile) and minimum fracture spacing for the F1, F2 and F3 fracture sets.

Fig. 10. Fracture spacing distributions from outcrops and deep wells. The number of F3 fracture spacings measured in outcrops was insufficient to present meaningful results.

Fig. 11. Experimental variograms for spacing of fractures with respect to the distance lag h along the horizontal legs of the deep wells (Utica Shale). A moving average curve was added for a better identification of the trends in the calculated variograms. The horizontal line corresponds to the variance of the entire fracture spacing sample. This representation highlights the limit beyond which fracture spacing is not correlated (range) for F1, F2 and F3.

Fig. 12. Fracture densities in the horizontal leg of the deep shale gas well A (Utica Shale). Fracture frequencies were calculated using a 20 m window length every 5 m.

Fig. 13. Fracture density and rock brittleness at depth: a. example of fracture density variation with depth in the deep vertical well B. Fracture densities were calculated using a 5 m window

length every 1 m and the values were corrected for sampling bias; b: mineralogical and acoustic Brittleness Index variations with depth (data from Séjourné (2017)).

Fig. 14. Examples of fractures affecting siltstone beds (a and c: site 9; b: top view of the outcrop at site 11). The gray dots highlight the abutting relationships between fracture sets.

Fig. 15. Geometrical characteristics of fractures in siltstone units: a. Examples of fracture attitudes measured in siltstone outcrops at sites 9 and 11; b. Linear relationship between fracture spacing and siltstone bed thickness (data from outcrops 1, 6, 13 & 19); the term ratio in the plots corresponds to the fracture spacing to layer thickness ratio; the location of sites is shown in Fig. 1.

Fig. 16. Conceptual models of the fracture patterns: a. caprock units of the autochthonous domain; b. caprock units of the parautochthonous domain; c. deep shale gas reservoir. In a. and b., the shallow aquifers are not specifically represented because they are affected by the same fracture network than the caprock units. The fracture network is also represented at a smaller scale in REVs: d. shale units; e. siltstone interbeds.

Figure 1



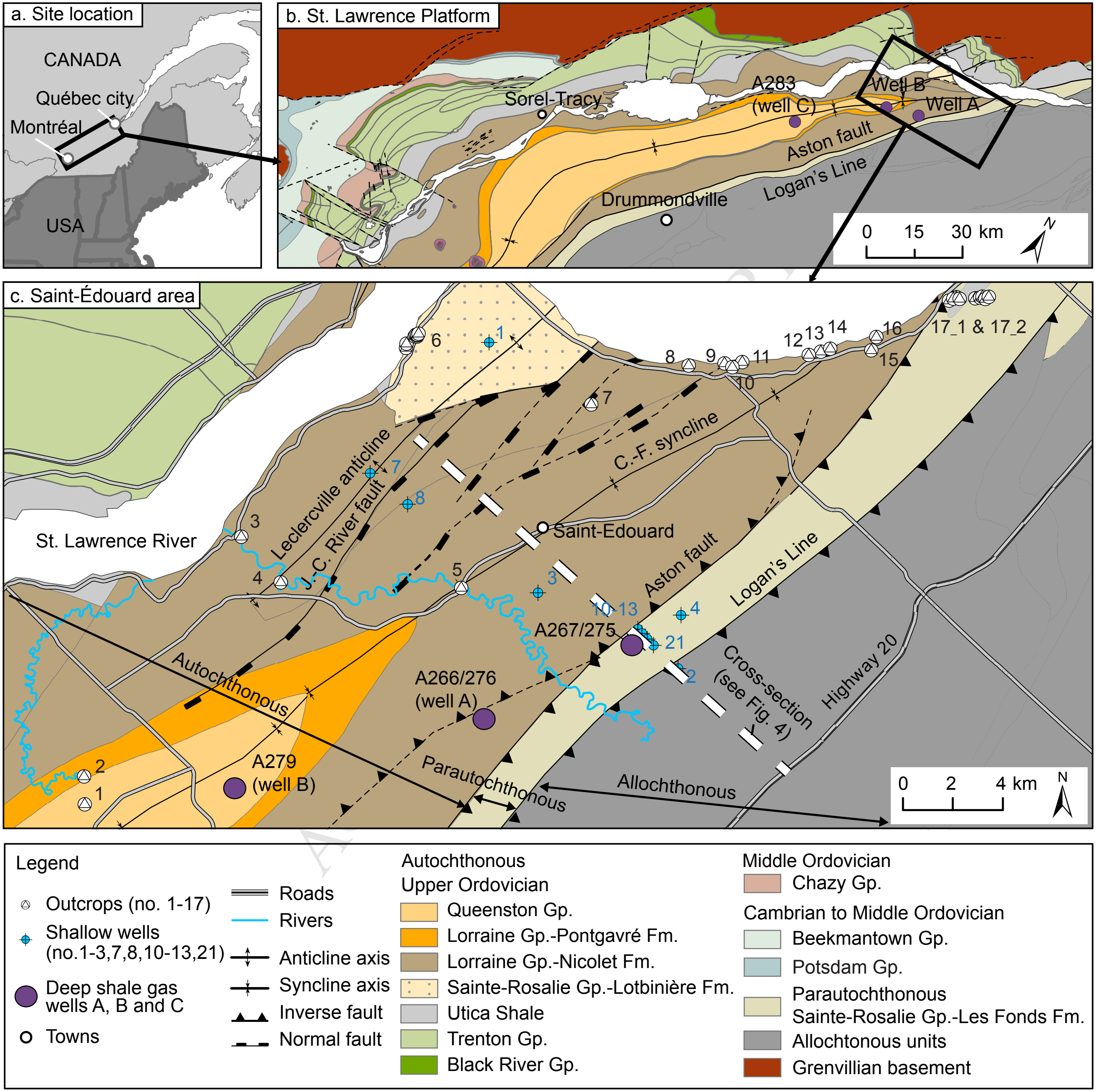
a. Site location
CANADA
Québec city
Montréal
USA
b. St. Lawrence Platform
Sorel-Tracy
A283
(well C)
Well B
Well A
Aston fault
Logan's Line
Drummondville
0 15 30 km
N
c. Saint-Édouard area
St. Lawrence River
Leclercville anticline
J. C. River fault
C.-F. syncline
Saint-Edouard
Aston fault
Logan's Line
A267/275
A266/276
(well A)
A279
(well B)
Autochthonous
Parautochthonous
Allochthonous
Cross-section
(see Fig. 4)
Highway 20
17_1 & 17_2
10-13
21
0 2 4 km
N
Legend
Outcrops (no. 1-17)
Shallow wells
(no.1-3,7,8,10-13,21)
Deep shale gas
wells A, B and C
Towns
Roads
Rivers
Anticline axis
Syncline axis
Inverse fault
Normal fault
Autochthonous
Upper Ordovician
Queenston Gp.
Lorraine Gp.-Pontgavré Fm.
Lorraine Gp.-Nicolet Fm.
Sainte-Rosalie Gp.-Lotbinière Fm.
Utica Shale
Trenton Gp.
Black River Gp.
Middle Ordovician
Chazy Gp.
Cambrian to Middle Ordovician
Beekmantown Gp.
Potsdam Gp.
Parautochthonous
Sainte-Rosalie Gp.-Les Fonds Fm.
Allochtonous units
Grenvillian basement

**Figure 2**

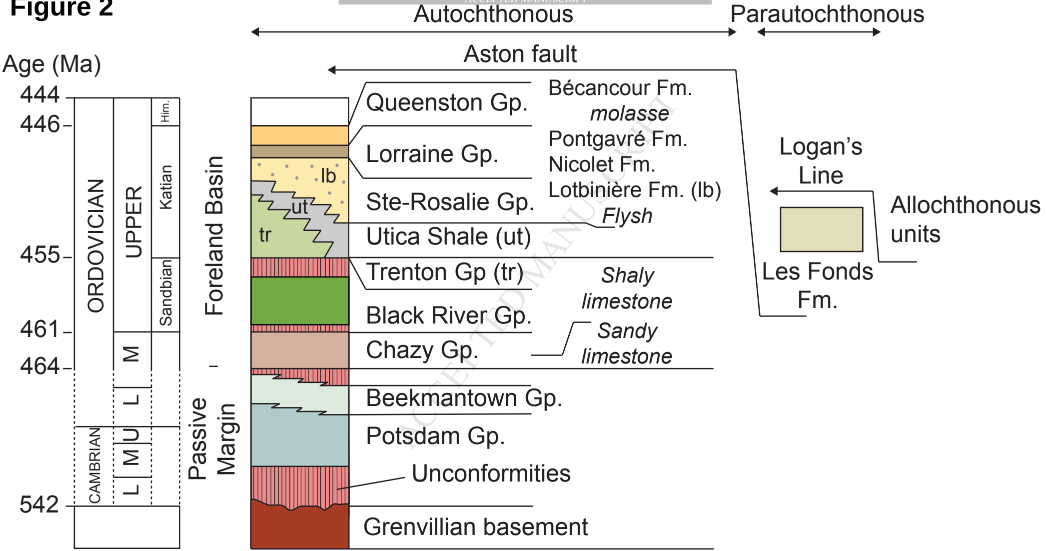
Autochthonous
Parautochthonous
Aston fault
Age (Ma)
444
446
455
461
464
542
ORDOVICIAN
UPPER
Hirn.
Katian
Sandbian
M
L
CAMBRIAN
U
M
L
Foreland Basin
Passive Margin
lb
ut
tr
Queenston Gp.
Lorraine Gp.
Ste-Rosalie Gp.
Utica Shale (ut)
Trenton Gp (tr)
Black River Gp.
Chazy Gp.
Beekmantown Gp.
Potsdam Gp.
Unconformities
Grenvillian basement
Bécancour Fm.
molasse
Pontgavré Fm.
Nicolet Fm.
Lotbinière Fm. (lb)
Flysh
Shaly limestone
Sandy limestone
Logan's Line
Allochthonous units
Les Fonds Fm.

# Figure 3



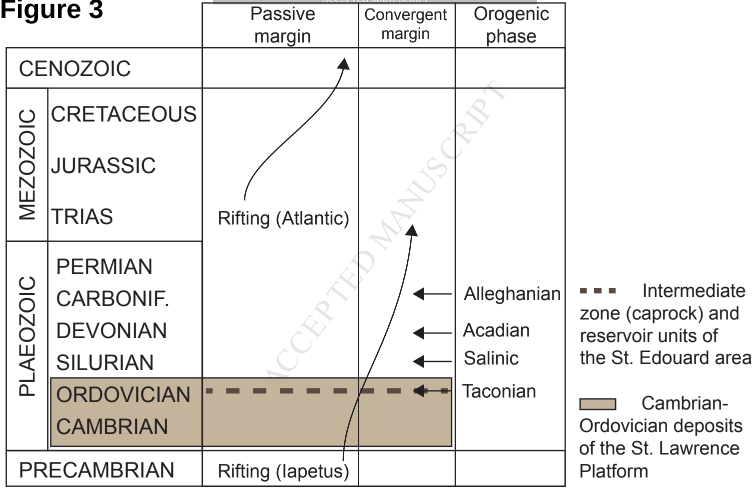

Passive margin
Convergent margin
Orogenic phase
CENOZOIC
MEZOZOIC
CRETACEOUS
JURASSIC
TRIAS
Rifting (Atlantic)
PLAEOZOIC
PERMIAN
CARBONIF.
DEVONIAN
SILURIAN
ORDOVICIAN
CAMBRIAN
PRECAMBRIAN
Rifting (Iapetus)
Alleghanian
Acadian
Salinic
Taconian
Intermediate zone (caprock) and reservoir units of the St. Edouard area
Cambrian-Ordovician deposits of the St. Lawrence Platform

**Figure 4**

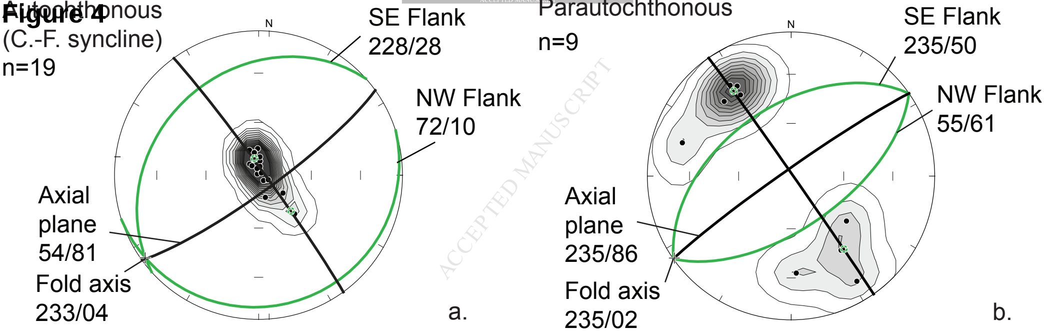
Autochthonous
(C.-F. syncline)
n=19
N
SE Flank
228/28
NW Flank
72/10
Axial
plane
54/81
Fold axis
233/04
a.
Parautochthonous
n=9
N
SE Flank
235/50
NW Flank
55/61
Axial
plane
235/86
Fold axis
235/02
b.

**Figure 5**



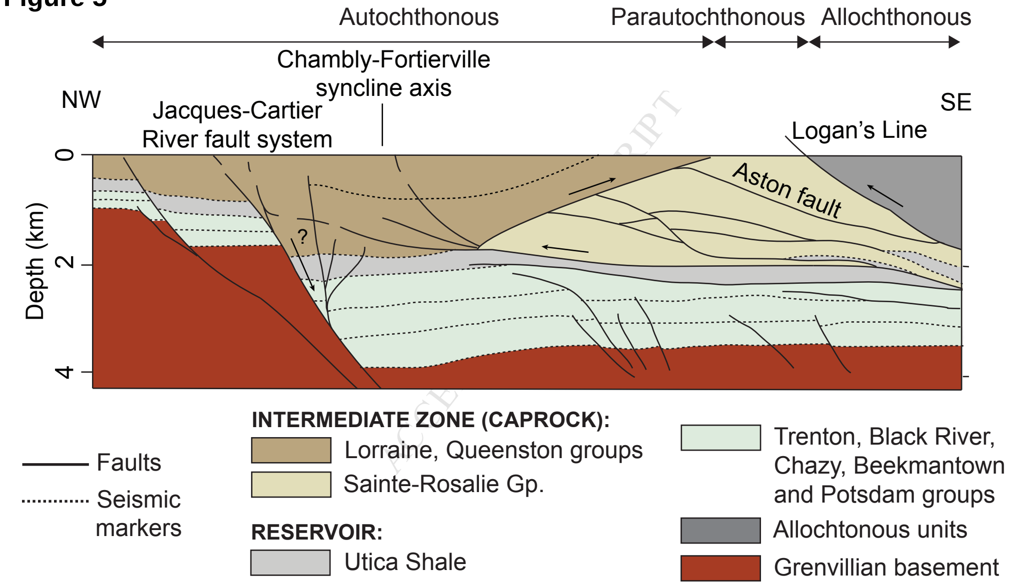

Autochthonous
Parautochthonous
Allochthonous
Chambly-Fortierville syncline axis
NW
SE
Jacques-Cartier River fault system
Logan's Line
Aston fault
?
0
2
4
Depth (km)
INTERMEDIATE ZONE (CAPROCK):
Lorraine, Queenston groups
Sainte-Rosalie Gp.
RESERVOIR:
Utica Shale
Faults
Seismic markers
Trenton, Black River, Chazy, Beekmantown and Potsdam groups
Allochtonous units
Grenvillian basement

Figure 6



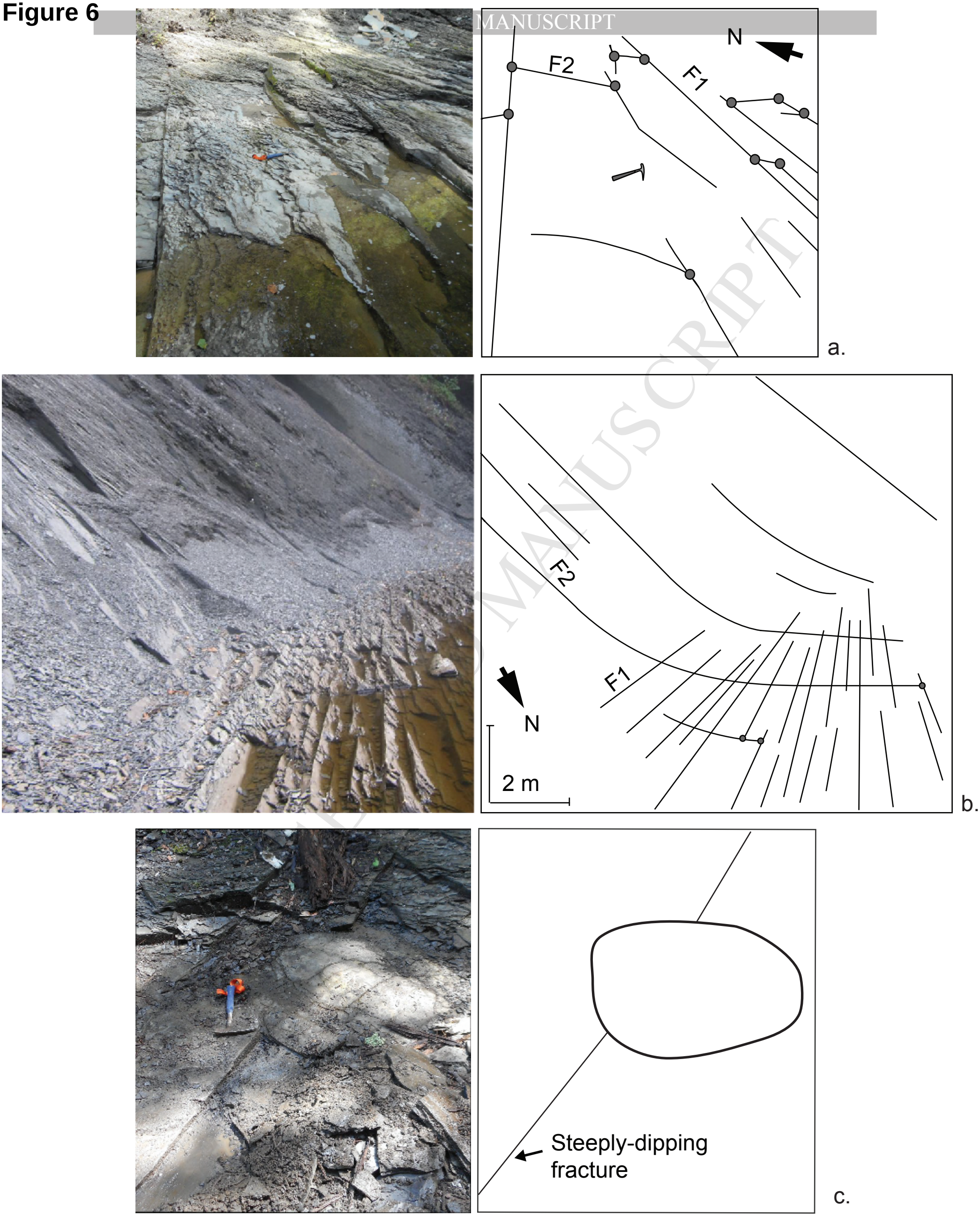

Figure 7



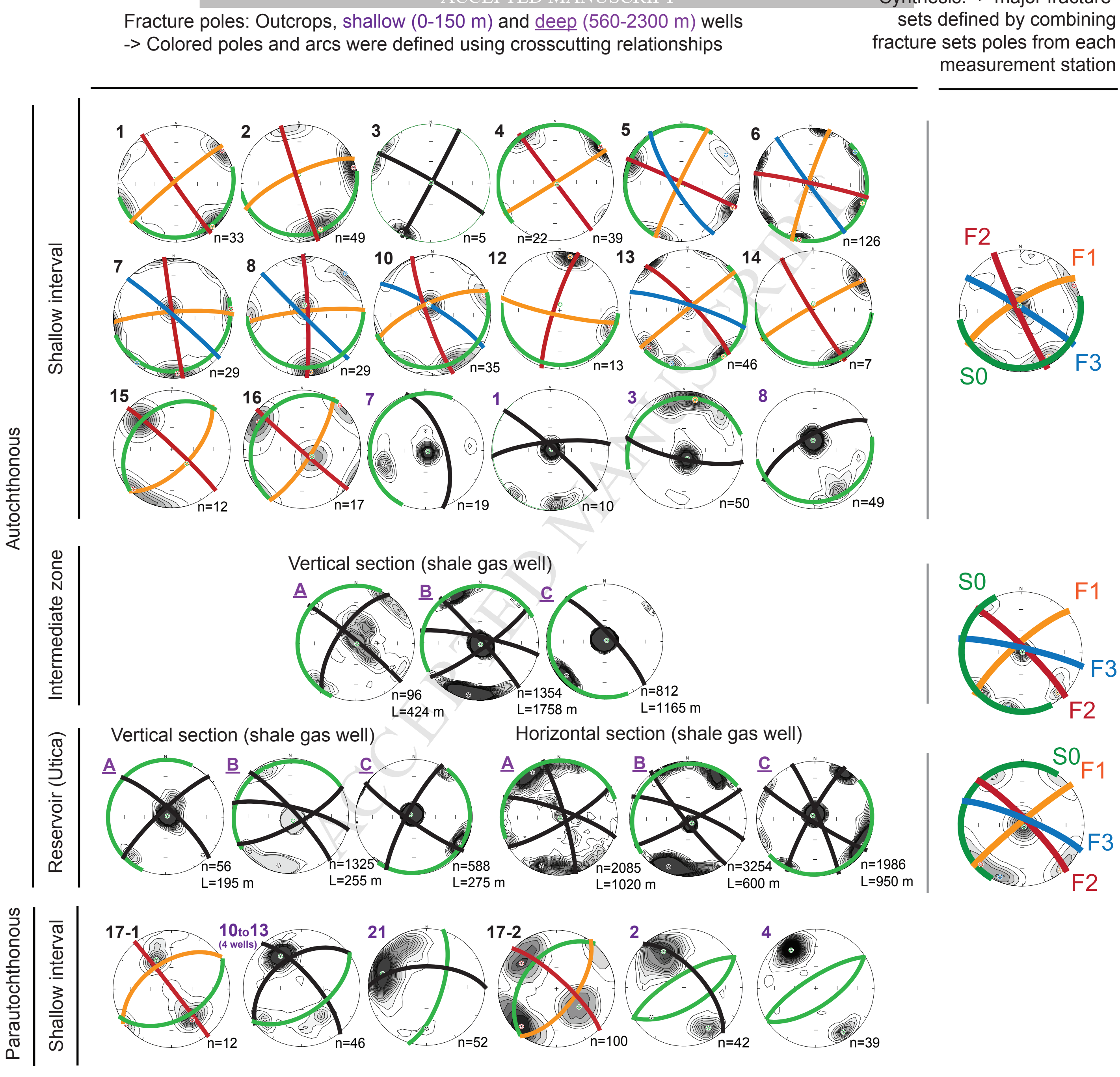

Fracture poles: Outcrops, shallow (0-150 m) and deep (560-2300 m) wells
-> Colored poles and arcs were defined using crosscutting relationships
Synthesis: -> major fracture sets defined by combining fracture sets poles from each measurement station
Autochthonous
Shallow interval
1 n=33
2 n=49
3 n=5
4 n=22 n=39
5
6 n=126
7 n=29
8 n=29
10 n=35
12 n=13
13 n=46
14 n=7
15 n=12
16 n=17
7 n=19
1 n=10
3 n=50
8 n=49
F2 F1 F3 S0
Intermediate zone
Vertical section (shale gas well)
A n=96 L=424 m
B n=1354 L=1758 m
C n=812 L=1165 m
S0 F1 F3 F2
Reservoir (Utica)
Vertical section (shale gas well)
A n=56 L=195 m
B n=1325 L=255 m
C n=588 L=275 m
Horizontal section (shale gas well)
A n=2085 L=1020 m
B n=3254 L=600 m
C n=1986 L=950 m
S0 F1 F3 F2
Parautochthonous
Shallow interval
17-1 n=12
10to13 (4 wells) n=46
21 n=52
17-2 n=100
2 n=42
4 n=39

Figure 8



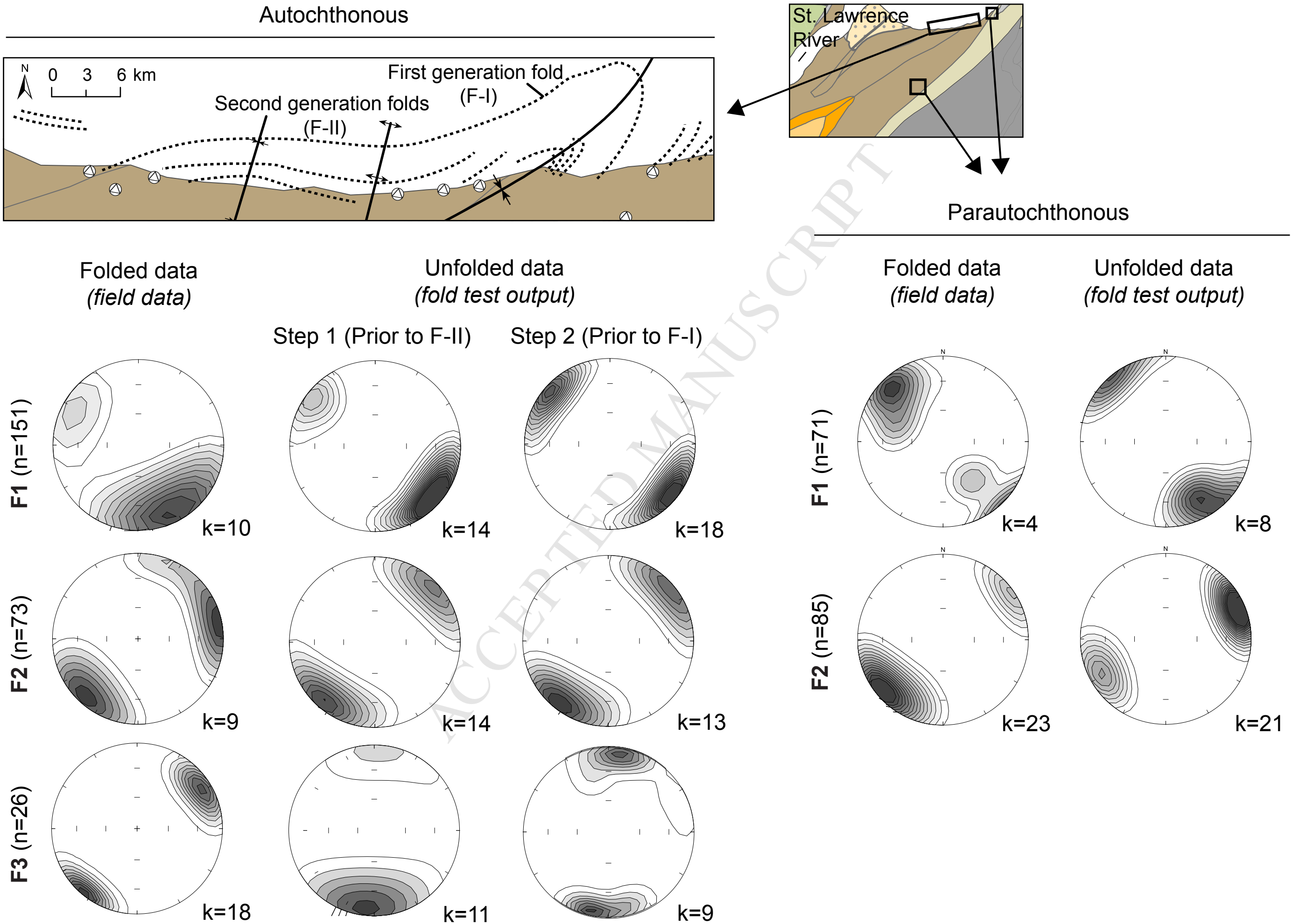

Autochthonous
N
0 3 6 km
First generation fold (F-I)
Second generation folds (F-II)
St. Lawrence River
Parautochthonous
Folded data (field data)
Unfolded data (fold test output)
Step 1 (Prior to F-II)
Step 2 (Prior to F-I)
F1 (n=151)
k=10
k=14
k=18
F2 (n=73)
k=9
k=14
k=13
F3 (n=26)
k=18
k=11
k=9
Folded data (field data)
Unfolded data (fold test output)
F1 (n=71)
k=4
k=8
F2 (n=85)
k=23
k=21

**Figure 9**

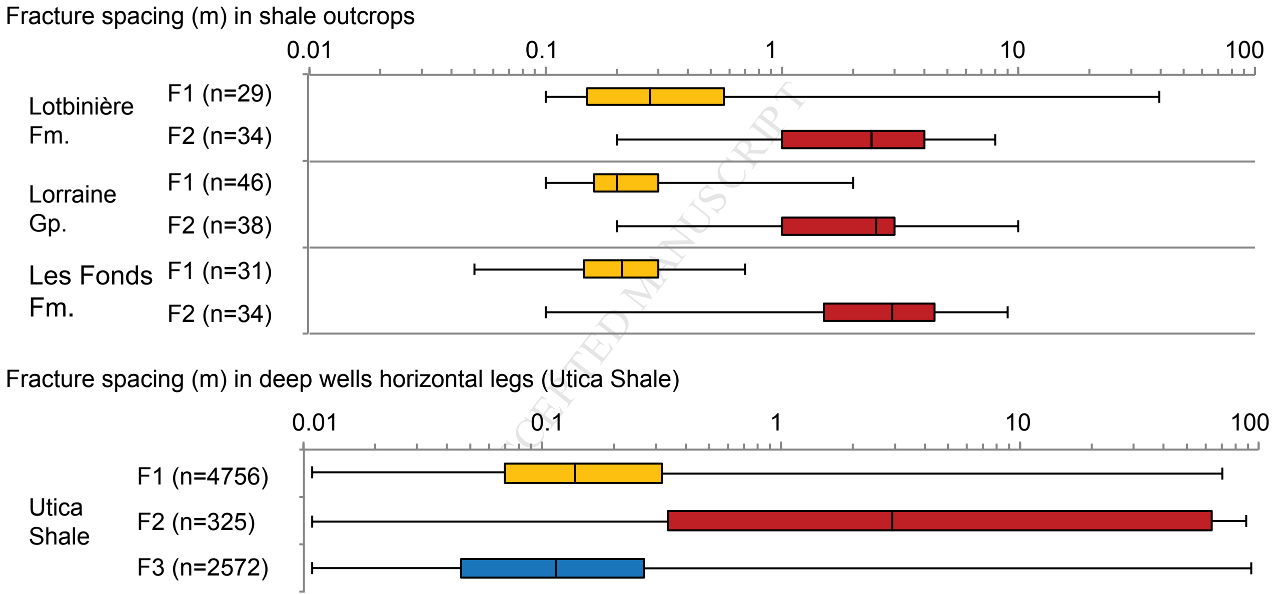

Fracture spacing (m) in shale outcrops
0.01
0.1
1
10
100
Lotbinière Fm.
F1 (n=29)
F2 (n=34)
Lorraine Gp.
F1 (n=46)
F2 (n=38)
Les Fonds Fm.
F1 (n=31)
F2 (n=34)
Fracture spacing (m) in deep wells horizontal legs (Utica Shale)
0.01
0.1
1
10
100
Utica Shale
F1 (n=4756)
F2 (n=325)
F3 (n=2572)

**Figure 10**

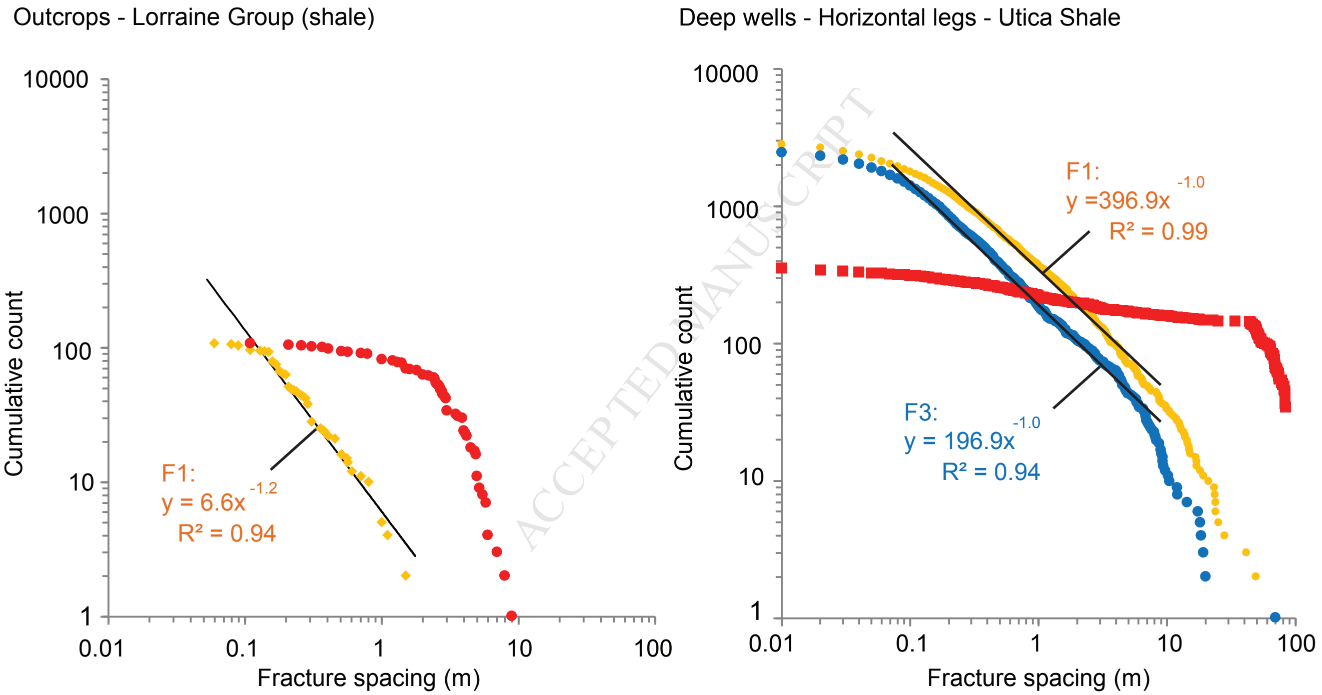
Outcrops - Lorraine Group (shale)
Cumulative count
10000
1000
100
10
1
0.01
0.1
1
10
100
Fracture spacing (m)
F1:
y = 6.6x -1.2
R² = 0.94
Deep wells - Horizontal legs - Utica Shale
Cumulative count
10000
1000
100
10
1
0.01
0.1
1
10
100
Fracture spacing (m)
F1:
y =396.9x -1.0
R² = 0.99
F3:
y = 196.9x -1.0
R² = 0.94

**Figure 11**

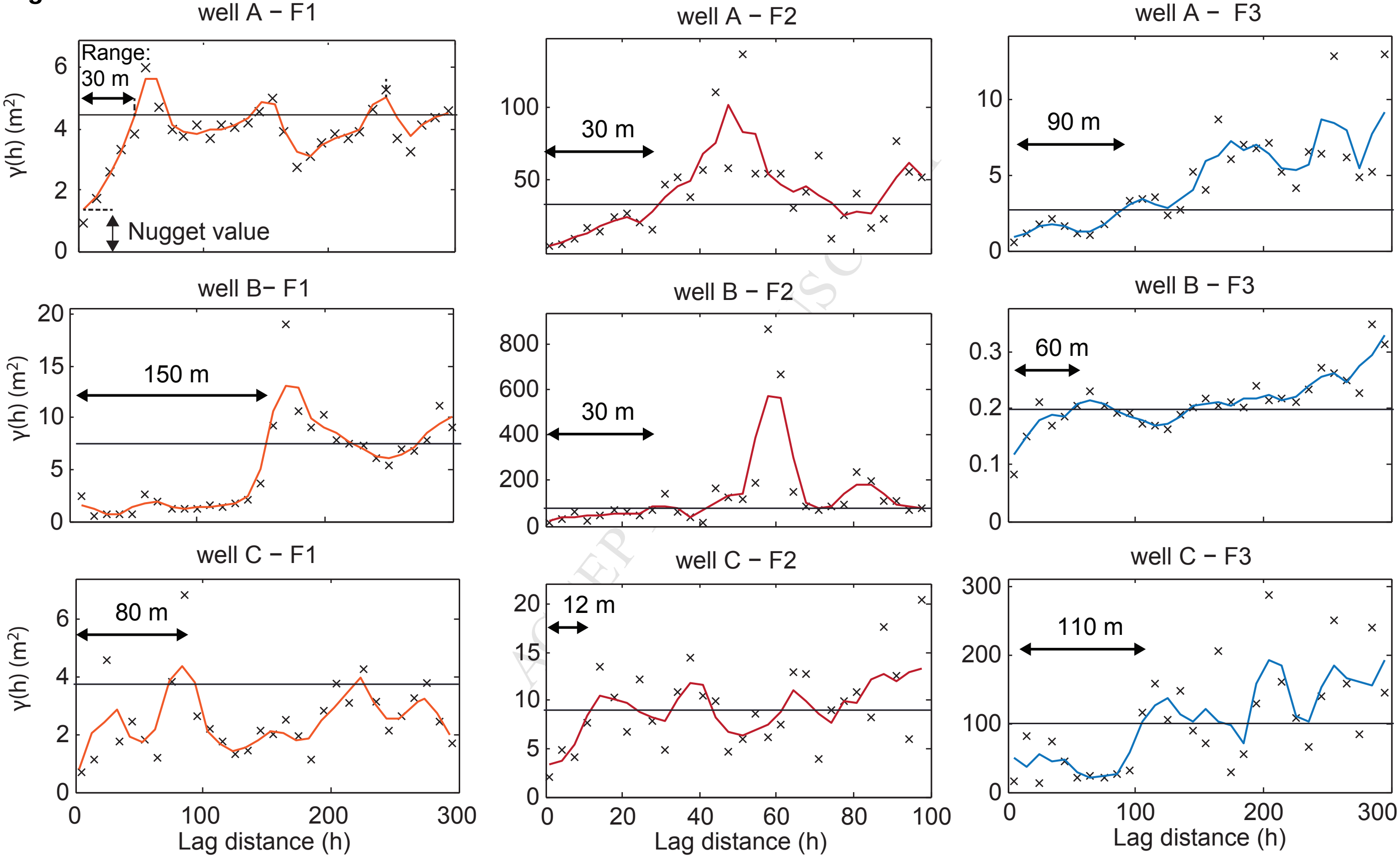

well A − F1
Range:
30 m
Nugget value
γ(h) (m²)
well A − F2
30 m
well A − F3
90 m
well B− F1
150 m
γ(h) (m²)
well B − F2
30 m
well B − F3
60 m
well C − F1
80 m
γ(h) (m²)
Lag distance (h)
well C − F2
12 m
Lag distance (h)
well C − F3
110 m
Lag distance (h)

# Figure 12

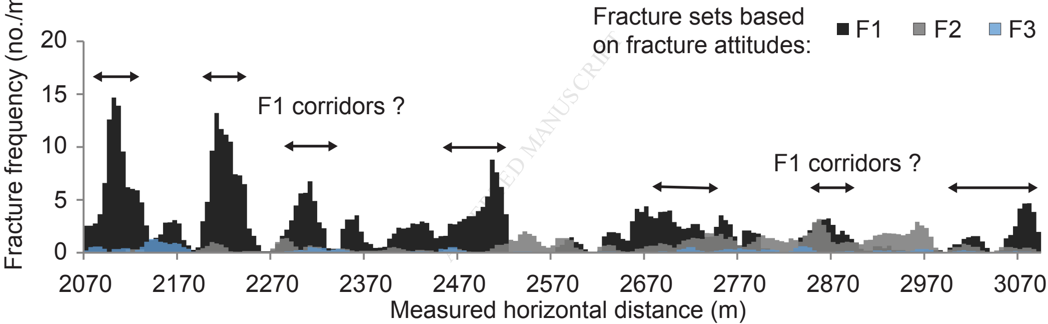
Fracture sets based on fracture attitudes:
F1
F2
F3
Fracture frequency (no./m)
20
15
10
5
0
F1 corridors ?
F1 corridors ?
2070
2170
2270
2370
2470
2570
2670
2770
2870
2970
3070
Measured horizontal distance (m)

# Figure 13



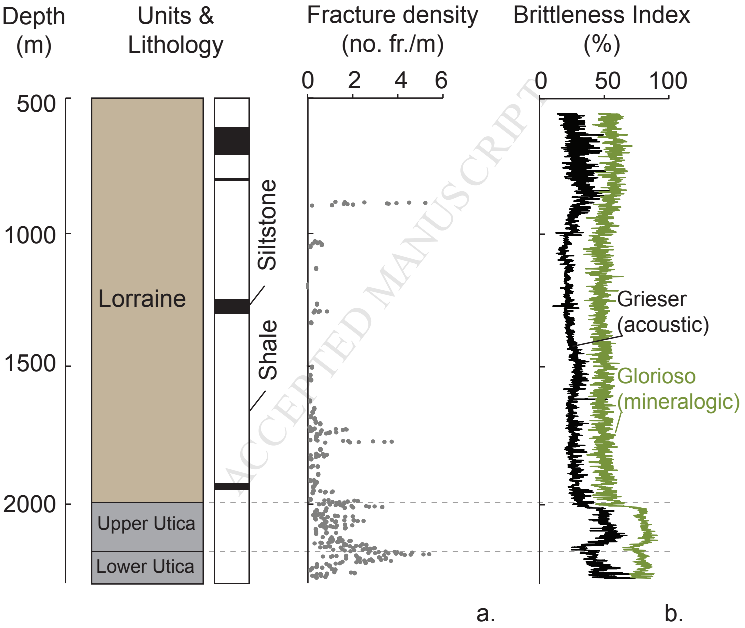

Depth (m)
Units & Lithology
Fracture density (no. fr./m)
Brittleness Index (%)
0
2
4
6
0
50
100
500
1000
1500
2000
Lorraine
Upper Utica
Lower Utica
Siltstone
Shale
Grieser (acoustic)
Glorioso (mineralogic)
a.
b.

## Figure 14



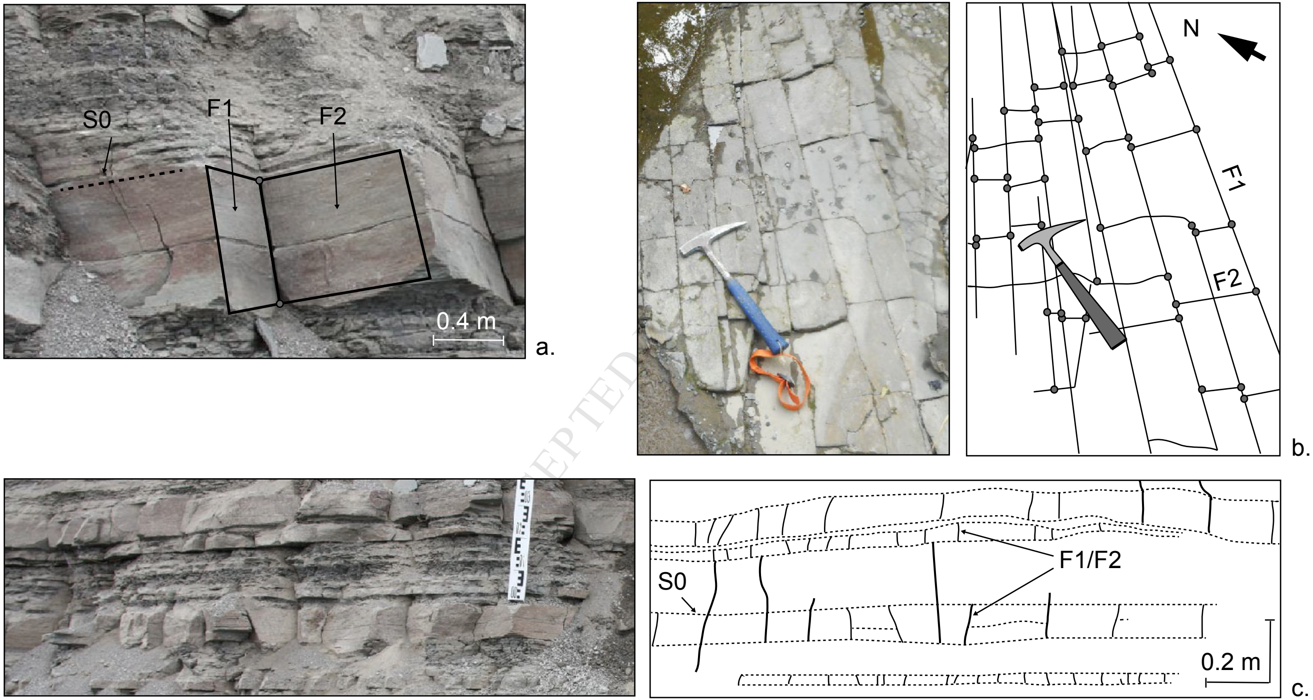

**Figure 15**

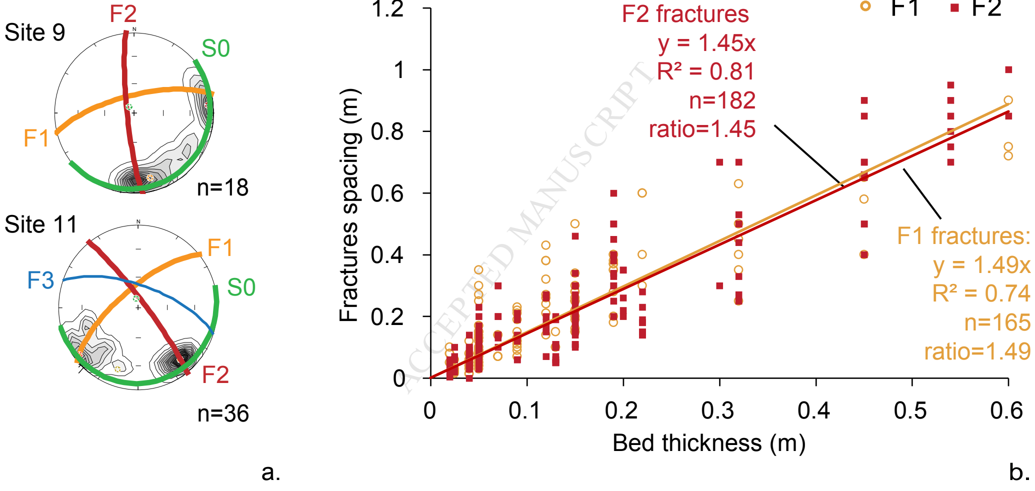

Site 9
F2
S0
F1
n=18
Site 11
F1
F3
S0
F2
n=36
a.
F1
F2
F2 fractures
y = 1.45x
R² = 0.81
n=182
ratio=1.45
F1 fractures:
y = 1.49x
R² = 0.74
n=165
ratio=1.49
Fractures spacing (m)
Bed thickness (m)
0
0.2
0.4
0.6
0.8
1
1.2
0
0.1
0.2
0.3
0.4
0.5
0.6
b.

Figure 16

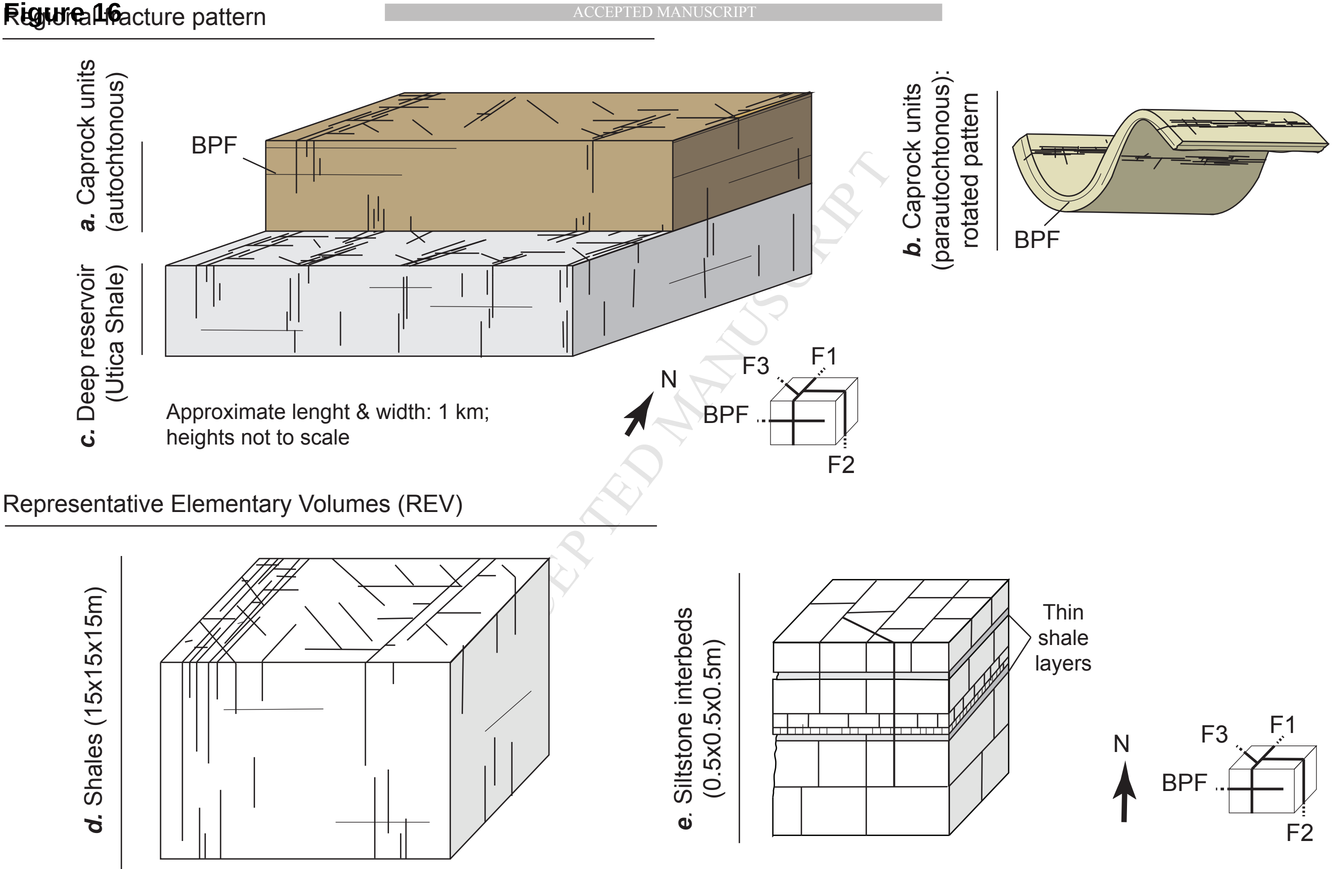

Regional fracture pattern
a. Caprock units
(autochtonous)
BPF
c. Deep reservoir
(Utica Shale)
b. Caprock units
(parautochtonous):
rotated pattern
BPF
Approximate lenght & width: 1 km;
heights not to scale
N
F3
F1
BPF
F2
Representative Elementary Volumes (REV)
d. Shales (15x15x15m)
e. Siltstone interbeds
(0.5x0.5x0.5m)
Thin
shale
layers
N
F3
F1
BPF
F2

**Table 1**



| Measurement station | ID | UTM coordinates (NAD83 19N) | | | Lithology | Group | Number of fractures | Outcrop size (approxima-tivelly) / borehole lenght in the bedrock (m) | Outcrop or well direction (°N) |
|---|---|---|---|---|---|---|---|---|---|
| | | X (m) | Y (m) | UTM Zone | | | | | |
| Outcrop (river bed) | 1 | 263815 | 5151764 | 19T | Shale | Queenston | 33 | 60 | 90 |
| Outcrop (river bed) | 2 | 263877 | 5152879 | 19T | Shale | Lorraine | 49 | 50 | 120 |
| Outcrop (river bed) | 3 | 270891 | 5161970 | 19T | Shale | Lorraine | 5 | 10 | 10 |
| Outcrop (river bed) | 4 | 272323 | 5160028 | 19T | Shale | Lorraine | 45 | 15 | 340 |
| Outcrop (river bed) | 5 | 279520 | 5159255 | 19T | Shale | Lorraine | 22 | 20 | 90 |
| Outcrop (river bed) | 6 | 278734 | 5169518 | 19T | Shale | Sainte-Rosalie | 126 | 4 x 20 | 44; 120; 150; 160 |
| Outcrop (river bed) | 7 | 285270 | 5166177 | 19T | Shale | Lorraine | 29 | 60 | 160 |
| Outcrop (river bed) | 8 | 289280 | 5167441 | 19T | Shale | Lorraine | 29 | 15 | 10 |
| Outcrop (vertical wall) | 9 | 290718 | 5167411 | 19T | Siltstones | Lorraine | 18 | 20 | 40 |
| Outcrop (river bed) | 10 | 290937 | 5167320 | 19T | Shale | Lorraine | 35 | 50 | 160 |
| Outcrop (vertical wall) | 11 | 291434 | 5167412 | 19T | Siltstones | Lorraine | 28 | 150 | 90 |
| Outcrop (vertical wall) | 12 | 294107 | 5167496 | 19T | Shale | Lorraine | 13 | 20 | 70 |
| Outcrop (vertical wall) | 13 | 294715 | 5167631 | 19T | Shale | Lorraine | 46 | 20 | 70 |
| Outcrop (vertical wall) | 14 | 294989 | 5167677 | 19T | Shale | Lorraine | 7 | 20 | 70 |
| Outcrop (river bed) | 15 | 296619 | 5167487 | 19T | Shale | Lorraine | 12 | 10 | 0 |
| Outcrop (river bed) | 16 | 296866 | 5168006 | 19T | Shale | Lorraine | 17 | 50 | 140 |
| Outcrop (river bed) | 17 | 299783 | 5169320 | 19T | Shale | Sainte-Rosalie | 120 | 2 x 20 | 130; 30 |
| Shallow well | 1 | 281370 | 5168963 | 19T | Shale | Sainte-Rosalie | 10 | 47 | vertical |
| Shallow well | 2 | 287925 | 5155391 | 19T | Shale | Sainte-Rosalie | 42 | 46 | vertical |
| Shallow well | 3 | 282584 | 5158820 | 19T | Shale & Siltstone | Lorraine | 50 | 30 | vertical |
| Shallow well | 4 | 288214 | 5157504 | 19T | Shale | Sainte-Rosalie | 39 | 20 | vertical |
| Shallow well | 7 | 276263 | 5164099 | 19T | Shale | Lorraine | 19 | 40 | vertical |
| Shallow well | 8 | 277620 | 5162758 | 19T | Shale & Siltstone | Lorraine | 49 | 50 | vertical |
| Shallow well | 10 | 286450 | 5157073 | 19T | Shale | Sainte-Rosalie | 25 | 15 | vertical |
| Shallow well | 11 | 286396 | 5156776 | 19T | Shale | Sainte-Rosalie | 19 | 50 | vertical |
| Shallow well | 13 | 286807 | 5156653 | 19T | Shale | Sainte-Rosalie | 2 | 59 | vertical |
| Shallow well | 21 | 287026 | 5156377 | 19T | Shale | Sainte-Rosalie | 52 | 148 | vertical |
| Deep well | A | 280035 | 5154051 | 19T | Shale | Sainte-Rosalie | 96 | 424 | vertical |
| Deep well | B | 269837 | 5152004 | 19T | Shale | Sainte-Rosalie | 1354 | 1758 | vertical |
| Deep well | C | 707892 | 5133892 | 18T | Shale | Sainte-Rosalie | 812 | 1165 | vertical |
| Deep well | A | 280035 | 5154051 | 19T | Shale | Lorraine | 56 | 195 | vertical |
| Deep well | B | 269837 | 5152004 | 19T | Shale | Lorraine | 1325 | 255 | vertical |
| Deep well | C | 707892 | 5133892 | 18T | Shale | Lorraine | 588 | 275 | vertical |
| Horizontal well | A | 280035 | 5154051 | 19T | Shale | Lorraine | 2085 | 1020 | 316 |
| Horizontal well | B | 269837 | 5152004 | 19T | Shale | Lorraine | 3254 | 600 | 316 |
| Horizontal well | C | 707892 | 5133892 | 18T | Shale | Lorraine | 1986 | 950 | 307 |

**Highlights**

- This study integrates shallow and deep multisource fracture datasets

- An analog approach was used to characterized the caprock of the Utica Shale reservoir

- Four fracture sets affects the entire shale succession

- A conceptual model of this fracture network is proposed